IOJAP: MORPHOLOGICAL AND PHYSIOLOGICAL PHENOTYPE CHARACTERIZATION IN ARABIDOPSIS

A Dissertation Presented for the

Doctor of Philosophy

Degree

The University of Tennessee, Knoxville

Thomas Jay Payne

December 2020

DEDICATION

"What is wanted is not the will to believe, but the wish to find out, which is the exact opposite." – Bertrand Russel

This dissertation is dedicated to my family. A father, a mother, a brother, a sister, and a nephew. Your love and support were unyielding.

ACKNOWLEDGEMENTS

"The methods of science, as stodgy and grumpy as it may seem, is far more important than the findings of science." –Carl Sagan

I want to thank the University of Tennessee Graduate School for allowing me to pursue my Ph.D., and for awarding me funding through Student Faculty Research Award.

I want to thank my committee members, Dr. Brad Binder, Dr. Jennifer Franklin, Dr. Bruce McKee, and Dr. Elena Shpak for listening and watching the presentations of my work, over and over. Their criticism helped me grow as a scientist and their doors were always open to offer guidance and encouragement. Without their overabundance of patience, I would not have made it this far.

Special thanks to my PI, Dr. Andreas Nebenführ, who taught me so much about critical thinking, how to read scientific papers, and showed me the American and European way of scientific inquiry. His support, encouragements and optimism, lifted me up from the toughest times. I would not have gotten this far without him.

Thank you to all my undergraduate who help gather data to fill these pages.

ABSTRACT

IOJAP protein is found in all organisms that contain a ribosome of bacterial origin. The majority of studies suggest that IOJAP plays a role in translation, although this has yet to be thoroughly investigated in plants. Using *Arabidopsis thaliana*, an extensive phenotype characterization of *iojap* mutants was performed. Many processes of plant growth were slightly impaired at optimal temperature (22˚C) but became severely hindered at low temperature (12˚C and 4˚C). These cold temperature defects manifested in an overall reduction of plant growth as well as variegation, chlorosis, leaf hyponasty, as well as reduced maximum quantum yield (F_v/F_m) in young leaves and during de-etiolation. Interestingly other developmental processes such as bolting time, germination, and etiolation were unaffected by low temperature. The observed exacerbation of defects was unique to low temperature as other abiotic stresses such as heat, osmotic, salinity, and high light were ineffective at eliciting similar responses. Tracking relative transcription and translation levels early in de-etiolation, chloroplast encoded transcripts were skewed towards low translation populations, suggesting a translation defect. Further investigation is required to pinpoint the involvement of IOJAP in translation, as well as better understanding of the detrimental deficiencies brought about by low temperature.

TABLE OF CONTENTS

LIST OF TABLES

LIST OF FIGURES

CHAPTER ONE

INTRODUCTION AND GENERAL INFORMATION

Discovery and of Characterization *Iojap* Mutant in *Zea Mays*

In 1924, Dr. Merel T. Jenkins wanted to know if there were recessive defects in maize crop varieties that had not been detected previously (Jenkins, 1924). He found 86% of the Iodent corn variety had variegation, displayed as white stripes parallel to the axis of the leaf mid vein. This striping in the mature plants resembled that of *japonica* striping and thus was dubbed IOJAP for *Iodent japonica* (Jenkins, 1924). Variegation is the random distribution of healthy green cells and unhealthy virescent, yellow, or albino cells, (Jenkins, 1924), resulting from an asymmetric population of dysfunctional chloroplasts. This can occur through mutations in the mitochondrial, chloroplast, or in the case of *iojap*, nuclear genomes. The striping of *iojap* phenotype persists through maturity but oddly can also persist through the maternal line even in the heterozygous condition (Rhoades, 1943, 1946, 1950). Interestingly, the phenotypic severity in leaf morphology, striping thickness and frequency, and overall plant stature was dependent on maize variety rather than environmental conditions (Coe et al., 1988). The exact reason for this variation of phenotypic expression is unknown but may be attributed to an unknown nuclear factor, such as the *R* gene. The R gene is a cluster of genes responsible for developmental and tissue specific responses involving pigmentation (Consonni et al., 1993). It was found that certain allelic combinations of dominant R genes could suppress, mitigate, or influence the *iojap* phenotype (Coe et al., 1982). Either way, the genetic background is a factor for phenotypic presentation of *iojap*.

Variegation is caused by heteroplastidic asymmetrical distribution that can be observed in various tissues, such as leaf epidermis, mesophyll, bundle sheaths, tassels, ears, and other shoot areas

(Coe et al., 1988). Though most maize varieties expressed similar phenotypes, such as variegation, the viability and stature of the plant was relatively unchanged, while a few varieties of maize were drastically reduced in size (Coe et al., 1988). Much of the difference depended upon in the varying degrees of variegation or stripe frequency and width across maize varieties. Interestingly, the white tissue adjacent to green tissue remained undistorted in size and shape relative to the healthy tissue. Another observable abnormality was the size and graininess (fine gradient of color change) of the leaves. A priori, we would predict that white tissue contains cells void of green healthy chloroplasts, but instead white tissue is often heteroplastidic, where some cells contain a few healthy green chloroplasts. A closer look at differences in chloroplasts of white and green tissue by electron microscopy found that white tissue chloroplasts were highly underdeveloped, with few to no internal thylakoid membranes, while green tissue chloroplasts were normal (Shumway and Weier, 1967). Likewise there were other defects in physiological processes in *iojap* plastids (Walbot and Coe, 1979). An easy guess would be to expect white tissue chloroplasts were void of pigment, and that is what they found. Extraction of white tissue chloroplast pigment contained 1% to 2% of carotenoids and 0.1% of chlorophyll relative to green tissue chloroplast in both *ij/ij* and *ij/+* genotypes (Siemenroth et al., 1980). Plastid ribosomes were not detected when viewed through electron microscopy. A molecular look into chloroplast translation defects discovered that several plastid proteins, specifically large subunit ribulose-1 5-bisphosphate carboxylase/oxygenase (RbcL), ATPase, and phosphoenolpyruvate carboxylase were undetected (Siemenroth et al., 1980). This suggests that there was a problem in plastid protein synthesis. Later it was verified that isolated chloroplast from white tissue were unable to incorporate amino acids into peptides, and lacked plastid rRNA (16S and 23S) suggesting a defect in ribosome formation or translation (Walbot and Coe, 1979). The other important biochemical process, plastid transcription, was

also investigated, and it was found that in white tissue, chloroplast transcript amounts were lower than in WT, as well as having large transcripts that were under processed (Han et al., 1993). In summary, the *iojap* mutation in maize causes a range of phenotypes in various tissues and molecular processes, but the precise function of the IOJAP protein is still not known. For the complete list of established characterizations of *iojap* mutations in plants, see **Table 1.**

IOJAP is a nuclear encoded plastid protein, which means that it is transcribed in the nucleus, translated in the cytosol, and imported to the plastid, in most cases the chloroplast form of the plastid. In order for proteins to be imported into the chloroplast, they must have a transit peptide. Transit peptides have sequence motifs and physicochemical properties that enable them to be targeted and imported into the chloroplast (Bruce, 2000). These properties have been well studied and are conserved enough that they can be used to predict the protein destinations. For instance, analysis of transit peptide of *Arabidopsis thaliana* IOJAP using TargetP software (Armenteros et al., 2019a), is 96% likely to be targeted to the chloroplast. This has also been shown empirically for both *Zea mays* (Han and Martienssen, 2001) and *A. thaliana* (Olinares et al., 2010; Wang et al., 2016a; Zybailov et al., 2008). After import, the transit peptide is cleaved off, leaving a mature functioning protein, which, in the case of IOJAP, is primarily made up of a domain of unknown function 143 (DUF143). The evolutionary conservation of DUF143 and its importance in IOJAP function will be discussed later in this chapter.

Chloroplast Basics and Function in Plants

Around 1.2 to 1.6 billion years ago a single ancient eukaryotic cell containing mitochondria engulfed an ancient cyanobacterial-like organism to establish an endosymbiotic bond

Table 1: Established phenotypes of *iojap* mutants in plants.

Organism	Paper	Phenotype
Z. mays		
	(Jenkins, 1924)	Variegation of the leaves
	(Shumway and Weier, 1967)	Arrested chloroplast development in white tissue
		Plastid rRNA depletion
		Plastid ribosome depletion
		Loss of plastid translation
	(Siemenroth et al., 1980)	Reduction of pigments
		Undetectable plastid proteins ATPase, RbcL
	(Coe et al., 1982, 1988)	Arrested leaf growth (background dependent)
		Grainy leaves (background dependent)
		Arrested embryo growth
		Reduced germination
		Albino tillers
		Reduced plant size
	(Han et al., 1992)	Transcript processing aberrations
A. thaliana		
	(Wang et al., 2016a)	Reduced maximum quantum efficiency in young leaves
		Delayed greening in cotyledons
		Chlorosis of young leaves
		Delayed chloroplast development
		Reduced (altered) plastid translation
		Reduced (altered) plastid transcription

(Bogorad, 2008; Dyall et al., 2004; Reyes-Prieto et al., 2007; Yoon et al., 2004; Zimorski et al., 2014). Three plastid-containing lineages evolved from this event, glaucophytes, red, and green algae (Wise, 2006). The green lineage gave rise to plastids we observe in the earliest terrestrial plants, around 450 million years ago (Pennington, 2002) and which we now call chloroplasts.

Plastids retained a small degree of autonomy and biochemistry of their ancient free-living ancestors, although their functions have been greatly reduced (Timmis et al., 2004). Many of the original chloroplast genes (>95%) (Leister, 2016; Tiller and Bock, 2014) have been transferred to the nucleus, yet chloroplasts contain their own DNA. In higher plants, the plastid genomes range from 120 to 160 kb, where Arabidopsis has 154 kb (Sugiura, 1992). The 100 to 150 (Jarvis and López-Juez, 2013; Lopez-Juez and Pyke, 2004) genes that remain primarily encode ribosome proteins, RNA polymerases, rRNA and tRNA, and photosynthetic machinery. The remaining proteins (around 3000) are imported from the cytosol into the plastid (Jarvis and López-Juez, 2013; Lee et al., 2017; Leister, 2016; Tiller and Bock, 2014).

Plastids in plants take on many different forms that are dependent on tissue type and developmental stage of the plant. Each form of plastid has a specific function that is both unique and overlaps with the other plastid forms. The main types of plastids studied are proplastids, leucoplasts, chromoplasts, gerontopoplasts, etioplasts, and chloroplasts.

Proplastids are the most simple form of plastids and the progenitors of all plastids in the plant's life cycle (Pyke, 1999). These undifferentiated (Marinos, 1967) plastids are small and around 1 μm in diameter (Lancer et al., 1976), having poorly defined internal membranes (Whatley, 1977). Being undifferentiated, they are most often found in tissues at early stages of growth such as seeds, embryo development and meristems. Most studies of proplastids are done in the meristem, where they

differentiate into chloroplasts and leucoplasts during leaf and root development, respectively (Wise, 2006). However, they also have more roles than merely differentiate. Studies of seed germination found proplastids contain high levels of gibberellic acid, a phytohormone stimulating seed germination. This was further supported by the localization of *ent*-kaurene synthases, an enzyme needed for gibberellic acid synthesis (Aach et al., 1997).

Leucoplasts are colorless, non-pigmented plastids that encompass three functionally unique sets of plastids, amyloplasts, elaioplasts, and proteinoplasts (Wise, 2006). Amyloplasts primarily function for starch synthesis and storage (Yu et al., 1998). Like other plastids they are surrounded by a double membrane however their internal membrane structure is reduced in size. During the day, starch is synthesized and stored until nightfall when is it used by the plant for energy (Zeeman et al., 2004). A more long-term version of starch storage in the amyloplast exists in fruit, seeds, and tubers. Another function of amyloplasts is gravity response. Within root columella cells, amyloplast increase starch density to form statoliths, which sediment in response to gravity for plant orientation (Sato et al., 2015). Elaioplast are small, round and primarily function to store oil in droplet-like forms (Wise, 2006). The synthesis of lipid is similar to the prokaryotic fatty acid synthesis pathway. Oil synthesis is important in oil seed plants such as rape seed, but also plays a role in pollen maturation (Hsieh and Huang, 2004; Pacini et al., 1992; Ross et al., 2000; Ting et al., 1998). Hence their abundance in anther tapetal cells during pollen development (Hernández-Pinzón et al., 1999). The least understood and most questionable category of leucoplasts are proteinoplasts. Internally, they are made up of large visible protein inclusions (Bain, 1968; Casadoro and Rascio, 1977; Esau, 1975; Hurkman and Kennedy, 1976; Thomson and Whatley, 1980). They are postulated to function as protein storage in a time when nitrogen is low (Price and Thomson, 1967), but not much research has been done since the 1980s.

Chromoplasts are responsible for the vibrant colors of fruits, flowers, leaves and some roots. These colors come from a family of chemicals called carotenoids, usually in the form of yellow, orange and red (Juneau et al., 2002). The carotenoids are stored in large supermolecular fibril structures. Unlike the other plastids, chromoplasts have an external function and are thought to have evolved to attract pollinators or animals needed for fruit distribution (Deruère et al., 1994). Chromoplasts don't usually arise from proplastids, but tend to come from the differentiation of already existing chloroplast (Bouvier et al., 1998; Ljubesic, 1972).

A gerontoplast is an interesting plastid that is formed by the degradation of chloroplasts in senescing foliar tissue. Even though it is technically dying, it has a distinct biochemical and metabolic signature (Harris and Arnott, 1973; Parthier, 1988). As the leaf proceeds towards complete senescence, grana stacks in the gerontoplast begin to unstack in conjunction with a drop in protein levels, gas exchange decreases, and yellowing of the leaf (Harris and Arnott, 1973). This unstacking event is a slow process, allowing the gerontoplast to remain relatively stable until the very end of senescence (Martinoia et al., 1983; Yamasaki et al., 1996). The exact function of gerontoplasts is still being investigated, but since the plastid contains around 75% of plant protein, this could be a nutrition reservoir for the process of senescence (Peoples and Dalling, 1988).

Etioplasts are plastids that develop from proplastids in the absence of light, in both leaf and stem tissues, but not in roots (Newcomb, 1967). Their existence is a transient form of arrested development towards becoming a chloroplast (Domanskii et al., 2003; Harsányi et al., 2005). Internally they contain an intermediate membrane structure called prolamellar body (PLB) arranged in tetrahedrally-branched tubules (Ellis, 1979; Gunning, 2001; Menke, 1962), along with plastoglobuli, ribosomes, some proteins of PSI, carotenoids, and prochlorophyllide a (Park et al., 2002). Upon exposure to light, etioplasts

differentiate, quickly converting prochlorophyllide a to chlorophyll, allowing for PSI and PSII to be activated within 15 hours and 1 hour respectively (Wellburn and Hampp, 1979).

Of all the plastids, the best characterized plastid is the chloroplast (Rolland et al., 2018), most likely due to its ubiquity and being the primary workhorse for plant energy and essential biochemical synthesis. There are 10 to 100 chloroplasts per cell depending on the tissue and their size ranges from 5 to 10 μm diameter in length and 3 to 4 μm in thickness, having 10 to 100 chloroplasts per cell, depending on the tissue (Lopez-Juez and Pyke, 2004; Waters et al., 2004). A chloroplast is made of four basic compartments: the envelope (outer and inner membrane), stroma, thylakoid membrane, and thylakoid lumen. The outer and inner membranes function to import proteins that have been translated in the cytosol, and importation of small molecules such as phosphorus, carbon dioxide, and water (Rolland et al., 2018). Furthermore the membrane is responsible for sustaining communication via ions, metabolites, proteins, and hormone precursors, between the chloroplast and other compartments of the cell (Rolland et al., 2012). The stroma is analogous to the cytoplasm of the cell. Here the majority of soluble proteins reside and reactions such as Calvin-Benson cycle take place. The thylakoid is made up of a bounding membrane and an enclosed inner area called the lumen. The main function of the thylakoid is for oxygenic photosynthesis (light energy assimilation production of ATP and reduction of redox compounds), and fueling ATPase activity by holding a proton gradient from the cracking of water molecules (Rolland et al., 2018).

Chloroplasts are found in various sizes and numbers in various tissues. Leaves contain various populations of chloroplasts in ground tissue (a large chloroplast with a high photosynthetic activity), epidermal guard cell chloroplast (smaller in size, for support of guard cell function), epidermal pavement cell (leucoplast, possibly degenerate chloroplast, that sometimes contains thylakoid

membranes) (Gutteridge et al., 2018). On top of that, chloroplasts synthesize almost everything that is essential for the production of biomass from vitamins, hormones, starch, sugar, galactolipids, amino acids, photo reduction of nitrogen, biological acquisition of sulfur for synthesis, biosynthesis of fatty acids, the shikimate pathway (phenolic group aromatics), synthesis of purine and pyrimidines bases, synthesis of tetrapyrroles needed for pigments, isoprenoids (terpenoids, steroids, carotenoids), methylerythritol pathway, and the carbohydrate oxidation through oxidative pentose phosphate pathway (Lopez-Juez and Pyke, 2004; Neuhaus and Emes, 2000; Rolland et al., 2018; Waters and Langdale, 2009). As one would suspect with chloroplasts being pervasive in the plant and having numerous roles in development, mutations of chloroplast genes often lead to variegations, aberrant leaf morphology, germination termination and sometimes embryo lethality (Majeran et al., 2012; Myouga et al., 2010; Tiller and Bock, 2014). For instance, mutations in 26 out of 39 tested genes encoding chloroplast ribosome proteins (66%) resulted in embryo lethality (Tiller and Bock, 2014). Similarly, out of the 16 plastid encoded RNA polymerase (PEP) genes tested, mutations in 13 (81%) were found to be lethal or albino (Pfalz and Pfannschmidt, 2013). Thus, many mutations in chloroplast genes, either nuclear or plastid encoded, that result in failure to establish photosynthesis, will result in the halt of chloroplast development, and show most likely albino or lethal phenotype (Savage et al., 2013).

Low Temperature Acclimation in Plants and Plastids

Unlike animals, plants are sessile organisms, which prevents them from moving away from threats, such as abiotic stress. Chloroplasts must respond to stress for both plant growth and development and its survival (Taylor et al., 2009). Abiotic stress is not a single entity, but is multifaceted, encompassing various conditions such as drought, osmotic stress, salt toxicity, low nutrients, toxic metals, high light, and high, low, to freezing temperatures (Bechtold and Field, 2018a).

Although all of these stresses elicit unique responses, but a commonality they all share is the production of reactive oxygen species (ROS). ROS production in chloroplasts is primarily derived from PSII producing superoxide ion ($^1O_2$) and PSI producing hydrogen peroxide (H_2O_2) (Allen, 1995). During normal photosynthetic activity a low level of ROSs are produced, which act as a signal to the nucleus, altering nuclear transcription for the chloroplasts, a process called retrograde signaling (Tripathy and Oelmüller, 2012). This communication maintains homeostasis in the chloroplast. As the chloroplast redox levels change and ROS accumulates, certain metabolites and proteins such as GUN1 send the signal to the nucleus, leading to an increase or decrease in the expression of many genes, which are often part of the photosynthetic machinery (Bobik and Burch-Smith, 2015; Hernández-Verdeja and Strand, 2018; de Souza et al., 2017). Abiotic stress often causes an over-excitation of photosynthesis or a highly reduced state that accumulates $^1O_2$ or H_2O_2, leading to irreversible damage to proteins, DNA, and membranes (Bechtold and Field, 2018a). For the plant, it is important for the chloroplast to maintain a steady state of energy generation and consumption (Suzuki et al., 2012). If they fail to maintain homeostasis, ROSs, like superoxide ion and hydrogen peroxide, can accumulate to such a degree (Miller et al., 2010; Mittler, 2002; Takahashi and Asada, 1988; Takahashi and Murata, 2008) that the chloroplast signals the cell to undergo apoptosis (Laloi and Havaux, 2015). One of the largest contributors and well-studied forms of abiotic stress is low temperate (chilling stress), on which we will focus on here.

One of the largest contributors to agricultural loss is low temperature stress (He et al., 2018; Lukatkin et al., 2012; Olen et al., 2019; Yadav, 2010). This happens at temperatures below 15˚C and above freezing, but can be as high as 20˚C for more sensitive species (Ciarmiello et al., 2011; Theocharis et al., 2012; Wang et al., 2016c). It is also one of the most significant limitations for plant

diversity on earth. This is because low temperature can hinder any point in plant development, from germination to maturity, thus leading to a dramatic shift in plant species diversity where the climate is much cooler (Liu et al., 2018). Signs of cold-sensitivity for plants not suited for low temperature usually are leaf wilting, chlorosis, and necrosis (Ruelland and Zachowski, 2010). To prevent these deleterious effects from occurring, plants need to not only react to environmental stimuli but also to anticipate changes in the environments that may cause them harm (Bechtold and Field, 2018a). Adjustments for low temperature can be a short process or a long process (Goulas et al., 2006). A long term adjustment to the environment, acclimation, is especially important to organisms that are sessile, such as plants (Bechtold and Field, 2018a). Not all plants are capable of doing this. Tropical plants like rice or maize are sensitive to low temperature climates, but cereals and plants like Arabidopsis are cold resistant (Stitt and Hurry, 2002; Wang et al., 2016b).

Most low temperature responses of the plant are activated via the chloroplast (Crosatti et al., 2013), although other mechanisms like the rigidification of plasma membrane also contribute. Together, these sensors lead to the expression of a cascade of cold response genes (COR), that prevent cellular damage and maintain homeostasis under low temperature conditions. A study of the transcriptome of *Arabidopsis* at 13˚C reported the expression of around 8,000 genes, which consequently influence lipid membrane composition (Uemura et al., 2006), osmolyte accumulation, ABA response, cold specific gene pathways (Thomashow, 1999), adjustment of metabolism and adjustment of photosynthesis (Stitt and Hurry, 2002), much of which is to mitigate the production of reactive oxygen species (ROS) accumulation. (Chinnusamy et al., 2010; Provart et al., 2003).

The chloroplast is arguably the primary sensor for the low temperature response(Fernández and Strand, 2008), due to the fact that low temperature has a large effect on photosynthetic activity

(Ensminger et al., 2006). Light is not hindered by low temperature, thus both photophysical and photochemical processes maintain a charge separation that takes place in 10^{-12} to 10^{-15} seconds (Ensminger et al., 2006) for photosynthesis. Unlike light, most enzyme activities and biochemical processes are reduced in low temperature, such as the synthesis of NADPH, ATP, and the Calvin-Benson cycle (Huner et al., 1998). All together this produces an excess of electrons and the accumulation of ROS's, primarily in the form of singlet oxygen species ($^1O_2$) produced by PSII (Fernández and Strand, 2008). Singlet oxygen species ($^1O_2$), along with intermediate carotenoids or the tetrapyrrole intermediate Mg-protoIX, signal the chloroplast and nucleus to adjust to low temperature (Fernández and Strand, 2008; Heidarvand and Maali Amiri, 2010). These signals activate the COR response genes which alter lipid composition of the thylakoid, capture ROS, and result in various other biochemical changes. Lipid composition is important for the chloroplast to function properly, thus changing the lipid composition of thylakoid membrane has consequences to photosynthetic capability (Gombos et al., 1994). During cold temperatures, the thylakoid membrane becomes rigid, reducing the activity of photosynthesis complexes. To combat this various enzymes such as glycerol-3-phosphate acyltransferase (GPAT) increase the unsaturated fatty acid content, allowing the thylakoid membrane to maintain normal fluidity preventing excess photoinhibition (Gombos et al., 1994; Uemura and Steponkus, 1997). To mitigate ROS damage, chemicals and enzymes are produced that capture or scavenge ROS molecules, thus preventing their damage elsewhere. Much of the scavenging is done by antioxidant molecules, such as flavonoids and anthocyanins (Soitamo et al., 2008). Other scavengers are enzymes, like glutathione S-transferases and peroxidases, which convert ROS's into a more stable molecule (Kindgren et al., 2015). In order for these processes to occur, along with the expression of other COR genes, the chloroplast needs to be fully developed. For example, *albino* and *xantha* mutants

in barley, that have plastids unable to complete chloroplast development, have only 11% of the total COR gene expression in response to cold (Svensson et al., 2006). In a similar fashion, light is required to activate a full COR response. In *Arabidopsis*, over-expression of COR gene transcriptions factors, only express 12% of COR genes in response to low temperate in the absence of light, even with fully functional chloroplasts. Many COR genes exist but only those proteins that locate to the chloroplast have a linear correlation to low temperature and frost tolerance (Francia et al., 2004; Houde et al., 1992; Vágújfalvi et al., 2003). This demonstrates chloroplasts are essential for low temperate response.

Evolutionary Comparison of IOJAP Homologs

IOJAP is one of the most widely conserved proteins with an uncharacterized function (Butland et al., 2005). As of 2004, it was ranked in the top-ten for well conserved hypothetical proteins (Soll and Schleiff, 2004) and suggested for prioritization of targets for experimental study (Galperin, 2004). Interestingly, it is excluded from any organism that lacks a ribosome of bacterial origin (Häuser et al., 2012; Wanschers et al., 2012). The main portion of the protein that is conserved is the domain of unknown function 143 (DUF143). *Arabidopsis thaliana* chloroplast IOJAP is more closely related to autotrophic lineages such as cyanobacteria and chloroplast (**Figure 1**). Although chloroplasts and mitochondria both exist in a plant cells, the mitochondrial homologs are farther away in evolutionary relation to chloroplast IOJAPs, most likely due to their two separate ancient lineages. The prevalent nature of IOJAP across life is noticeable, being found in species that live in very difference environments. These environments range from *Zostera marina* (common eel grass) found in the marine environments to *Glaciecola puncie,* a psychrophilic bacterium, found in Antarctic sea-ice habitats. This span of evolutionary time across species could suggest that any conservation of sequence is highly important in both structure and function in a variety of habitats.

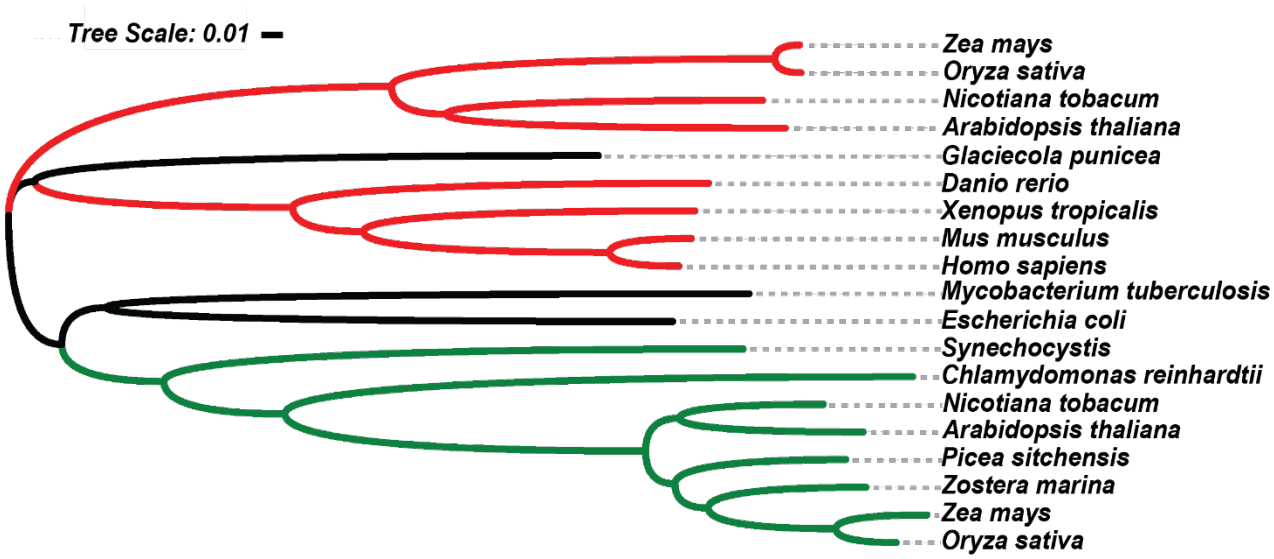

Figure 1: Phylogeny tree of DUF143 domain of IOJAP homologs.

Organisms that contain sequenced IOJAP homolog and represent a small but varied sample across evolutionary relationships to chloroplastic IOJAP in *Arabidopsis*. The tree shows three main clades, mitochondria (red), bacteria (black), and photosynthetic/plastid (green). Organisms that contain mitochondria are the least related to chloroplast IOJAP, compared to bacteria. The phylogenic tree was created by blasting both bacterial IOJAP homolog and *Arabidopsis* chloroplast IOJAP. Full length protein sequences were found using Blast NT (NCBI) downloaded from NCBI. These protein sequences where aligned via MegAlign Pro (DNA Star Inc), and imported into interactive Tree of Life (Letunic and Bork, 2019).

DUF143 structure consists of α1-α2-β-sheet-α3 where the five-stranded beta sheet is sandwiched between the alpha helices (Li et al., 2015). This structural arrangement is found in all the current crystal structure of IOJAP homologs. The alignment of the DUF143 from a broad spectrum of species, along with predicted secondary structures based on homology models with published crystal structures, shows this same pattern (**Figure 2**). All but *G. punicea* maintain the α1-α2-β-sheet-α3 topology. *G. punicea* is a cold-loving bacterium with a shorter sequence than the rest of the species presented. This may be the cause of it breaking the consensus pattern of DUF143, matching every secondary structure beside alpha helix 1 (**Figure 2**). Regardless of *G. punicea* being an outlier, there is still complete conservation of four amino acids among all species presented. Relative to *Arabidopsis* chloroplast IOJAP these amino acids are tryptophan (W195), aspartate (D199), histidine (H206), and arginine (R213). Three of the four of the conserved amino acids are positioned on beta sheets 4 and 5, which along with the other beta sheets interact with ribosome large subunit protein 14 (RPL14) in *M. tuberculosis* (Li et al., 2015). Despite this high conservation in the binding region and common topology of the secondary structures, there is only 21% protein sequence similarity. Nevertheless, DUF143 domain is evolutionarily conserved, being found in a broad spectrum of organisms, and most likely necessary for the function of IOJAP. In vitro, a homolog of IOJAP in *Mycobacterium tuberculosis* was found to dimerize, where much of this interaction happens within the beta-sheet and involves around 15% of its surface area (Li et al., 2015). Earlier investigation into DUF143 found it was related to a nucleotidyltransferase (NTase) superfamily but a closer look revealed that IOJAP homologs did not have the catalytic pocket needed for the transfer of a nucleotide triphosphate (Rorbach et al., 2012). DUF143-encoding genes are single copy genes universally conserved in organisms that have a ribosome of bacterial origin (Sorek et al., 2007). DUF143-encoding genes are single copy genes universally

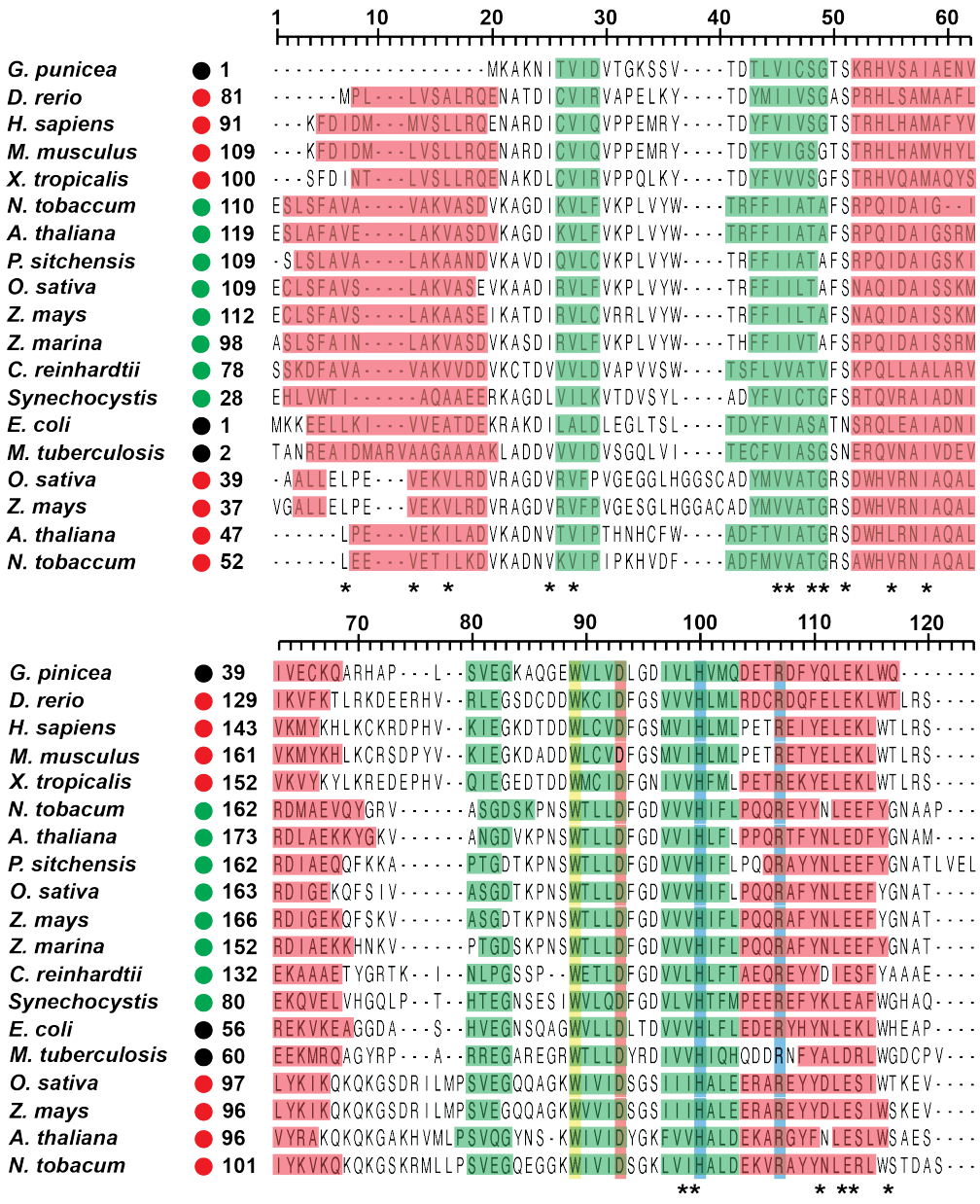

Figure 2: Alignment of DUF143 domain and predicted modeled secondary structure.

The sequence of the DUF143 domain of IOJAP homologs were found using Pfam software (El-Gebali et al., 2019) and then aligned using Megalign Pro (DNASTAR, Inc). The prediction of alpha helices (red) and beta sheets (green) is based on homology models of the given protein with published crystal structures. The features of alpha helixes and beta sheets were overlayed on top of sequences as horizontal rectangles. The vertical bars (yellow, orange, cyan) show conservation among all organisms listed. The dots listed by the organism label represent bacterial (black) mitochondria (red) and chloroplast/autotroph (green). Amino acid number on left and right were calculated using the full-length sequence. Asterisk (*) denotes sequence similarity.

conserved in organisms that have a ribosome of bacterial origin (Sorek et al., 2007). However, in plants there are two copies, one of mitochondrial origin and the other of plastid origin. When comparing *Arabidopsis thaliana* chloroplast IOJAP DUF143 domain's protein sequence to homologs in other species we see high amino acid conservation of *Zea mays* chloroplast IOJAP (73% identity) but very low conservation of both *Zea mays* (25% identity) *Arabidopsis thaliana* (28% identity) mitochondrial versions (**Table 2**). Interestingly, the IOJAP homologs of *Homo sapiens* mitochondria and bacteria are more conserved than those of plant mitochondria, falling in the range of 30% to 40% identity. It is worthy to note that comparing protein sequence relative to conservation of amino acid physiochemical properties, the percent similarity increases on average by 18%, suggesting a conserved physiochemical property that may also be important in IOJAP function. Another feature to note in regard to DUF143, is that bacterial DUF143 homologs have very short termini compared to those found in eukaryotic organelles (**Table 2**). This may suggest co-evolutionary changes for the same function or changes that alter its function. Interestingly, *IOJAP* orthologs have not been found to undergo gene transfer in the prokaryotes (Sorek et al., 2007), thus it is found to be universally a single copy gene (Sorek et al., 2007). IOJAP orthologs in prokaryotes are conserved among α-proteobacteria and cyanobacteria, that gave rise to mitochondria and chloroplast respectively; not only they are similar at the sequence level but also by a similar operon arrangement and neighboring genes. The main components of this conservation are proteins L21 (*rplU*) and ribosomal protein L27 (*rpmA*) (Wanschers et al., 2012).

Although this arrangement is inversed in cyanobacteria, having both genes upstream rather than down stream of *IOJAP* orthologs, this may suggest IOJAP is associated with ribosome assembly or translation for these species. However, this gene arrangement falls apart in eukaryotes, probably due to the mass transfer of mitochondrial and chloroplast genes to the nucleus over the course of evolution.

Table 2: Percent amino acid identity, N- and C-terminal length comparison of IOJAP homologs.

Organism	Organelle	DUF143	DUF143+	N-Term (aa)	C-Term (aa)
Arabidopsis thaliana	**cp**	100%	100%	54	18
Arabidopsis thaliana	mt	28%	48%	19	36
Zea mays	cp	73%	85%	55	15
Zea mays	mt	25%	43%	19	33
Synechococcus pcc 6080	–	39%	58%	31	25
Homo sapiens	mt	31%	47%	31	25
Escherichia coli	–	38%	59%	7	13

Protein alignment of DUF143 domain protein sequences relative to *Arabidopsis thaliana* chloroplast localized IOJAP. Organelle column, chloroplast (cp) and mitochondria (mt). DUF143 column is the percent of identically conserved amino acids relative to *Arabidopsis* chloroplast IOJAP. DUF143+ denotes the protein percent similarity of conserved amino acids with similar physicochemical properties. N-terminus (aa) and C-terminus (aa) denote the amino acid sequence length of the N-terminal domain and C-terminal domain, respectively, outside of the DUF143 domain. Alignment was perform using Clustal Omega (Madeira et al., 2019)

Similarly, both the N-terminal and C-terminal portions of IOJAP are poorly conserved. For one, in prokaryotes the entire protein is primarily made up of DUF143 domain, while eukaryotes have longer N-terminal and C-terminal extensions. When comparing the termini between eukaryotic species, *A. thaliana* IOJAP has 66% and 73% amino acid similarity with *Z. mays* N-terminal and C-terminal sequences, respectively. However, the alignment failed to find any conservation with its mitochondrial counterparts in plants, or homologs in humans or cyanobacteria. This may suggest that the function of the DUF143 domains may be highly conserved, with the N- and C-termini providing additional or a modified function. To better understand the function of IOJAP and any possible differences we must look at studies of homologs in various species.

Primary studies of IOJAP homologs looked at prokaryotes in *Escherichia coli* and *Mycobacterium tuberculosis,* chloroplastic IOJAP in *A. thaliana* and *Z. mays* and human mitochondrial IOJAP. The *E. coli* IOJAP orthologue, ribosomal silencing factor A (RsfA), binds to RPL14, where it is suspected to work as a translational silencer (Häuser et al., 2012). Deletion of Δ*rsfa* causes no morphological changes in either *E. coli* or *M. tuberculosis* (Häuser et al., 2012; Li et al., 2015). As for function, when RsfA is present, there is an increase in both 30S and 50S levels compared to 70S, while in a RsfA knock-out line (Δ*rsfa*), there is an increase of the fully assembled 70S ribosome and a decrease in both 50S and 30S large and small subunits, respectively. The regulation of 70S ribosome formation by RsfA is likely to play a role in amino acid availability homeostasis. When Δ*rsfa* was grown on nutrient rich media (amino acid additives) then transferred to nutrient poor media, the cells went into a premature stationary phase, while WT continued logarithmic growth (Häuser et al., 2012). It was found that the mutant in this early stationary phase translated more protein, relative to WT. Interestingly, both during log and stationary phase RsfA and ribosomal protein mRNA levels remained constant, thus

suggesting the gene regulation on the protein level (Galagan et al., 2010). This was bolstered by the fact that the Δ*rsfa* mutant was unable to form the 100S ribosome, an inactive form of a dimerized 70S ribosome necessary for protein homeostasis (Kijek, 2013; Shcherbakova et al., 2015). Thus RsfA seems to reduce translation by binding to the 50S ribosome to inhibit the formation of the 70S monosome (Häuser et al., 2012). This function was also observed in M. tuberculosis (Li et al., 2015). In fact, introduction of *E. coli* RsfA into *M. tuberculosis* was found to work similarly to native RsfA, suggesting high conservation across prokaryotes (Li et al., 2015). Just like *E. coli*, RsfA of *M. tuberculosis* binds to RPL14 on the 50S ribosome large subunit, which results in lower 70S formation (Li et al., 2015). However, if 70S is already formed, RsfA, even in excess, is unable to disassemble 70S, suggesting it controls translation through free 50S ribosome (Häuser et al., 2012).

Studies of the IOJAP homolog in human mitochondria, *C7orf30*, tell a different story than their prokaryotic counterparts. Knock-down of *C7orf30* shows abnormal mitochondrial network morphology (Rorbach et al., 2012). Reduced levels of C70rf30 resulted in a decrease in protein production, only reaching 60% of that of the control (Rorbach et al., 2012). This resulted in a decrease in the oxygen consumption rate (OCR) of 50% that of the control (Rorbach et al., 2012). The cause of this reduction may be due to a decrease of overall translation of mitochondrially encoded proteins, but it was found that the levels of rRNA and of ribosomal proteins were also reduced (Wanschers 2012, Fung 2013), suggesting a ribosomal assembly malfunction. Obviously, if transcription was also reduced, the translation could also be affected, but mRNA levels of ribosomal proteins and mitochondrial encoded transcripts remained similar to control (Rorbach et al., 2012). The relationship of C7orf30 to translation was bolstered by the binding of C7orf30 to the 39S (50S equivalent) ribosomal large subunit (Rorbach et

al., 2012), more specifically to the ribosomal protein of the large subunit 14 (RPL14) (Häuser et al., 2012).

As noted earlier, deletion of chloroplastic *iojap* in *Z. mays* reduced translation and ribosome availability. This coincided with the binding of IOJAP to the 50S ribosomal large subunit via the RPL14 ribosome (Han and Martienssen, 2001; Han et al., 1993; Häuser et al., 2012). However, it was also noted that the *iojap* mutant had altered chloroplast transcripts, causing transcripts to be larger or under-processed to various degrees (Han et al., 1993). Recently, more research was done in chloroplastic IOJAP using *A. thaliana*. Mutation in *iojap* revealed slight chlorosis in young leaves and cotyledons, which also had reduced F_v/F_m, evidence of low photosynthetic efficiency (Wang et al., 2016a).
It seems likely that IOJAP orthologues play opposing roles in prokaryotes and in eukaryotes. As we see in **Table 3,** deletions of the *iojap* gene have no observable defect on the morphology of prokaryotes, but often cause morphological abnormalities in mitochondria and *Z. mays* chloroplasts (Fung et al., 2013; Shumway and Weier, 1967). Yet, in *Arabidopsis*, the chloroplasts are merely delayed in development, but remain similar to WT in both internal structure and shape (Wang et al., 2016a). Complicating the matter more, in prokaryotes the presence of RsfA (IOJAP homolog) inhibits translation and reduces the formation of the 70S monosome (Häuser et al., 2012; Li et al., 2015). This is in opposition to mitochondria and *Z. mays* chloroplasts where the presence of IOJAP is required for translation and ribosome formation (Fung et al., 2013; Rorbach et al., 2012; Shumway and Weier, 1967; Siemenroth et al., 1980). By contrast, a common feature of IOJAP homologs in maize, mitochondria, and bacteria is the ubiquitous binding of IOJAP to the ribosome large subunit (LSU), thus suggesting a strong correlation to some type translation function. This is further bolstered by the amino acids that interacted with RPL14 in the crystal structure of *M. tuberculosis* RsfA with the 50S subunit (Li et al., 2015). It was

Table 3: Summary of phenotypes of *iojap* in respective homologs.

Organism	Organelle	Morphology	Development	LSU	PEP	TransL	TransX
Z. mays	cp	Abnormal	Halted	Bound	n.t.	None	Abnormal
A. thaliana	cp	Normal	Delayed	n.t.	Interaction	Reduced	Reduced
Homo sapiens	mt	Abnormal	Normal	Bound	n.t.	Reduced	Normal
E. coli	–	Normal	Delayed	Bound	n.t.	Increased	Normal
M. tuberculosis	–	Normal	Normal	Bound	n.t.	Increased	n.t.

Morphology refers to changes in organelle or bacterial shape, either externally or internally. Development refers to any alternations in the organelle or bacteria in development, growth or differentiation. Chloroplast (cp), mitochondria (mt), Ribosomal large subunit (LSU), Plastid encoded RNA polymerase (PEP) of the respected polymerase of the organism, Translation (TransL), Transcription (TransX), Not tested (n.t.).

found that all the five beta sheets interacted with RPL14 but beta sheets 4 and 5 contain three out of the four conserved amino acids across the species analyzed (**Figure 2**). This may suggest that the translational function or at minimum the ligand interaction is highly conserved in *Arabidopsis*.

Unlike in non-plant species which show no detrimental effects in transcription, there was a reduction of transcript levels observed in young *Arabidopsis* leaves (Wang et al., 2016a), suggesting IOJAP may be a part of the chloroplast transcriptional machinery (Wang et al., 2016a). It was shown that the deletion of *iojap* in *Arabidopsis* resulted in a reduction in steady-state chloroplast protein levels in young leaves (Wang et al., 2016a). However, the *iojap* chloroplast protein levels of young leaves were normalized to WT mature leaves instead of young leaves which may have distorted the drop of translation. Although the reduction of translation chloroplast proteins could also have been due to lower mRNA levels, genes with unaffected mRNA abundance also had reduced protein levels (Wang et al., 2016a). Another wrinkle in the argument of IOJAP function is the finding that in *A. thaliana*, IOJAP is found to bind to nucleoid proteins, a compact organized structure of plastid DNA, RNA, ribosomes, and proteins for anchoring, replication and gene expression, (Powikrowska et al., 2014). Some of the components housed in the nucleoids are PEP and PEP associated nucleoid proteins, which were shown to interact with IOJAP (Wang et al., 2016a). But in this study no ribosomal proteins or ribosomal associated proteins were tested for a similar interaction. This is relevant because ribosomes are also involved in nucleoid complexes to translate recently transcribed genes relevant for thylakoid membrane biogenies and maintenance (Liang et al., 2018; Zhang et al., 1999). When DUF143 alone is expressed, having the N-terminal and C-terminal extension truncated, it locates to nucleoid, and is able to complement *iojap* mutant phenotype, however the interaction with PEP nucleoid proteins, like FLN1 is abolished (Wang et al., 2017). This evidence suggests that the conserved interaction of IOJAP with the

ribosome is enough to localize the protein to the nucleoid, but DUF143 alone is not sufficient for this interaction to occur with PEP (Wang et al., 2017). One can speculate that in plants, the extended N- and/or C-termini may be required to facilitate this interaction between IOJAP and PEP nucleoid proteins. This could be an added feature to IOJAP that evolved later, since bacterial IOJAP homologs are primary DUF143 without any N- or C-terminal extensions (**Table 2**). Like *Arabidopsis*, studies in maize reveal that *iojap* chloroplast have abnormal transcripts, both being reduced in amount and unprocessed to their mature form. Yet, these chloroplast also lack ribosomes, which could be the source for mRNA processing defects, and thus is caused by a lack of translational (Han et al., 1993; Shumway and Weier, 1967; Siemenroth et al., 1980; Walbot and Coe, 1979). Either way, the problem addressing the function of IOJAP, particularly in plants, resembles the kind of the chicken or the egg. To ascertain the way forward, it is necessary to understand the translational and transcriptional machinery in higher plant chloroplasts.

Mechanisms of Gene Expression in Plastids

During the endosymbiotic event, an ancient cyanobacterium was engulfed by a proto-eukaryotic cell, which eventually became the plant cell containing a chloroplast we know today. Over evolutionary time, the chloroplast genome shrunk significantly (Timmis et al., 2004), transferring most of its genes to the nucleus while other genes were discarded (Martin et al., 2002). Many of the genes still encoded in the chloroplast resemble those of its ancient prokaryotic ancestor, where the gene expression and genome organization, operon-like structures, and the composition of the protein synthesis machinery remain similar (Zoschke and Bock, 2018). The genome of the plastid contains genes that are vital for the viability of the chloroplast and the plant, for without the chloroplast, the plant's chances of survival are limited. Primarily, the genome is made up of two categories of genes, the photosynthetic components

and the gene expression components. Around half of the photosynthetic components (rbcL, around half of the PSI, PSII, cytochrome b6f complex, ATP synthase) are encoded in the chloroplast, while most of gene expression system (bacterial type RNA polymerase, rRNA, tRNA, and around one third of its ribosomal proteins (Zoschke and Bock, 2018) are encoded in the plastid genome. Although the plastid gene expression machinery has many orthologs to that of its bacterial ancestry, there are a few important differences in translation, ribosome structure, and transcription.

The ribosome of the plastid has a bacterial origin, having a 30S small subunit, 50S large subunit and 70S monosome (Sugiura, 1992). The plastid ribosome consists of a full set of bacterial rRNA: 23S, 16S, and 5S. The 23S rRNA has peptidyl transferase activity, but is broken into 23S + 4.5S (Whitfeld et al., 1978), while 16S is the docking center and is structurally similar to its bacterial counterpart (Maier et al., 2013; Shajani et al., 2011). In fact, the 16S maintains a highly conserved anti-Shine Dalgarno (anti-SD) sequence. Given that there is overall conservation among the plastid and bacterial ribosome, it is no surprise there is similarity in the translation mechanism including initiation, elongation and termination of translation (Millen et al., 2001). For initiation, plastids have orthologs of all the initiation factors bacteria contain (IF1, IF2, and IF3), but also have 2 or more paralogs of IF3 (Nesbit et al., 2015). As mentioned before, the 16S anti-SD sequence is highly conserved, this corresponds to the fact that more than 2/3 of transcripts have SD sequences for translation initiation. The other 1/3 have evolved to rely on other motifs and secondary structures for assistance in detection of the initiation site (Nakagawa et al., 2017; Scharff et al., 2011, 2017). Like their bacterial cousins, plastid ribosomes can translate both unprocessed polycistronic transcripts and processed transcripts (Jackson et al., 2007; Kiel et al., 2007). Even though the pools of unprocessed and processed mRNA are different, the overall efficiency of translation is unaffected (Barkan, 1988; Yukawa et al., 2007).

The plastid ribosome, as a whole, also has high conservation with its bacterial counterpart. As said previously, most of the plastid ribosome proteins have been identified to have bacterial orthologs (Yamaguchi and Subramanian, 2000; Yamaguchi et al., 2000). Additionally, it was found that higher plants have nuclear encoded plastid specific ribosomal proteins (PSRP). In the case of *Arabidopsis*, there have been six PSRPs found, where PSRP2 and PSRP3 bind to the 30S small subunit and PSRP5 and PSRP6 bind to the large ribosome subunit. The others, PSRP1 and PSRP4, associate with the ribosome but are only present under certain stimuli or developmental stages (Sharma et al., 2007, 2010; Yamaguchi and Subramanian, 2000; Yamaguchi et al., 2000). Another feature that separates the bacterial ribosome from the one in plastids is the mass and ratio of protein to rRNA. The plastid ribosome is around 170 kDa and has a lower rRNA mass of 0.4 kDa. This makes the protein to rRNA ratio 2:3 while in *E. coli* it is 1:3 (Zoschke and Bock, 2018). The ratio difference observed is primarily due to many of the ribosome protein orthologs of the plastid having N or C-terminal extensions (Ahmed et al., 2016; Bieri et al., 2017; Graf et al., 2017). This makes the ribosomes of plastids more porous and less densely packed.

Plastid transcriptional machinery also has some similarity to its prokaryotic ancestors, but there are some crucial differences. In bacteria, only one RNA polymerase is used to control transcription while higher plant plastids have two. One is a nuclear encoded plastid RNA polymerase (NEP), made up of a single subunit, and is, as the name implies, encoded in the nucleus. The other is a plastid encoded RNA polymerase (PEP) made up of multiple subunits [(Börner et al., 2014) Chapter 1 pp 3-47]. Because of the two sets of RNA polymerases, the gene expression can be categorized by the promoters which these RNA polymerases recognize, of which there are three classes, class I PEP only, class II NEP and PEP, and class III NEP only genes (Liere et al., 2011).

NEP evolved from a T3/T7 phage type RNA polymerase (Hess and Börner, 1999). Monocots contain RpoTp NEP, which is directed exclusively to the plastid, while dicots also have RpoTmp, which is targeted to both the mitochondria and the plastid (Hess and Börner, 1999; Kühn et al., 2007; Tarasenko et al., 2016). These NEPs recognize genes that contain three promoter types, Ia, Ib, and II, to which no promoter recognition factor has yet been found (Richter et al., 2010). There are a few genes that are specific to NEP in most plant species, which are the *RPO* operon, *ACCD*, and *YCF2* (Pfannschmidt et al., 2015).

PEP's are a prokaryotic type RNA polymerase that is made up of four core proteins, RPOA, RPOB, RPOC and RPOC1 (Hu and Bogorad, 1990; Ohyama et al., 1986; Shinozaki et al., 1986; Sijben-Müller et al., 1986). The genes for the PEP are located in the plastid and are transcribed by NEP. *RPOA* is located near a gene cluster containing ribosomal proteins, while *RPOB*, *RPOC* and *RPOC1* make up their own operon (Barkan, 2011; Börner et al., 2015; Lyska et al., 2013). Together these proteins make up the central core of PEP. Unlike NEPs, PEPs require a nuclear encoded sigma factor to recognize promoter sequences (Link, 1996). These sigma factors are nuclear encoded, and resemble *E. coli* sigma 70 promoters which recognize -35 to -10 consensus sequence elements (Gatenby et al., 1981; Gruissem and Zurawski, 1985; Strittmatter et al., 1985). In *Arabidopsis*, there are six sigma factors, each involved in different gene regulation and developmental stages.

Traditionally, NEPs were thought to transcribe housekeeping genes, while PEPs were assumed to transcribe photosynthetic genes. (Hess et al., 1993; Hübschmann and Börner, 1998; Kapoor et al., 1997; Vera et al., 1996). This was supported by green chloroplasts having PEP transcripts over-represented while NEP transcripts were lower abundance (Hess et al., 1993; Shiina et al., 2005). However, a closer look at promoter sequences revealed that there is no distinct division of labor between the two RNA

polymerases. Most genes have PEP and NEP promoters, but in different frequency (Kapoor et al., 1997; Vera and Sugiura, 1995; Zhelyazkova et al., 2012). However, evidence supports various trends in levels of activity of each RNA polymerase. NEP is more represented in non-green plastids, and during differentiation to chloroplasts. In this case, NEP is primarily responsible for transcription but PEP takes over later in chloroplast development (Baumgartner et al., 1993; Courtois et al., 2007; Emanuel et al., 2004; Hajdukiewicz et al., 1997; Kapoor et al., 1997; Mullet, 1993; Swiatecka-Hagenbruch et al., 2008; Zoschke et al., 2007).

There is some overlap in space when it comes to transcription and translation, and that space is the nucleoid. The nucleoid is an organization of DNA in plastids made up of a complex of RNA, proteins for replication, DNA repair, recombination, transcription, and translation (Krupinska et al., 2013; Liere and Börner, 2013; Melonek et al., 2016; Pfalz and Pfannschmidt, 2013; Sakai et al., 2004). Nucleoids are highly dynamic and undergo extensive remodeling during tissue specific development, biogenesis, proplastid to chloroplast differentiation, and other plastid interconversions (Chi-Ham et al., 2002; Hashimoto, 1985; Kuroiwa, 1991). This is why nucleoids contain differing amounts of the 150 proteins and RNA that have been found there (Majeran et al., 2010; Melonek et al., 2016; Pfalz and Pfannschmidt, 2013). Both transcription and translation take place in the nucleoid, thus both ribosomal proteins and PEP proteins can be found there. Interestingly, there has been no evidence for NEP localization to the nucleoid, even in the proplastids, which is a high activity stage of NEP (Majeran et al., 2010, 2012). Other nucleoid proteins are necessary for the nucleoids response to redox homeostasis, or they anchor DNA, RNA, membrane, or other proteins (Pfalz and Pfannschmidt, 2013; Powikrowska et al., 2014; Savage et al., 2013; Tadini et al., 2016, 2020).

As previously described, IOJAP and its homologs were found to bind to the large subunit of the ribosome (Han and Martienssen, 1995; Häuser et al., 2012; Li et al., 2015; Wanschers et al., 2012), and also affecting translation (Häuser et al., 2012; Li et al., 2015; Rorbach et al., 2012; Siemenroth et al., 1980). However, a study in *Z. mays*, also showed that mutations in *iojap* lead to aberrant transcript levels and processing (Han et al., 1993), suggesting a possible role in transcription. A further study in *Arabidopsis* demonstrated that IOJAP may play a role in plastid encoded RNA polymerase (PEP) regulated transcription. When the *iojap* gene was knocked out, there was a reduction of mRNAs that are transcribed by PEP. PEP transcripts of *RBCL*, *PSAA*, and *PSAB* were somewhat reduced in mature leaves but more strongly reduced in young leaves by a factor of 4 to 10-fold. Additionally, other genes transcribed by plastid nuclear encoded plastid RNA polymerase (NEP), were significantly higher in young leaves, but only by around 30% (Wang et al., 2016a). Evidence for a possible role of IOJAP in transcription was supported by interaction with a nucleoid associated PEP protein, FLN1 (Gilkerson et al., 2012; Wang et al., 2016a). Although not all nucleoid proteins interacted with IOJAP, some other nucleoid proteins do. Nucleoid associated proteins MRL7 and FSD3 interacted with IOJAP, but failed to interact when only the DUF143 was expressed without the N- or C-terminal sequences (Wang et al., 2017). Thus, the driving factor for this interaction does not appear to be the DUF143 conserved domain, but rather one of the termini.

Like PEP, IOJAP is also found to locate to the nucleoid, while the presence of nucleoid bound NEP has not been observed (Liere et al., 2011). Additionally, IOJAP was found in low quantities in the nucleoid at all stages of development, from proplastids to mature chloroplasts using mass spectrometry on isolated nucleoids (Majeran et al., 2012). Since, IOJAP is found in the nucleoid, and interacts with

PEP associated nucleoid proteins (Wang et al., 2017), any possible role it has in transcription mostly likely involves PEP and not NEP.

All these elements of gene expression demonstrate various layers for regulation with regard to development and adjustment to environmental stimuli. In plants, plastid gene expression regulation has limited influence on transcription with most of the regulatory control taking place post-transcriptionally or translationally (Barkan, 2011; Sun and Zerges, 2015a). Relative translational outputs are adjusted during developmental transitions so that the relative stoichiometric amounts of proteins for a given complex are constant (Chotewutmontri and Barkan, 2016). Land plants such as *Arabidopsis* and tobacco showed higher regulations of translation output rather than a change in transcripts, when compared to *Chlamydomonas* to (Trösch et al., 2018).

In plants, mutations of *iojap* result in variegation that results from chloroplast arrest (Jenkins, 1924; Shumway and Weier, 1967), or delayed development (Wang et al., 2016a). The cause of the variegation is still unknown, and further confusion is driven by the fact that some white tissues contain healthy green chloroplasts (Coe et al., 1988; Shumway and Weier, 1967), a phenomenon known as heteroplastidicity. The function of IOJAP in prokaryotes and human mitochondria is suggested to regulated translation (Häuser et al., 2012; Li et al., 2015) and ribosome assembly (Rorbach et al., 2012), respectively. Compared to its homologs the understanding of the function of IOJAP in plants less well developed. Studies in *Z. mays* suggest that it functions in plastid translation, since *iojap* chloroplasts (white) are unable to synthesize plastid-encoded protein (Siemenroth et al., 1980; Walbot and Coe, 1979) and lack ribosomes (Shumway and Weier, 1967). On the other hand in *A. thaliana,* there is evidence that suggests IOJAP plays a role in transcription, showing interaction with PEP nucleoid proteins (Wang et al., 2016a, 2017). Yet in *Z. mays* mutations in *iojap* also lead to aberration in mRNA

processing (Han et al., 1993), while in *A. thaliana* translations of plastid-encoded protein were also altered (Wang et al., 2016a). The primary component of IOJAP function is thought to be the conserved DUF143 domain. This domain was shown to be necessary to bind to the plastid ribosome protein L14 (PRPL14) of the large 50S subunit in prokaryotes (Häuser et al., 2012; Li et al., 2015), human mitochondria (Wanschers et al., 2012) and *Z. mays* (Han and Martienssen, 1995). Furthermore, mutations in PRPL14 resulted in a similar phenotype as *iojap* mutants (Fung et al., 2013; Häuser et al., 2012). The importance of the DUF143 domain comes up in an amino acid mutations study. Wang et al (2017), aligned IOJAP homologs from *Z. mays*, *E. coli*, *Saccharomyces cerevisiae*, human mitochondria and *A. thaliana*, and found 8 highly conserved amino acids. Single site alanine substitutions on *A. thaliana* IOJAP, D138, I156 and S161 (N-terminal portion of DUF143), resulted in a WT phenotype, while a truncation of amino acids 193 to 217 (C-terminal region of DUF143) mimic knock-out phenotype. Surprisingly, this region contains the only highly conserved amino acids W, D, H and R when a more extensive alignment is performed (**Figure 2**). This may imply that the binding of DUF143 to PRPL14 remains and thus functions in translation. Yet, IOJAP may have a duality, given by its N- and C-terminal extensions, shown by its location to the nucleoid and integration with PEP nucleoid associated protein that requires these extensions (Wang et al., 2016a, 2017).

From 1924 to 2001 there was extensive work on the characterization of *iojap* phenotype and inquiry into IOJAP's function in *Z. mays*, and only until 2012 was more work on IOJAP, mainly in non-plant systems. Even with the recent studies performed in *A. thaliana* there is still much that is unknown in plants. For one, unlike in *Z. mays*, phenotypes of *iojap,* in *Arabidopsis* they are subtle, only effecting modest delay in chloroplast development in young developing leaves (Wang et al., 2016a). However, we still don't know the ramification of this delay. Does delay in chloroplast development systemically

affect plant growth, size, bolting time, root growth, skotomorphogenesis, and other processes? Also, unlike the *Z. mays*, which is chilling sensitive, *A. thaliana* acclimates to temperate environments. On top of this, the chloroplast is sensitive to low temperature and other abiotic stresses, thus begging the question whether delayed chloroplast development is more susceptible to abiotic stresses, especially in young leaf tissue. Furthermore, there is substantially more evidence from non-plant systems, and *Z. mays*, that IOJAP functions in some process of translation, yet in *A. thaliana* some evidence suggests a duality of function, in both translation and transcription. Here I will further characterize the phenotype of *iojap* mutants in *A. thaliana* in several plant tissues and physiological processes, during response to abiotic stress, and attempt to decipher whether IOJAP is involved in transcription or translation.

CHAPTER TWO
PHENOTYPE CHARACTERIZATION OF *IOJAP* MUTANT IN *ARABIDOPSIS THALIANA*

Introduction

The model plant *Arabidopsis thaliana* has well characterized phenotypes in all aspects of anatomy, development, and under various conditions. This is useful when characterizing the unknown effects of genetic mutations, such as *iojap.* Additionally, *Arabidopsis* offers another trait that is beneficial to this study, which is the ability to acclimate to low temperature (Gilmour et al., 1988). In this chapter, I characterized the main phenotypic changes from mutations in *iojap.* These macroscopic scale observations of rosette size, shoot and leaf morphology, root length, and some basic physiological processes such as germination and skotomorphogenesis were recorded at normal temperature (22˚C) and under low temperature conditions (12˚C and 4˚C).

Plant growth and development is influenced by the chloroplast as a result of its myriad of functions such as amino acid and lipid biosynthesis, and essential metabolite production (Pogson et al., 2015). The shoot, the photosynthetically active tissues of the plant, is comprised of hypocotyl, stem, and leaves. One of the main functions of the chloroplast is to provide energy in the form of sugars to sustain shoot growth and accumulate biomass (Van Dingenen et al., 2016). Often, impairment of the chloroplast or inability of proplastids to differentiate into the chloroplast reduces plant growth or alters flowering time (Albrecht et al., 2006). In maize, mutations in *iojap* lead to various alternations in shoot and leaves such as smaller and narrower leaves, and overall reduced height in many variants. These phenotypes of *iojap* maize remained throughout the life of the plant, and were not altered in growing temperatures of 25˚C to 15˚C (Coe et al., 1988). Maize optimal growing temperatures span the range of 21˚C to 27˚C,

having detrimental effects below 20˚C (Greaves, 1996). This suggests that the phenotype was relatively stable and resilient through slightly different, suboptimal environmental conditions.

Another large and important part of the plant is the root system. The main function of the root is to collect water and nutrients and deliver them to the rest of the plant. Since the roots contain mostly non-photosynthetic plastids, such as leucoplasts, they rely on the shoot to supply energy for their growth (Kobayashi et al., 2012). During the day, the shoot accumulates energy in the form of starch and sugar, that then can be supplied to the root (Kobayashi et al., 2012; Stitt and Zeeman, 2012). Thus, many mutants that affect chloroplast development or production of energy, also affect the root growth. An example of this is a mutation in the gene encoding plastid ribosomal protein of the small subunit 17 (*prps17*), which results in reduced photosynthetic efficiency, which coincided with a reduction of primary root length (Nakata et al., 2018). Likewise, the shoot abnormalities caused by *iojap, Z. mays* variegation (Coe et al., 1988; Jenkins, 1924) and chlorosis in young leaves in *Arabidopsis* (Wang et al., 2016a), may result in deleterious root effects. Yet, the effects on the roots in both plant systems have not been tested. Here we investigate whether mutations in *iojap* hinder root growth.

Plastids play an important role in leaf development. As soon as the leaf primordium forms, proplastids begin to differentiate into chloroplasts. Once matured, the chloroplasts divide in synchronous fashion with division of cells (Charuvi et al., 2012; Nelissen et al., 2016; Pyke and Leech, 1994; Sun and Zerges, 2015b). During this developmental transition from proplastids to chloroplast and dividing cells to mature leaf, there is an extensive interconnected regulatory network between the nucleus and the plastid, where transcription and translation are tightly controlled to allow proper execution of photosynthesis and biosynthesis (Nelissen et al., 2016). This delicate balance is often altered by mutations that affect chloroplast development, photosynthesis or other essential chloroplast functions.

Many of those mutations are lethal but many result in virescent or variegated leaves (Myouga et al., 2010; Pogorelko et al., 2016; Yu et al., 2007). Variegation is categorized as green and white (yellow) tissue, containing populations of heteroplastidic (healthy and unhealthy chloroplast) cells (Yu et al., 2007). In *Z. mays iojap* mutants, leaf variegation is displayed as white and green stripes. Unlike in maize, variegation in *Arabidopsis* leads to a random pattern of patches of various size (Aluru et al., 2006; Pogorelko et al., 2016; Yu et al., 2007). However, in standard growth conditions the mutation of *iojap* does not elicit variegation, but leads subtle chlorosis in the proximal end of young leaves (Wang et al., 2016a).

Skotomorphogenesis (etiolation) occurs when a plant grows from germination in darkness, which happens when a seed is beneath the soil. During that time, the primary allocation of energy from the endosperm is concentrated to the elongation to the hypocotyl, in order for the plant to reach the surface and be exposed to light (Josse and Halliday, 2008; Sinclair et al., 2017). Plastids in the hypocotyl are leucoplasts that are not photosynthetically active, and don't play a central role during skotomorphogenesis.

Plastids affect germination in two ways. First, establishment of the embryo, and second during the germination process (Hsu et al., 2010). During embryogenesis the plastids begins as proplastids then differentiate into chloroplasts in order to provide energy for the future seed, and accumulate protective metabolites (raffinose, non-amino acid GABA, Late Embryogenesis Associated proteins) to survive desiccation (Angelovici et al., 2010; Goldberg et al., 1994). Once this is accomplished the chloroplast itself reverts back to a proplastid state, to survive the desiccation process of seed maturation (Mansfield and Briarty, 1991). For this process to occur about one third of the genes are plastid related (Hsu et al., 2010; Meinke et al., 2008). During germination the plastid differentiates back to the chloroplast, which

is required for successful germination. Thus many mutations that hinders or halts chloroplast development during germination lead to germination defects (Hsu et al., 2010; Meinke, 2020; Pogson et al., 2015; Savage et al., 2013). Many of the essential genes are required for the transcriptional and translational machinery (Majeran et al., 2012; Meinke, 2020; Meinke et al., 2008; Pfalz and Pfannschmidt, 2013; Savage et al., 2013; Tiller and Bock, 2014). This correlated with a rapid increase in NEP-dependent transcripts such as ribosomal proteins during germination (Demarsy et al., 2012; Tadini et al., 2020). This may explain why, in *Z. mays iojap* mutants have a high rate of seed abortions and low germination percentages of around 50 to 20 percent, respectively (Coe et al., 1982, 1988). Here I more fully characterized the *iojap* mutant phenotype in *A. thaliana* at both optimal (22˚C) and low temperatures (12˚C and 4˚C).

Methods

Plant growth conditions: All seeds were passed through sieves, only using seeds greater than or equal to 250 µM. Seeds of WT (Col-0), *ijT1* (this study), *ijT2* (SALK_121803.40.80.x), *ijT3* (SALKseq_053017.1) were sterilized in a bleach (30% v/v), triton-x100 (0.1% v/v) solution for 8 minutes on a rotator, then rinsed 5 times in sterile deionized distilled water under a sterile hood. Seeds were either left submerged in water, stratified at 4˚C for 2 days, then transferred to a plate. Standard media was Murashige and Skoog Basal Salt Mixture ½ strength (Sigma), 1% sucrose (Fisher), 0.5% Phytagel™(Sigma), pH5.8 and sterilized by autoclaving. Seeds were germinated and grown at 22˚C in long day conditions (16 h light/8 h dark) at 100 $\mu E \cdot m^{-2} \cdot s^{-1}$ illumination. Standard media and temperature were used unless otherwise stated.

Statistical Analysis: All statistical analysis was carried out using Graphpad Prism (v8). For histograms, One-Way ANOVA for multiple comparison between mean of each columns was used including a

Tukey's correction. Scatter plots were analyzed against a WT reference via a Two-Way ANOVA multiple comparison within each row, comparing the column, with a Dunnett correction. Scatterplot analysis compares all genotypes (not displayed in figures), using a Two-Way ANOVA multiple comparison within each row comparing the column, with a Tukey correction was used. ($p < 0.05$).

Thermal asymmetric interlaced polymerase chain reaction: DNA was extracted from cold-sensitive mutant using an in-house DNA extraction protocol. Three to four leaves were placed in a microfuge tube (1.5 mL, Fisher), and homogenized with 400 µL of DNA extraction buffer (200mM tris(hydroxymethyl)aminomethane hydrochloride, pH 8.0; 250mM NaCl; 25mM Ethylenediaminetetraacetic acid, pH 8.0; 0.5% w/v sodium dodecyl sulfate). Samples were heated for 5 minutes at 95˚C, then spun down at maximal speed for 10 minutes at room temperature using a bench top centrifuge. The supernatant was transferred to a new microfuge tube, and the same volume of 100% isopropanol (Fisher) was added and incubated for 15 minutes at room temperature. The samples were centrifuged at maximal speed for 15 minutes, the supernatant was decanted, and the pellet was washed twice with 70% ethanol. The pellet was allowed to dry at room temperature, then resuspend in sterile distilled water, and stored at -20˚C. Thermal asymmetric interlaced (TAIL) PCR protocol was taken from (Liu et al., 1995), using ambiguous primers AD1 and AD2 (see primer list in 'Appendix'), and nested primers. Electrophoresis of the primary, secondary and tertiary reactions were done on 1% agarose gel, in TAE buffer. The most prominent band was excised using the Wizard® SV Gel and PCR Clean-Up System (Promega), then sequenced via UT Genomics Core sequencing lab (https://dna.utk.edu/). This was completed sequentially for a total of three TAIL-PCR reactions, having three distinct nested primers sets, giving three products. Sequences were analyzed using SeqBuilder Pro (DNASTAR, Inc) and verified their source via nucleotide blast provided by National Center for

Biotechnology Information. The adjacent gene of the T-DNA insert was further verified by PCR genotyping, using primers sets that flanked both the right and left borders (see primer list **Table 10** in 'Appendix').

Root Length Measurements: Stratified seeds of WT, *ijT1*, and *ijT2* were grown on square grid plates (100 x 15 mm, Fisher) containing standard media. For 22˚C, stratified seeds were placed along the top-most gridline, in groups of 6 to 7 seeds per genotype. For 12˚C and 4˚C conditions, seeds were plated on the top grid and middle grid line. Plates were wrapped in parafilm and placed vertically at 22˚C for 2 days to germinate, then moved to their respective temperatures. Whole plate images were taken using a camera stand with an attached Canon Rebel XS camera (55 mm lens) every day for 12 days for 22˚C or 17 days for 12˚C, while 4˚C plants were imaged every 4 days for 72 days. To measure primary root length, the segmented line tool in ImageJ was used to trace the primary root from the shoot-root node to the end of the root cap. Statistical analysis in GraphPad Prism (v.8) was used to compare the average primary root length by Two-Way ANOVA with Dunnett's correction, comparing each colum mean to WT column mean, and Tukey's correction comparing each mean to every other mean. Three replicates were completed, each having a sample size of N=12 to 14 with $p<0.05$.

Rosette Radius: Seeds were germinated and grown on standard media plates vertically for 4 days at 22˚C. One seedling of each genotype was transferred to the center of a pot (top 3 in^2, height 2.5 in, bottom 2.2 in^2), packed lightly with germination soil (Fafard Superfine Germination Mix, by SunGro Horticulture, Agawam, MA). Each pot was placed in a tray, making 8 pots per genotype, and one tray for each temperature of 22˚C, 12˚C, and 4˚C. After transferring to soil, the tray was covered with a plastic dome, incubated at 22˚C under long day conditions (16 hours day, 8 hours night) for one day. Afterward, each tray was transferred to its respective temperature, under long day conditions. Whole

plant images were taken using a camera stand with an attached Canon Rebel XS camera (55 mm lens) at bolting. To measure rosette radius, the line tool in ImageJ was used to trace the three longest leaves from the center of the rosette to the tip of the leaf to produce an average radius for each plant. Although three leaves were measured, each plant counted as one sample. One-Way ANOVA with Tukey's correction, comparing each column mean to mean of every other column. Three replicates were completed, each having a sample size of N=6 to 8 with $p<0.05$.

Leaf Morphology: Stratified seeds of WT, *ijT1*, and *ijT2* were grown on square grid plates (100 x 15 mm, Fisher) containing standard media. Each grid contained one seed at its center, having six seeds total, per genotype, per plate. The plates were incubated at 22˚C in long day conditions (16 hours day, 8 hours night) for two days, then transferred to their respective temperature of 22˚C, 12˚C and 4˚C. Once the first or second true leaf reached around 3 to 4 mm in length (from shoot apical meristem to leaf tip), images were taken using a Zeiss stereoscope with an attached Canon Rebel XS camera. All images were taken at 20 times magnification. Three replicates were completed, each having a sample size of N=8.

Hypocotyl Length: Stratified seeds of WT, *ijT1*, and *ijT2* were grown on square grid plates (100 x 15 mm, Fisher) containing standard media. Plates were divided into 4 sections, in which 3 sections contained eight 13 x 13 mm square grids, and one section contained twelve grids. Around 36 seeds were placed in each section of the plate. The plates were then illuminated (100 µE) for four hours at 22˚C. Afterward, each plate was covered in aluminum foil, and placed vertically in their respective temperature of 22˚C, 12˚C or 4˚C. Plates were imaged 3, 4 and 5 days after illumination for 22˚C, 12˚C, and 4˚C respectively. Whole plate images were taken using a camera stand with an attached Canon Rebel XS camera (55 mm lens). To measure hypocotyl length the segmented line tool in ImageJ was used to trace from the shoot-root node to the end of the cotyledon. Statistical analysis in GraphPad Prism

(v.8) was used to compare the average hypocotyl length by One-Way ANOVA with Tukey's correction, comparing each column mean to mean of every other column. Three replicates were completed, each having a sample size of N=36 with $p<0.05$.

Germination: Stratified seeds of WT, *ijT1*, and *ijT2* were grown on square grid plates (100 x 15 mm, Fisher) containing standard media. Plates were divided into 4 sections, in which 3 sections contained eight 13 x 13 mm square grids, and one section contained twelve grids. Around 50 seeds were placed in each section of the plate. The plates were placed vertically in their respective temperature of 22˚C, 12˚C or 4˚C. Plates were imaged after WT seedling cotyledons emerged. Whole plate images were taken using a camera stand with an attached Canon Rebel XS camera (55 mm lens). The seeds were counted using the counting tool in ImageJ then the percentage germinated was calculated. Five replicates were completed and the average percentage germination for each genotype for their respective temperature was calculated, each having 50 seeds per replicate. Statistical analysis in GraphPad Prism (v.8) was used to compare the average hypocotyl length by Two-Way ANOVA with Tukey's correction, comparing mean within each row with the means in the respective column, N=5 with $p<0.05$.

Cloning of IOJAP tagged constructs: Two Gene Entry Clone plasmids were ordered through TAIR, GEC-C-3xMyc (Fu48) and GEC-C-CFP (Fu44) which have a C-terminal 3x Myc tag and C-terminal Cerulean Fluorescent Protein tag (Wang et al., 2013). Cultures of DB3.1 *E. coli* containing the vectors were inoculated in sterile LB liquid cultures plus 34 µg/ml chloramphenicol and incubated for 10 to 16 hours at 37˚C with shaking in a 50 mL Falcon® tube. Plasmids were then isolated following the Zyppy™ Plasmid Miniprep Kit instructions.

Primers to amplify the insert for GEC-C-3xMyc consisted of GW-cpij-CL-F1 and GW-cpIJ-CL-R, having restriction enzymes SpeI-HF (New England Bio Labs) and EcoRI-HF (New England Bio

Labs), respectively, on the 5' end of the primer. While the primers for the insert into GEC-C-CFP GW-cpIJ-CL-F and GW-cpIJ-CL-R, having restriction enzymes XhoI (New England Bio Labs) and EcoRI-HF (New England Bio Labs), respectively on their 5' ends. Genomic DNA was extracted from WT (Col-0) *Arabidopsis thaliana*, to serve as the templated for insert amplification using Phusion PCR (New England Bio Labs). Inserts where separated via electrophoresis (see Electrophoresis Method) with the addition of guanosine (1 mM) to the gel and buffer. The inserts were excised out of the gel and purified using Wizard® SV Gel and PCR Clean-Up System (Promega), and stored at 4˚C.

Restriction enzyme reactions were set up for both the plasmids and the inserts following the instruction provided by the manufacturer. Digests of the products were then purified using Wizard® SV Gel and PCR Clean-Up System (Promega), and ligated with the appropriate plasmids using T4 DNA Ligase (New England Bio Lab) on a four cycle temperature gradient of of 4˚C, 6˚C, 8˚C, 10˚C 12˚C, and 16˚C, for 1 hour at each temperature. Ligase mixture was then used to transform TOP10 cell through heat shock transformation protocol (http://nebenfuehrlab.utk.edu/prot/E-coli-Transformation.pdf). Transformed *E. coli* were inoculated on LB chloramphenicol plates and incubated at 37˚C for 10 to 16 hours. Positive transformation was verified via colony PCR, then cultured in liquid LB plus 34 μg/mL chloramphenicol.

Plasmids of GEC-IOJAP-3xMyc, GEC-IOJAP-CFP and Early Gate pEG100 were isolated from overnight cultures using Zyppy™ Plasmid Miniprep Kit. Each GEC plasmid was the used in a 1 to 1 ratio with pEG100 LR reaction using Clonase (New England Bio Lab), following manufactures instructions. LR reaction solutions were then used to transform TOP10 *E. coli* cells through heat shock transformation. Transformed cultures were plated on LB selection plates containing 50 μg/mL kanamycin and incubated for 10 to 16 hours at 37˚C. Positive transformed colonies were verified via

colony PCR, then inoculated in liquid LB kanamycin selective media at 37˚C, shaking for 10 to 16 hours. Transformed cultures of pEG-iojap-3xMyc and pEG-iojap-CFP were isolated and transformed in *Agrobacterium tumefaciens* (GV3101) using BioRad Gene Pulser-Xcell following lab-based protocol (http://nebenfuehrlab.utk.edu/prot/Agrobacterium-Transformation.pdf). Transformed *Agrobacterium* were inoculated on YEP selection plates contain 50 µg/mL kanamycin and incubated for two days at 27˚C. Positive colonies were verified by colony PCR, then cultured in liquid YEP kanamycin selection media, to incubate at 27˚C for another two days. Cultures were stored at 4˚C, until further use.

Making of complement transgenic lines: *ijT1* plants were grown in soil in optimal conditions until there were two to three inflorescences with around ten siliques. All the siliques were removed the night before transformations. Additionally, transformed *Agrobacterium* culture containing the pEG100-iojap-CFP and pEG100-iojap-3xMyc plasmids were transferred from YEP to LB liquid media and incubated at 27˚C with shaking, the night before so that the O.D. was greater than 0.6 and to induce virulence. The cultures were spun down in a fixed-angle rotor using an Optima XE centrifuge (Beckman-Coulter), at 5000xg for 5 minutes, decanted and washed gently with chilled water twice. Pellets were resuspended in 'Dipping Solution' (Sucrose 5% w/v, Benzylaminopurine 44 nM, and pH of 6) and kept on ice. At the point of use, silwet L-77 was added to make a 0.05% v/v solution. Using a 1000 µL pipette, the agrobacterium dipping solution mixture was dripped onto every flower or bud. Plants were then placed under a dome and incubated at optimal temperature for an hour. Excess *Agrobacterium* dipping solution was removed by gently shaking followed by water spray bottle mister. Afterward, the plants were incubated under a dome for 16 hours, then the dome was removed. The flower inoculation process was repeated 7 days after first inoculation for old and new flowers. Seeds were harvested when the shoot was

golden brown. Seeds were then filtered through a wire sieve of 300 μm (Fisher), then dried in 1.5 mL Eppendorf tube for 1 week at room temperature.

Phenotypic selection of complement transgenic lines: T1 seeds were surface sterilized, and plated on standard media, and stratified at 4˚C in for 2 days, around 200 seeds per plate. The plates were placed horizontally at 22˚C in long day conditions (16 hours light, 8 hours dark), then transferred to 12˚C until four true leaves formed, where the fourth leaf was > 3 mm in length. Seedlings where the low temperature phenotype was absent, were transferred to soil, and grown in optimal conditions. Genomic DNA was isolated from 1 to 2 leaves from each plant and genotyped to verify a positive transformant. These plants were then grown until ready for harvest, making homozygous T2 seeds containing either 35S-IOJAP-CFP in an *ijT2* background or 35S-iojap-3xMyc in an *ijT1* background.

Confocal microscopy of transiently expressed IOJAP-CFP in *Nicotiana benthamiana*:

Nicotiana benthamiana plants were grown in soil in the same conditions as *Arabidopsis*, for about 3 weeks or until 4 leaves were longer than 4 cm. Agrobacterium were cultured that contained plasmids pEG100-iojap-CFP, pAN363 (prSSU-YFP), or pAN159 (cox-YFP), which are C-terminally tagged iojap to cerulean fluorescent protein, plastid and mitochondrial markers fused to a yellow fluorescent protein. Cultures were grown in YEP liquid media until an O.D. of > 0.8. Cultures were then centrifuged as described before and washed gently twice with chilled water. Each culture was resuspended in transient expression media (sucrose 5% w/v, 6-Benzylaminopurine 10 μg/mL, acetosyringone 100 μM, and silwet L-77 0.02% v/v). Culture containing pEG100-iojap-CFP was mixed with either pAN363 (prSSU-YFP) or pAN159 (cox-YFP) culture in a 1 to 1 ratio. A scalpel was used to place a small nick at the abaxial side of the leaf, then using a 3 mL syringe, the bacterial solution was injected into the leaf. All four leaves were used, and each combination was used to inoculated two plants. Plants were then incubated

for 1 to 2 days. Multiple 1x1 cm cuts were taken from each leaf, placed between a glass slide and a cover slip, filling any void space with water. Samples were then view using a Leica SP8 White Laser Confocal System.

Results

A T-DNA insertion line in the myosin *XIK* gene, *kt5**, had a cold-sensitive phenotype of short roots at 12˚C, while other myosin *xik* mutant alleles did not show this defect (data not shown). A backcross to WT allowed us to separate the *kt5* insertion having an *xik* typical phenotype of short root hairs from the cold sensitivity phenotype (suspected secondary mutation) observed in *kt5**. Of those seedlings containing short roots at 12˚C, but normal length root hairs, a genotype analysis was done, and no T-DNA was found in the location of *kt5* within the myosin *XIK* gene. In order to find the mutation, which was presumed to be a secondary T-DNA insertion, thermal asymmetric interlaced (TAIL) PCR (Liu *et al*, 1995), was performed.

The procedure of TAIL-PCR described in Liu *et al* (1995) was followed, using LBa1 for the primary reaction and LBb1 for the secondary and tertiary reaction as specific primers located near the left border of the T-DNA. For the arbitrary degenerate primer, we used AD2 described in Lui *et al* 2010. The product of the tertiary reaction was excised from electrophoresis gel, purified and sequenced. Analysis of the first TAIL-PCR product (1’’’) sequencing results showed the product was made up of T-DNA and the flanking region of the binary vector, with a length of 500 base pairs (**Figure 3A**). Three new nested specific primers were made (SP1, SP2.2, and Sp2.1) and reactions were run using AD1. Second TAIL-PCR product (2’’’) was approximately 1.5 Kb but only contained the sequence of the N-region (**Figure**

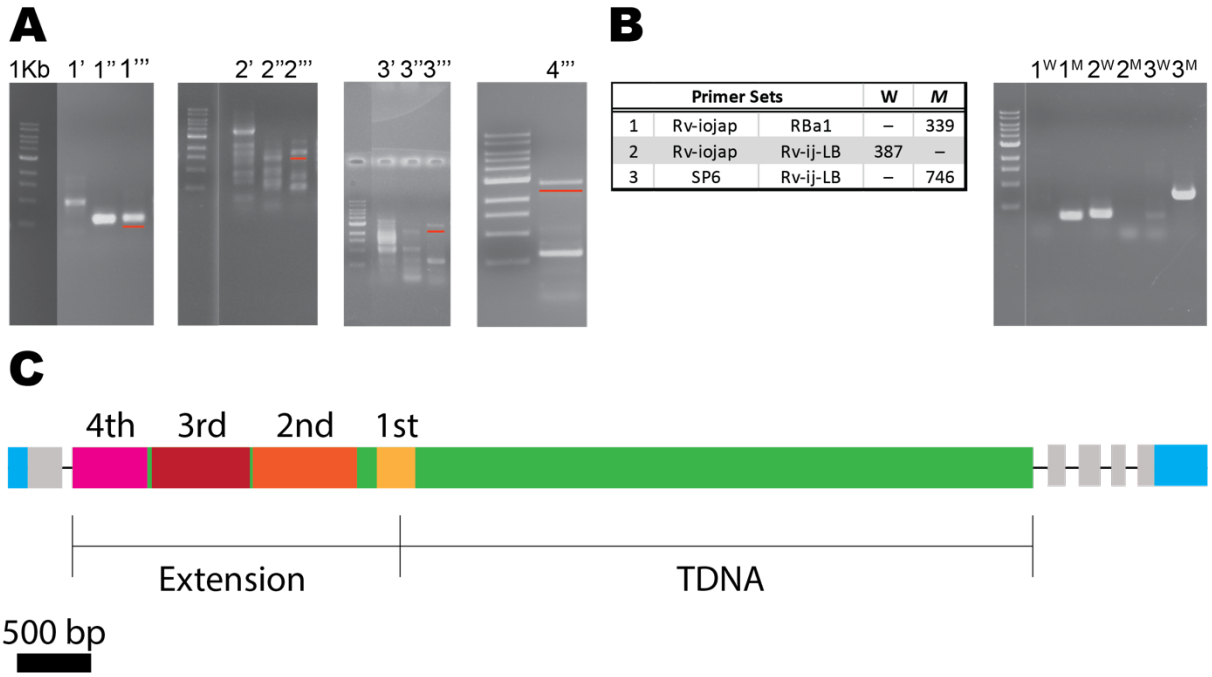

Figure 3: Secondary mutation verification through TAIL-PCR.

A) TAIL PCR products, 1, 2, 3, and 4 denote first, second, third, and fourth reactions. For each reaction there were three sequential reactions, primary (N'), secondary (N''), and tertiary (N'''). TAIL-PCR reactions 1''', 2''', 3''' of 500 bp, 1.5 kb, and 3.0 kb were sequenced, while 4''' (same as 3''') was re-sequenced using a primer more downstream. Red bar denoted excised band. B) Genotyping of WT (W) and isolated homozygous secondary mutation (M), were amplified using PCR primers sets, 1, 2, and 3. C) Schematic T-DNA insert in first intron of *IOJAP* (At3g12930), named *ijT1*. 5'-UTR and 3'-UTR (cyan), exons (gray), introns (black line), T-DNA insertion and binary vector extension (green), sequenced TAIL-PCR products first (yellow), second (orange), third (red), and fourth (magenta). Scale bar 500 bp (black).

3A). Again, three specific primers were made and along with AD2, produced the third TAIL-PCR product, with the reaction of 3''' having a band of 3 kb (**Figure 3A**). The sequencing results of this isolated band showed more of the N-region. Since the sequencing limitation is around 1.5 kb, I designed one more specific primer (SP6) and used that for sequencing fourth TAIL-PCR product (4''') (**Figure A**). Sequencing results showed the product contained the binary vector sequence and the start of the flanking genomic DNA. The flanking genomic DNA sequence was compared to sequences in GenBank using nucleotide BLASR (NCBI), resulting in a match to At3g12930, iojap-like protein.

The total insertion was approximately 4.5 Kb in length, having 2.3 Kb of the T-DNA insert and 1.2 Kb binary vector flanking the T-DNA sequence (insertion extension). This large insertion was found to be located in the first intron of the *iojap* gene, but to verify this, two primer sets were made for the suspected gene, flanking each side of the T-DNA extended insertion (**Figure 3B**). Genotyping primer set 1, Rv-iojap and RBa1 for the right boarder was expected to not produce a band for WT, but to have a band for the mutation, at 339 bp. Likewise, the expected bands for primer sets, 2 (Rv-iojap and Rv-ij-LB) and 3 (SP6 and Rv-ij-LB) also were observed, further verifying that the T-DNA insertion was located in the first intron of iojap gene At3g12930. This mutant allele will be referred to as *ijT1* for first T-DNA insertion in IOJAP gene. To further verify that the short root phenotype at low temperature was attributed to mutations in the *iojap* gene, other *iojap* mutant alleles *ijT2* (SALK_121803.40.80.x) and *ijT3* (SALKseq_053017.1) were ordered from the *Arabidopsis* stock center to characterize cold dependence of root length.

The T-DNA inserts were found to be in different areas of the gene, having *ijT1* located in the first intron, *ijT2* located in the promoter region, and *ijT3* located in the third exon (**Figure 4A**). At the optimum temperature of 22˚C, we found that all mutant alleles roots were slightly shorter than WT

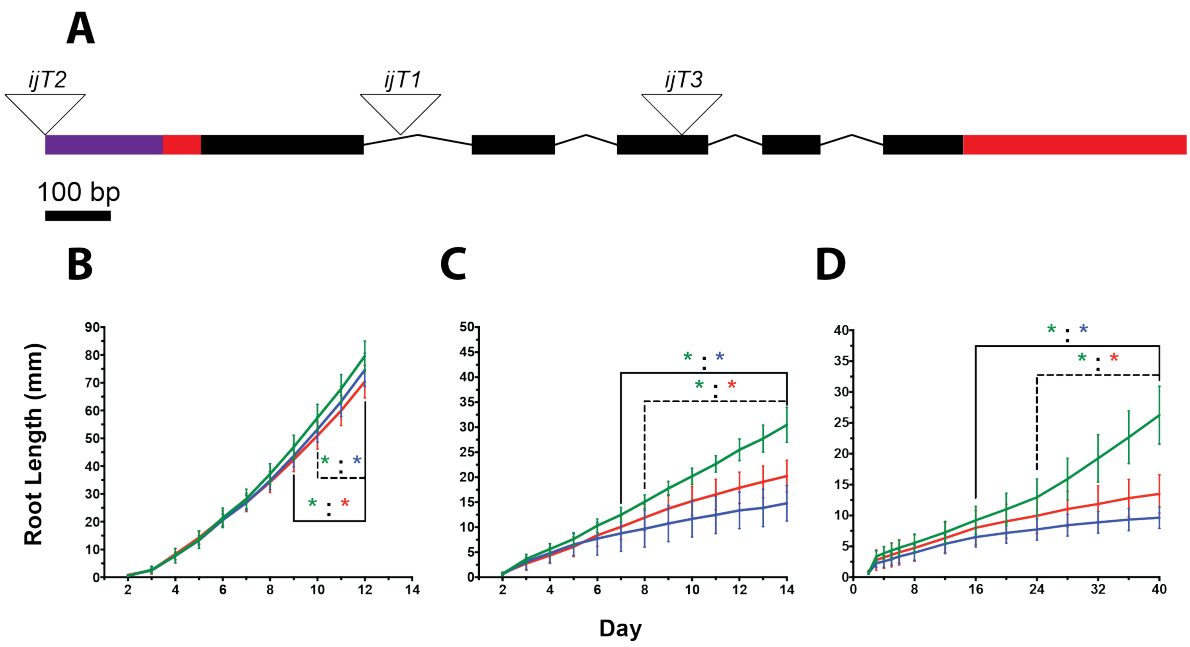

Figure 4: Reduced root growth manifest at low temperatures.

A) Schematic map of the IOJAP gene with its intron (lines), exon (blocks) structure plus the T-DNA insertion sites of the iojap mutant alleles. Plants of WT (Col-0), *ijT1*, and *ijT2* were grown vertically on a standard plate at 22˚C. Promoter (purple), UTR (red), exons (black box), introns (lines), T-DNA inserts (open triangles). (B) 12˚C (C), and 4˚C (D). Whole plate images were taken every day (22˚C and 12˚C) or every four days (4˚C) until termination. Primary roots were then measured using ImageJ. B) WT root length was significantly different ($p<0.05$) than *ijT1* and *ijT2* starting at day 10 and 9, respectively. C) Lower temperature exacerbated the growth defect in *ijT1* and *ijT2*, leading to significantly shorter roots than WT already on days 7 and 8, respectively ($p<0.05$). D) Both mutants root lengths were reduced, but *ijT1* was more effected, having a reduction at 16 days, 8 days earlier than *ijT2* ($P<0.05$, N=12 to 14). Error bars given by standard deviation. Two-Way ANOVA with Dunnette correction was performed, using WT as the reference. WT (green line), *ijT1* (blue line), *ijT2* (red line), and the asterisks denote significant difference, and the color denotes genotype.

(**Figure 4B)**. Curiously, the first days of growth from day 2 to day 8, there was no difference in root length between WT, and *ijT1* or *ijT2*. One day later, we observed that *ijT2* was statistically shorter than WT, and similarly, two days later for *ijT1*. You can see this trend continue by growth rate. At 22˚C WT averaged 8.07 mm/day, compared to 7.50 mm/day and 7.04 mm/day of *ijT1* and *ijT2* respectively. The growth rates of mutants is close to WT levels, having *ijT1* at 92.9% and ijT2 at 87.2% of the rate of WT. This accounts for the late significant difference between *iojap* mutant alleles and WT towards the end of the experimental time frame. It may also account for the significant difference between *ijT1* and *ijT2* root length at day 12. Preliminary work also noted that *iojap* mutant, *ijT1*, may be sensitive to chilling stress, thus we subjected all genotypes to low temperatures of 12˚C and 4˚C. We chose these temperatures to see if there was any correlation between the severity of the phenotype with that of the temperature decrease. As we see in both 12˚C and 4˚C, root lengths in *iojap* mutants were significantly reduced compared to WT (**Figure 4C & 4D**, while also visually extremely shorter than at 22˚C (**Figure 5C, D**). Mutant plants that were grown for 16 days at 12˚C, had statistically shorter roots than WT by day 7 (*ijT1*) and day 8 (*ijT2*). This reduction occurred a few days earlier than at 22˚C, suggesting WT was more resistant to chilling stress than both the mutants. This can also be observed looking at the growth rate differences. WT root growth rate was 2.48 mm/day, while *ijT1* and *ijT2* were 1.04 mm/day and 1.58 mm/day, respectively. Compared to 22˚C, the *ijT1* had a growth rate of 41.8% while *ijT2* was 63.7% compared to WT. Another interesting observation that the decrease of root growth rate from 22˚C to 12˚C was observed in all genotypes. While low temperature slows down most biological processes, WT root growth rate only reduced 3.3 fold, while *ijT1* and *ijT2* reduced 7.0 and 4.5 fold, respectively. This change in the magnitude accounts for an earlier significance difference of root length between *iojap* mutants and WT. This can be demonstrated further by the statistical analysis of root lengths between

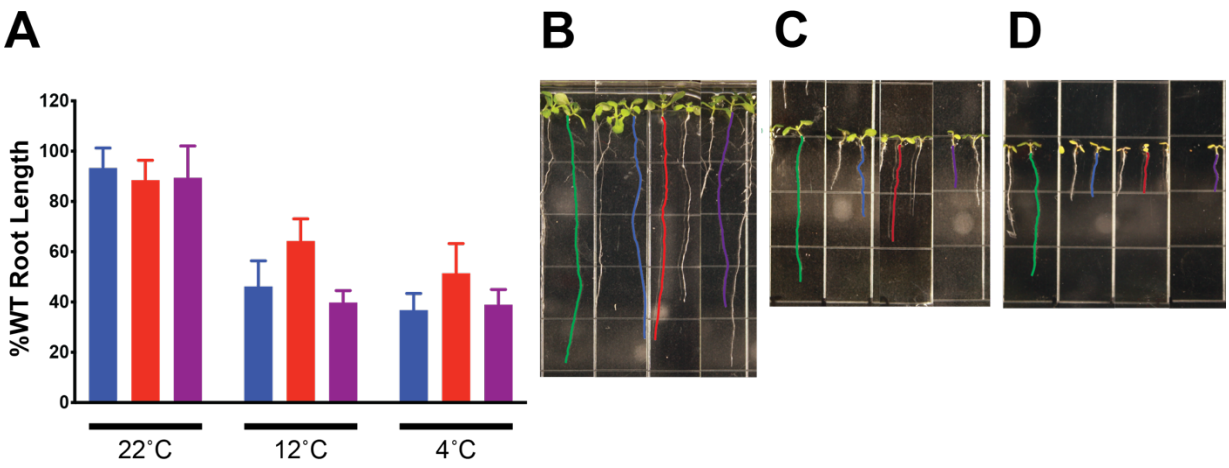

Figure 5: All iojap mutant alleles display root length deficiencies in response to low temperature.

WT, *ijT1*, *ijT2*, and *ijT3* were all plated on a standard plate and germinated at 22˚C. Whole plate images were taken 3 days after germination, then at 11, 16, and 36 days after transfer to their respective temperature of 22˚C, 12˚C, and 4˚C. Images were measured using ImageJ software, where their lengths were calculated as the percent relative to WT. A) All mutant alleles primary root lengths were similarly affected at each temperature, but *ijT2* showing the least effect at 12˚C and 4˚C. B-D) Images of primary roots measured for B) 22˚C, C) 12˚C, and D) 4˚C. WT (green), *ijT1* (blue), ijT2 (red), *ijT3* (purple).

iojap mutants, where *ijT2* becomes significantly longer than *ijT1* at day nine, and remains so throughout the course of the experiment. The severity of reduction of root length increases when grown at an even lower temperature. At 4˚C, both *iojap* mutants roots were shorter than WT. Additionally, *ijT1* root length became statistically significantly shorter on day 16 of growth, which was 8 days earlier than *ijT2* (day 24) (**Figure 4D**). Although, each genotype decreases in growth rate, mutant alleles root lengths alleles root lengths were not significantly different from one another. Similar to the other two mutant alleles, *ijT3* had a reduction in root length at all temperatures. This was demonstrated by the percent of root length relative to WT upon the termination of the experiment (**Figure 5A**). At 22˚C, the decrease was minimal for all genotypes, being around 85% to 95% of WT root length. However, at lower temperature of 12˚C and 4˚C, *ijT3* dramatically decreased to 40% of WT. Although all alleles were cold sensitive, the degree to which they were affected differed. At the optimal temperature, *ijT2*, was more affected than the other alleles, but grew better at both 12˚C and 4˚C. Additionally, at lower temperatures, *iojap* mutants had yellow or virescent cotyledons compared to WT and lacked pigmentation in emerging younger leaves. This seemed to be absent at 22˚C, where WT and *iojap* mutants looked similar (**Figure 5A**). This observation prompted the investigation into whether these earlier effects in young shoot tissue would alter leaf growth and development.

To characterize the *iojap* mutation's leaf phenotypes in Arabidopsis, we grew WT, *ijT1*, *ijT2*, and *ijT3* on standard media, and imaged them when the first two true leaves were around 3 mm in length (**Figure 6**). When grown at 22˚C, leaves of *ijT1* (**Figure 6D**) and *ijT2* (**Figure 6G**), looked similar to WT (**Figure 6A**). Their leaf shape, distribution of green pigment, trichome formation were visually similar. On the other hand, in *ijT3* (**Figure 6J**) we noticed slight yellowing of the basal area of the leaf, and small but slightly protruding hydathodes. This suggests that the mutation of *ijT3* is more severe than

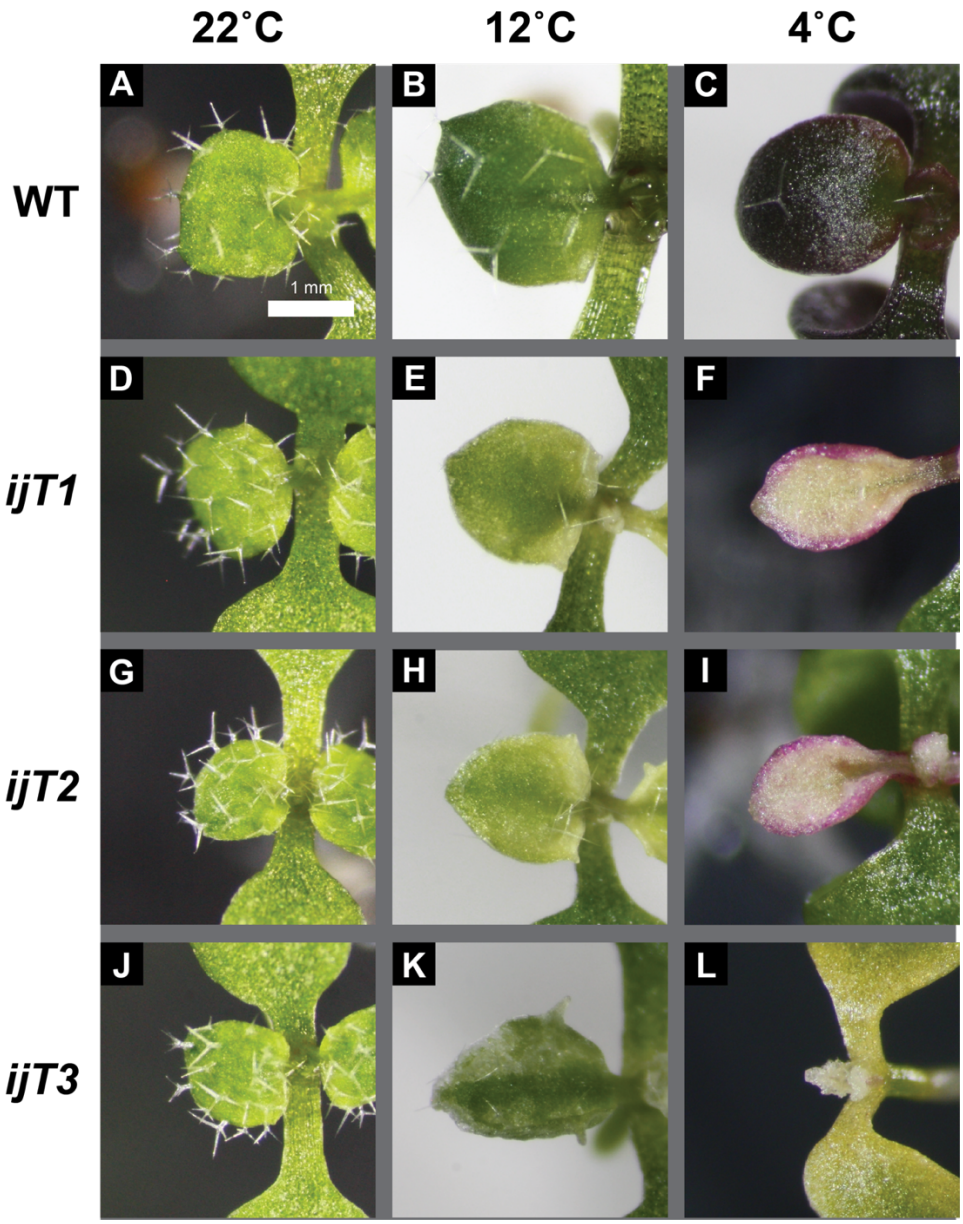

Figure 6: Sustained chilling stress leads to abnormal leaf morphology, degrees of chlorosis.

WT (A-C), *ijT1* (D-F), *ijT2* (G-I), and *ijT3* (J-L) plants were plated in standard media, germinated on horizontal plates at 22˚C, for two days then transferred to 22˚C (A, D, G, and J), 12˚C (B, E, H, and K), or 4˚C (C, F, I, and L). Images were taken when the first true leaves were of similar size between genotypes, using a camera attached to a stereoscope. WT at 22˚C appeared identical in shape and color to iojap mutant alleles (D, G, and J). Leaves at 12˚C mutant alleles were pale green (H), experience variegated (K), and chlorosis at the basal portion of the leaf (E). Also, *ijT1* (E) and *ijT2* (H), experience hydathode protrusion, while WT, unaffected by low temperature, has a smooth margin, and dark green color. At 4˚C, WT (C) has increase anthocyanin but retained a smooth margin and green color. All mutant alleles lost their green pigment, being pale yellow (F), albino (I), to albino, and purple (L). Both *ijT1* and *ijT3* increased in protrusions, while *ijT2* completely margins but a round-shaped compared to WT (C).

the others relative to leaf development. As with the roots, we looked at plants that were growing in low temperature conditions of 12˚C and 4˚C. In moderately low temperatures, 12˚C, WT (**Figure 6B**) appeared darker green compared to 22˚C, while seemingly having fewer trichomes. We also saw a slight accumulation of purple pigment, suspected to be anthocyanin, on the edge of the leaf margin. For the *iojap* mutants, the change was more drastic. Mutant *ijT1* (**Figure 6E**) was virescent near the distal portion of the leaf, but showed chlorosis in the proximal region, protruding hydathodes, and an upward curvature. The phenotype of *ijT2* (**Figure 6H**) had a more homogenous virescence but often lacked the curvature of *ijT1* (**Figure 6E**). Finally, the *ijT3* phenotype was also different than the other *iojap* mutant alleles, being highly variegated, with more narrow leaf morphology (**Figure 6K**). Just like the root phenotype, the severity of the leaf phenotype increased as temperature decreased. WT leaf shape was unchanged at 12˚C but leaves accumulated purple pigment, yet still contained green pigment near the center of the leaf (**Figure 6C**). All mutant alleles lost all green pigment at 4˚C, and experienced complete yellowing, albinism, and albino with anthocyanin accumulations (**Figure 6F, 6I, 6L**). These mutants' leaf shape was altered, as well. Often there was a narrowing of the leaf, and protrusions of the basal and apical hydathodes, or sometimes being completely smooth with no protrusions at the apex or basal edge. Another side effect of 4˚C was observed primarily in *ijT3*, in an instance where the leaf was albino, ensued a gradual decline in green pigment in the cotyledons, often leading to delayed growth or complete necrosis. Given that leaves are responsible for photosynthesis and thus energy production, deformations in morphology, variegation, and pigment alterations may also affect overall plant size, e.g., rosette radius.

To test whether the mutation of *iojap* affects overall growth of the plant, we used rosette radius as a reference. Plants of WT, *ijT1*, *ijT2*, and *ijT3*, were germinated on standard medium (see methods),

transferred to soil at 4 days old, and incubated for 1 day at 22˚C to acclimate to the new condition. After acclimation, potted plants were transferred into their respective temperatures of 22˚C, 12˚C, or 4˚C, were they experienced 100 μE light in long day conditions (16 hr day/8 hr dark). Each plant was collected and analyzed upon bolting, the emergence of inflorescence. When grown at 22˚C there was no difference in rosette radius between WT, *ijT1*, and *ijT2* (**Figure 7A**). However, there was a slight but significant decrease on *ijT3* rosette radius (**Figure 7A**). This seems to follow the root length trend, where the effect of *iojap* mutation is minute. However, like the root length experiments, the lower temperatures of 12˚C and 4˚C brought about a more severe phenotype. At both temperatures, we observe a drastic reduction in rosette radius in all *iojap* mutants, being around 2-fold smaller than WT (**Figure 7B**). Each *iojap* mutant allele was differentially affected by 12˚C. Another interesting observation was that WT at 12°C was around 15 mm larger than WT at 22˚C. Similar to 12˚C, *iojap* mutants were 3-fold smaller in rosette radius than WT (**Figure 7C**). But unlike at 12˚C, the severity of reduction was not significantly different from one another. Another observation was the differentiation in phenotypic pigmentation, represented by mutant alleles grown at 12˚C (**Figure 7D-F**). In soil, *ijT1* rosette leaves were variegated (**Figure 7D**), while *ijT2* (**Figure 7E**) and *ijT3* (**Figure 7F**) were virescent and albino respectively.

To take advantage of rosette data, I also recorded the number of leaves at bolting. The bolting process is the transition from the vegetative stage (rosette) to a reproduction stage (inflorescence), where flower buds form at the center of the rosette and the stem begins to grow (Koornneef et al., 1998). Flower time is regulated by day length, circadian clock, and other environmental cues such as cold. In some species induction of flowering by cold is called vernalization, where a cumulative and qualitative change occur when a plant is exposed to extended period or high frequency of low temperature periods

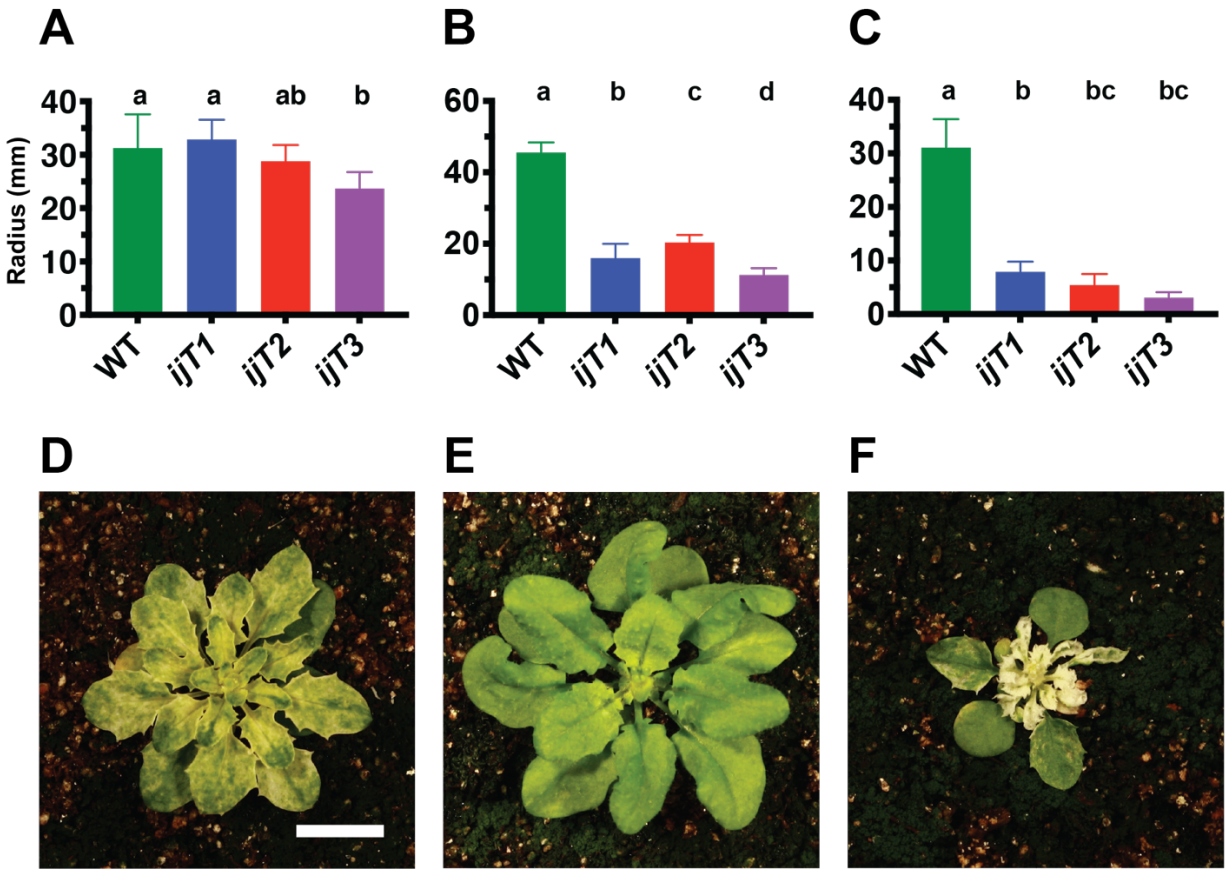

Figure 7: Rosette radius decreases as temperatures are reduced.

Four-day old seedlings germinated on standard media (22˚C, long day conditions), were transferred to soil, and incubated in optimal conditions for 24 hours. Next, the plants were transferred to their respective temperatures A) 22˚C, B) 12˚C, and C) 4˚C, to grow. D-F) Representative images of rosette images at 12C of D) *ijT1*, E) *ijT2,* and F) *ijT3*. At bolting, images were taken of the rosette. The three longest leaves were measured from the center of the plant to apex of the leaf, using ImageJ software, to which that average was used as the radius of the plant's rosette. A) Both *ijT1*, and *ijT2* had a similar radius as WT, but *ijT3* was significantly reduced in radius. B) All *iojap* mutant alleles were significantly reduced compared to WT. C) All *iojap* mutant alleles were significantly reduced compared to WT. Statistical analysis of Two-Way ANOVA with Tukey correction was performed ($p<0.05$, N=8). Scale bar (10 mm).

(Minorsky, 2002).

Often, low temperature exposure will cause the plant to bolt early but is not required for bolting to occur. One metric to indirectly measure any dysfunction in the transition to the reproductive stage, is to record the leaf number, which is highly correlated with the speed of developmental transition into reproductive phase (Pouteau and Albertini, 2009). At optimal temperatures and long day conditions (16 hour light and 8 hour dark), *Arabidopsis* has a range of 10 to 14 leaves at bolting (Boyes et al.; Lee, 2009; Miryeganeh et al., 2018), to which WT falls within this range having close to an average of 12 true leaves (**Figure 8A**). Both *ijT1* and *ijT2*, mutant alleles were similar to WT, unlike *ijT3* which had a significantly lower leaf number. When the plants were grown at lower temperatures two interesting observations arose. First the WT leaf number at bolting increased to around 30 leaves at 12˚C (**Figure 8B**), but went back down to around 12 leaves at 4˚C (**Figure 8C**). Second, all i*ojap* mutants had a significantly lower leave number than WT at 12˚C (**Figure 8B**), while only *ijT2* and *ijT3*, are significantly lower leaf number that WT at 4˚C (**Figure 8C**). Another interesting observation is that bolting time (data not shown) for WT and *iojap* alleles were the same relative to the temperature they were grown in. Although time for reproductive transition was not altered across temperatures, mutants in *iojap* resulted in lower leaf numbers for most alleles at lower temperatures.

Before further investigating the more specific dysfunction of *iojap* in the leaves, we first looked at the effect of *iojap* mutations on other developmental processes, germination and hypocotyl growth during etiolation. During germination the plastids differentiate from proplastids to chloroplasts and defects in plastid ribosomes might manifest themselves in reduced germination rates. Seeds of all genotypes were plated and placed in their respective temperatures of 22˚C, 12˚C, and 4˚C in long day

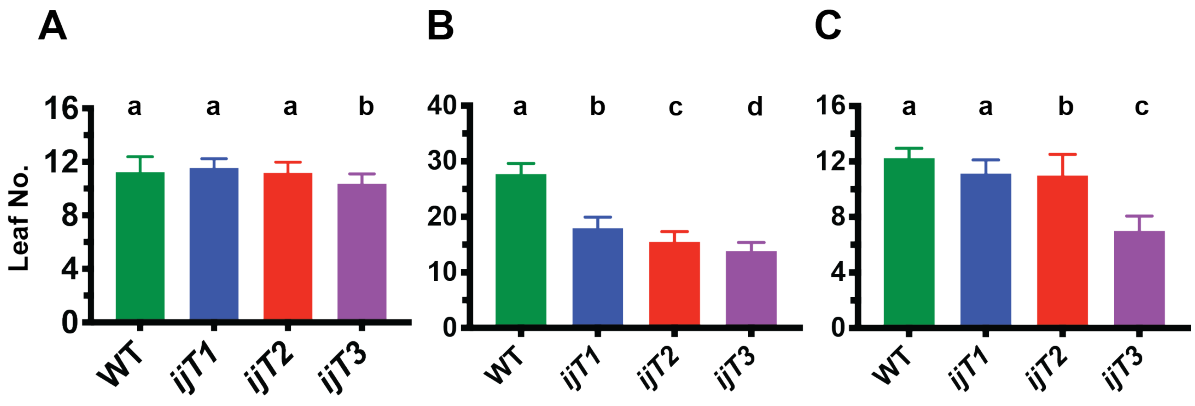

Figure 8: Leaf number variation in *iojap* mutant alleles:

Genotypes of WT, *ijT1*, *ijT2*, and *ijT3* were grown germinated on standard media plates at 22˚C for 4 days, then transferred to soil. Potted plants were allowed to recover at 22˚C for one day then transferred to A) 22˚C, B) 12˚C, and C) 4˚C until bolting, when the number of true leaves was determined.

conditions. For all temperatures, there was no observed decrease in germination in any of the *iojap* alleles (**Figure 9**).

So far there has been no characterization of the effect of *iojap* mutants on etiolation. Here we investigated whether *iojap* mutant in *Arabidopsis* affected etiolation as a measure of hypocotyl elongation. Similar to the results of germination there was no decrease in hypocotyl length at any temperature. In fact, the opposite was observed, having *ijT3* being somewhat longer than WT at 12˚C and 4 ˚C (**Figure 10**). Mutation of *iojap* showed no deleterious effects in either germination or hypocotyl length during etiolation. This suggests that the function of IOJAP was not required for these two processes to occur.

Although the TargetP transit peptide prediction software (Armenteros et al., 2019b) and experimental evidence (Wang et al., 2016a, 2017), support that IOJAP localizes to the chloroplast, I wanted to verify IOJAP's localization. The parent vector of pEG100 was used to house inserts of IOJAP fusion constructs of C-terminal cerulean florescence protein (**Figure 11A, top**) and C-terminal 3x-Myc (**Figure 11B, bottom**) constructs. The separate constructs were verified by PCR and Sanger sequencing (data not shown) and transformed into *Agrobacterium tumefaciens* (GV3101) by electroporation. *Agrobacterium tumefaciens* cultures containing either pEG100- IOJAP-CFP or pEG100-IOJAP-3xMyc were then used to transform *Arabidopsis ijT2* and *ijT1* mutants, respectively, by a modified dipping method (see 'Methods'). The T1 seeds were harvested and selected using phosphinothricin (BASTA) plates, with mixed results. Instead, I decided to select T1 seeds using a two-prong approach: those showing both evidence of positive transformation as well as complementation of the low temperature phenotype. To accomplish this, T1 seeds were plated on standard media, germinated at 22˚C for 2 days, then grown at 12˚C until 4 to 6 true leaves formed (**Figure 11D**). This allowed visualization of three

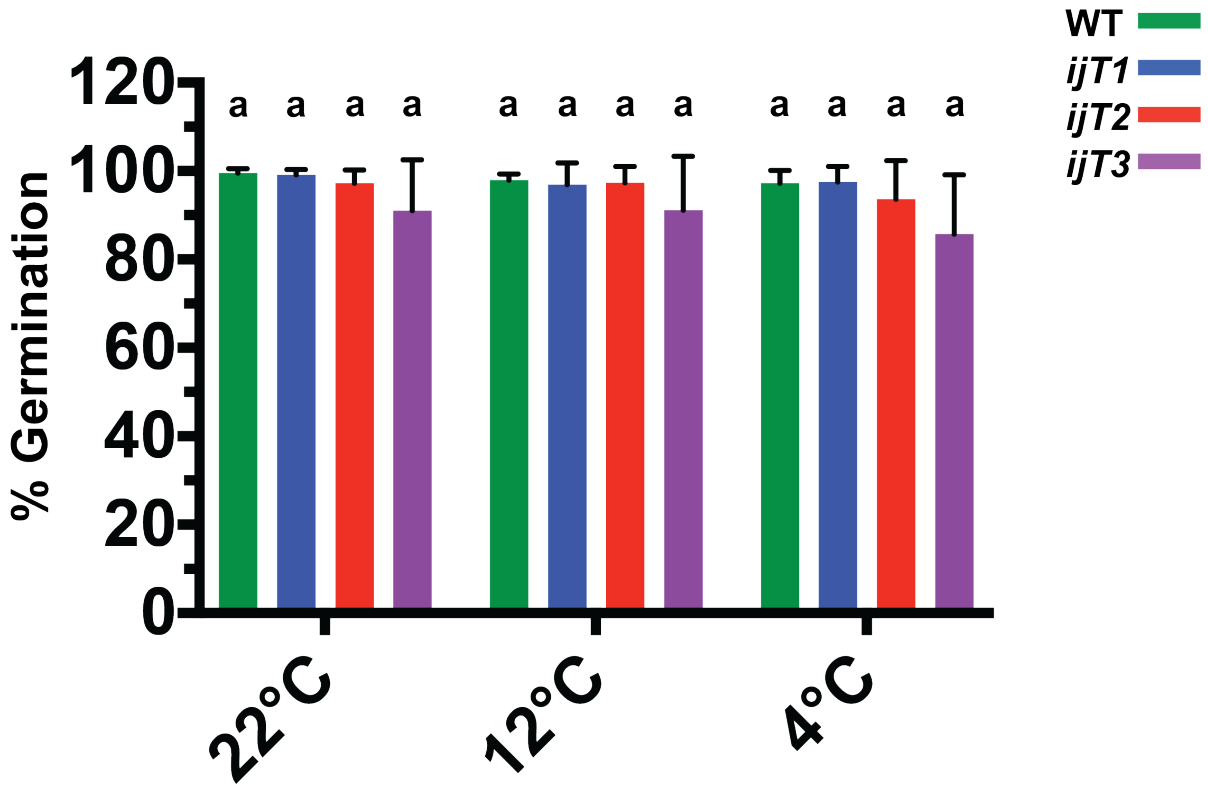

Figure 9: Germination unaffected by low-temperature stress

Seeds of WT, *ijT1*, *ijT2*, and *ijT3* were plated on standard media, and placed vertically in their respective temperatures, 22˚C, 12˚C, and 4˚C to germinate. Whole plate images were taken once WT stopped germinating. The percent germination was calculated using ImageJ software counting tool. No difference in germination at 22˚C, 12˚C, and 4˚C between all genotypes. The experiment was repeated 3 times, sample size 50 seeds per genotype for each temperature. Statistical analysis of Two-Way ANOVA with Tukey correction ($p<0.05$, N=3).

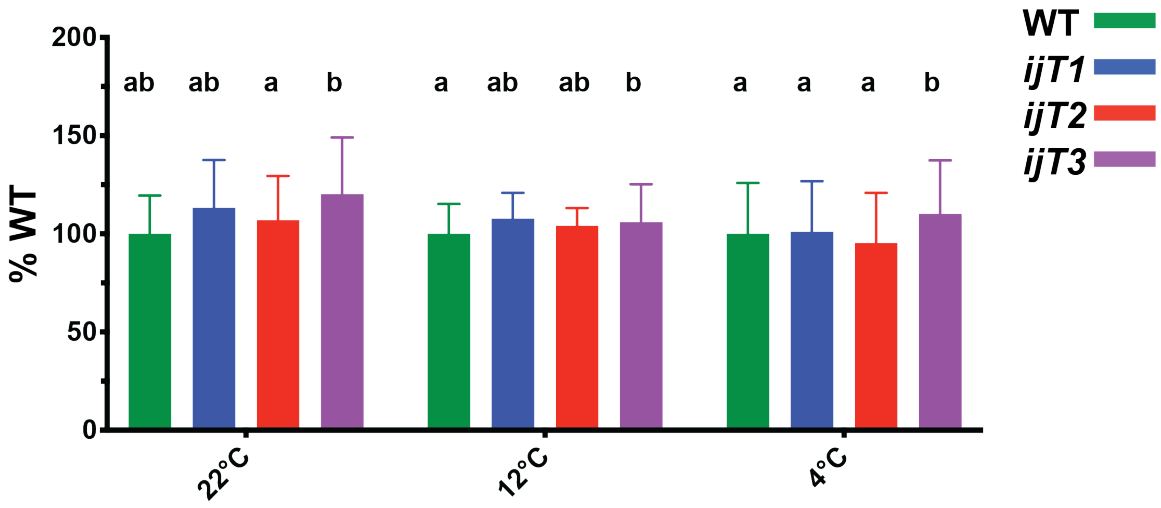

Figure 10: Hypocotyl length during etiolation is unaffected by low temperature

Seedlings were plated on standard media, vertically, and germinated at 22˚C for 24 hours. Plates were then transferred to their respective temperature to incubate for a total of 60 hours (22˚C), 84 hours (12˚C), and 108 hours (4˚C). Whole plate images were taken, and hypocotyls were measured using ImageJ software. A) No difference between WT and *iojap* mutant alleles, but *ijT3* was slightly taller. B) No difference between WT and *ijT1*, *ijT2*, or *ijT3*. C) No difference between WT and *ijT1* or but *ijT3* was significantly taller than all other genotypes. Statistical analysis was a Two-Way ANOVA with Tukey correction ($p<0.05$, N=50).

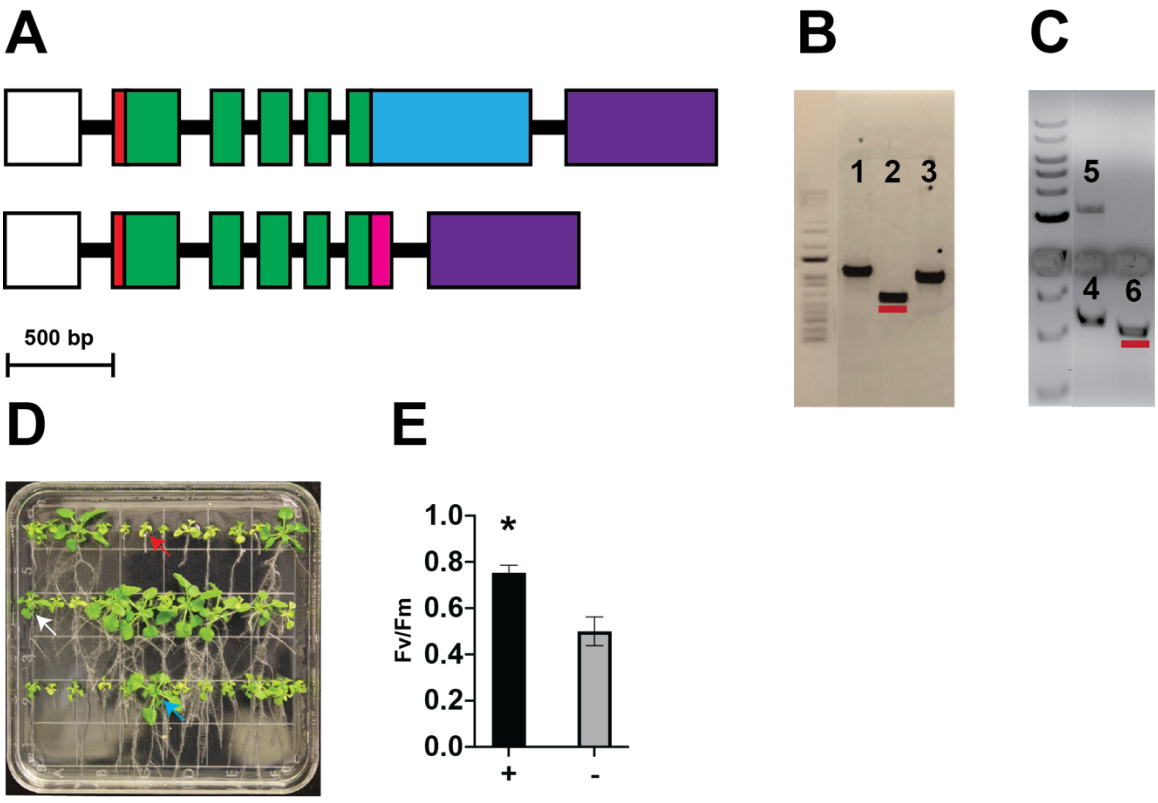

Figure 11: IOJAP tagged transgenic lines restore F_v/F_m *ijT1* to WT levels at 12˚C:

A) Gene schematic of IOJAP tagged construct in pEG100 vector, pEG100-IOJAP-CFP (top) and IOJAP-3xMyc (bottom). Constructs consist of 35S promoter (white box), 5'-UTR (red box), five exons (green box), intron (black line), CFP (blue box), three tandem Myc's (magenta box), and an OSC terminator (purple box). B) Genotype verification T1 transgenic line of IOJAP-CFP in *ijT2* background. Primer set 1) cp-ijT2-LP + SEQ-35S-F (900 bp), 2) IJ_e3-SEQ-F + GEC-alpha-CFP-R (440 bp), and 3) KT5-LP +KT5-RP control (850 bp). Red line band is the expected product if IOJAP-CFP was successfully inserted into the plant. C) Genotype verification T1 transgenic line of IOJAP-3xMyc in *ijT1* background. Primer set 4) IT5-RP + IT5-LP control (1.2 Kb), 5) cp-ijT2-RP + Lb1a (3.2 Kb), and 6) rv-ij-LB + GEC-3xMyc-R (1.0 Kb). Red line band is the expected product if IOJAP-CFP was successfully inserted into the plant. D) T1 seeds grown on standard media, at 12˚C until 4 to 6 true leaves. The seedlings without variegation where selected for genotyping. E) Representation of of the F_v/F_m values of a cold selection plates of contrasts, where the '+' represents phenotypic WT plants and '-' represents the expected cold phenotype of *ijT1*.

results: non-transformed (red arrow), poor vigor transformation (white arrow), and strong vigor transformation (blue arrow). T1 plants that had strong vigor were transferred to soil, and then the leaf was excised to isolate genomic DNA for genotyped PCR verification. Three primer sets were used to analyze T1 pEG100-IOJAP-CFP in *ijT2* background gDNA (**Figure 11B**). Primer set 1 (cpijT2-LP + SEQ-35S-F), having the expected band size 1.4 kb bp for *ijT2* genome, while primer set 2 (IJ_e3-SEQ-F + GEC-alpha-CFP-R) showed an expected band size of 440 bp (red line), suggesting the transformation was successful (**Figure 11B, red line**). Primer set 3 (KT5-LP + KT5-RP) was used as a control, having the expected band size of 850 bp. Similarly, a three-primer set was used to verify successful transformation of T1 IOJAP-3xMyc plants (**Figure 11C**). Primer set 4 (IT5-LP + IT5-RP) was used as a control and gave the expected band size of 1. 2 kb, while set 5 (cpijT2-RP + LBb1) band size of 3.2 kb, verified genomic background of *ijT1.* Primer set 6 (Rv-ij-LB + GEC-3xMyc-R) verified the successful transformation of IOJAP-3xMyc, having an expected band size of 1 kb (**Figure 11C, red line**). Genotyping confirmed the expected band size for both transgenic lines, for plants that had a WT phenotype at 12˚C. However, the appearance of WT-like does not guarantee true complementation of low temperature phenotype of *iojap* mutants.To address this issue, F_v/F_m measurements were recorded for negative transformation plants, denoted by '-', and positive transformed plants, denoted by '+' (**Figure 11E**). The negative transformed plants (displayed low temperature phenotype) were grouped together, having both non-transformed (red arrow) or poor vigor (white arrow), while positive group, displayed WT phenotype and contained only strong vigor (blue arrow) (**Figure 11D, E**). The positive transformed group averaged a F_v/F_m value of 0.74 which was significantly higher than an F_v/F_m 0.50 of the negative group. Thus, is it evident that transgenic line of IOJAP-CFP and IOJAP-3xMyc were successful and complement the low temperature phenotype of *iojap* mutants.

Successful complementation would suggest that IOJAP fusion constructs are expressed and functional, but IOJAP's location needed to be confirmed. To address this, vectors of pEG100-iojap-CFP, pAN363 (prSSU-YFP), and pAN159 (cox-YFP), were transiently expressed in *Nicotiana benthamiana* to be viewed using confocal microscopy (**Figure 12**). Transient expression of only pEG100-IOJAP-CFP resulted in various CFP signals. In some cases, the presence of CFP signal was absent from the majority of the chloroplasts, while in other cases the CFP signal was observed in most chloroplasts. When present, it was most often visualized as many large punctate signals around the periphery of the chloroplast (**Figure 12A, white arrow**). Furthermore, there was no CFP signal in other organelles or cytoplasm. Since some transit peptides are dual targeting, going both to the chloroplast and mitochondria, as well as the mitochondria having an IOJAP homolog, simultaneous transient expression of IOJAP-CFP and mitochondrial protein construct COX-YFP was completed (**Figure 12B**). Images of this co-expression confirmed COX-YFP construct (yellow, arrowhead) located to mitochondria, while IOJAP-CFP (blue, arrow) was localized to the chloroplast (magenta) (**Figure 12B**). Unlike the large punctate signals in IOJAP-CFP only transient expression (**Figure 12A**), the CFP signal was concentrated in regions of the chloroplast with an irregular structure (**Figure 12B, arrow**). Moreover, there was no observed signal of CFP signal overlapping with the YFP signal. To further verify IOJAP localization, another co-expression of IOJAP-CFP was done with chloroplast protein SSU-YFP (**Figure 12C-D**). In many cases, the CFP signals were observed as large punctate form (**Figure 12C, arrow**), sometimes alongside a YFP signal. However, more commonly, as in (**Figure 12C-D**), representing different planes of the same sample, CFP signal was strongest in small chloroplasts (**Figure 12C**), while YFP was more strongly represented in larger chloroplasts (**Figure 12D**), having a longest axial range of 5 to 6 μm and 7 to 11 μm, respectively. However, in both cases overlap between IOJAP-CFP and SSU-

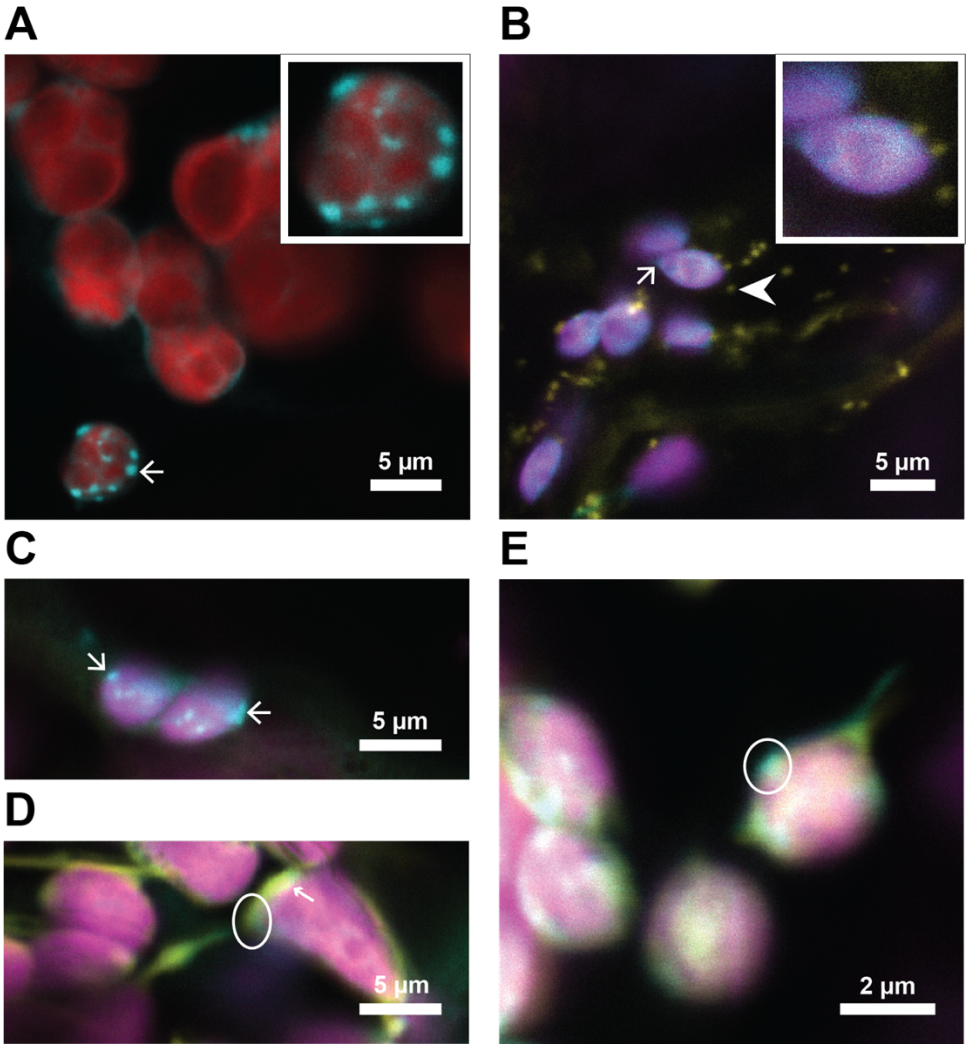

Figure 12: IOJAP localizes to chloroplast in the transient expression of *N. benthamiana*.

Confocal images using Leica SP8 White Light Laser Confocal System at 40x objective, with 1.1 NA motorized correction collar water immersion. A) Transient expression of IOJAP-CFP construct only, where chloroplast (red) visualized by autofluorescence, IOJAP-CFP (blue) and emphasized by white arrow. Larger image was scaled up by a factor of two. B) Simultaneous transient expression of IOJAP-CFP and cox-YFP, with chlorophyll autofluorescence (magenta), IOJAP-CFP (blue), mitochondria (yellow). IOJAP-CFP located to the chloroplast (small arrow) while the mitochondria clearly separate from chloroplast (arrowhead). Insert was scaled up by a factor of two. C-D) Simultaneous transient expression of IOJAP-CFP (blue) and prSSU-YFP (yellow). Both C and D are the from the same cell but focusing on a different plane, showing chlorophyll (magenta), IOJAP-CFP presence (arrow), prSSU-YFP (small arrow), and overlap of location of both proteins in the chloroplast as green and white circle. E) Simultaneous transient expression of IOJAP-CFP (blue) and prSSU-YFP (yellow) located to the chloroplast (magenta). Merged image depicts both fluorescent constructs in similar locations by green merged color (white circle).

YFP could be detected (**Figure 12D-E, circle**). Taking it all together, IOJAP-CFP localizes only to the chloroplast, and is found in both small and large chloroplasts.

Discussion

IOJAP was first characterized in maize in 1924 (Jenkins, 1924), which was followed by a thorough characterization of phenotype. Recently in *Arabidopsis*, the phenotype characterization was limited to chloroplasts of leaf tissue (Wang et al., 2016a). Here we are expanding this characterization, at both optimal temperature (22˚C) and lower temperatures (12˚C and 4˚C). At optimal growing temperature, *iojap* mutants in *Arabidopsis* showed mild but statistically significant differences in primary root length (**Figure 5**), but no differences in overall plant size (rosette radius, **Figure 7A**). Root length was analyzed on media enriched with sucrose, while for measuring rosette radius the plants were grown in soil. Since *iojap* delays the development of chloroplasts (Wang et al., 2016a), and is responsible for energy production (sucrose), one would expect to see a larger reduction in rosette radius than root length. However, the observed result could be due to the strategy for measuring rosette radius, which may be less precise due to leaf curling, and partial hyponasty. However, these subtle differences disappear at low temperature. The progression of increased severity of rosette radius with lower temperature was matched visually by variegation in *ijT1* (**Figure 7D**), virescent in *ijT2* (**Figure 7D**), and albinism in *ijT3* (**Figure7F**). As observed in *Z. mays*, variegation reduced plant size (Coe et al., 1988), most likely due to an extreme decrease in functioning chloroplast population. This is why we observed rosette radius of ~15% of WT with partial variegation or virescence at 12˚C and ~5% of WT at 4˚C with almost total loss of green pigment. This may also explain the similar pattern in root length. Although the root length studies were done on media containing sucrose, the increase in variegation also would reduce other essential compounds synthesized in the chloroplast, such as hormones, amino acids, and various

metabolites (Lopez-Juez and Pyke, 2004; Neuhaus and Emes, 2000; Rolland et al., 2018; Waters and Langdale, 2009) that are required for root growth. To put it simply, delayed chloroplast development or chloroplast dysfunction often has deleterious systemic effects on other non-leaf tissues.

Mutations in *iojap* also show a difference in variegation between monocots and dicots. In *Z. mays*, a monocot, *iojap* has permeant variegation at optimal conditions and even some instances of complete albinism in tillers and certain varieties (Coe et al., 1988). Among *Arabidopsis iojap* mutants there was no observed variegation in young or mature leaves at optimal conditions (22˚C) (**Figure 6**), except in *ijT3.* This difference in phenotypic expression may be due to T-DNA position in the *iojap* gene (**Figure 3A**) Even though all mutant alleles are due to a T-DNA insert, their loci span the primary section of gene structure: promoter, intron and exon. We observe the most severe phenotype in *ijT3*, which has the T-DNA insert located at the exon. Therefore, *ijT3* mutation is likely is a full knock-out since the C-terminus of the protein (starting in DUF143) could not be produced, hence no functional protein could be made. The weaker phenotypes in the *ijT1* and *ijT2* alleles could result from a leaky mutation, or to alter the functionality of the promoter, as with *ijT2*. Or in regard to *ijT1* a changing efficiency of splicing of the first intron, thus removing the T-DNA insert. For instance, *ijT1* T-DNA insert is located on the first intron, which may be inefficiently spliced out to produce low levels of functioning IOJAP that are below the threshold to produce visual damage. This hypothesis is similar to what is observed in *ijT2* where the T-DNA is located in the promoter region, which may alter its regulation but also express low levels of functioning IOJAP. Unlike the other two mutant alleles, *ijT3's* T-DNA insert is located in the third exon, which is the coding region of C-terminal region of the DUF143 domain. Even if this allele is expressed at low levels, the T-DNA insert most likely create a non-functioning IOJAP protein, producing the most severe phenotype even at 22˚C. This may be why

chlorosis is visually observed at 22˚C in *ijT3*, and not in the other mutant alleles (**Figure 6**). Additionally, the T-DNA position may also cause different levels of phenotypic expression of variegation at 12˚C. Both *ijT1* and *ijT3* have variegation, which is easily discernable in mature leaves, while *ijT2* leaves are often virescent, most notable in soil, having a uniform pale green of the whole leaf. This trend continued at 4˚C, where each *iojap* mutant allele had a different expression of its phenotype. At this low temperature, *ijT1* is often yellow. The yellow pigment is most likely due to the accumulation of carotenoids. Unlike *ijT1*, *ijT3* lack yellow or green pigments and is stunted compared to the other mutant alleles. Leaf pigment is not the only difference observed between all the alleles. Again, this variance in leaf morphology and growth, could be due to the location of T-DNA insertion, but *ijT2* is a verified knockout (Wang et al., 2016a), and *ijT3* insertion would render the protein dysfunctional given the location of the T-DNA insert. As a whole, all alleles respond to the drop in temperature in a similar manner, where both pigment and leaf morphology are progressively altered.

Leaf growth rate was also varied among *iojap* mutant alleles. Leaf number at 22˚C was similar in all mutant alleles, with the exception of *ijT3*, which had a significantly lower leaf number at all temperatures, possible due to lower growth rate (**Figure 8**). Even so, both *ijT1* and *ijT2* were also sensitive to low temperatures, showing a lower leaf number at both 12˚C and 4˚C. The speculation that the lower leaf number resulted from slower growth rates, stems from the observation that bolting time between WT and mutants were the same relative to each temperature. Another observation recorded was the rise in leaf number of WT from 22˚C to 12˚C, having close to the double the number of leaves. Yet, this trend did not continue at 4˚C, where WT leaf number closely resemble that at 22˚C. This trend could be due to stress differences between 12˚C and 4˚C. Firstly, 4˚C is more severe and reducing enzyme activity, viscosity, and most likely an increase in ROS's compared to 12˚C. While *Arabidopsis* can

acclimate to 4˚C, the threshold of stress may be far less at 12˚C, as such growth can continue with far less damage. This is in slight agreement with the trend we observe to a lesser degree in *iojap* alleles, where the leaf number increases from 22˚C to 12˚C but reduced from 12˚C to 4˚C. On the other hand, the leaf number increase of WT at 12˚C, suggests it is responding to cold signals, while *iojap* is unable to. This may suggest that at 4˚C, this response is also hampered in WT, resulting in a loss of a process that signals for an increase in leaf number. Secondly, bolting time was similar between WT and *iojap* alleles, suggesting that the malfunction observed in leaf number and morphology does not interfere with bolting time. It could be that the function of IOJAP in leaf development is isolated completely from the bolting pathways, yet ROS produced by chloroplasts have been shown to initiate bolting in response to high light (van Buer et al., 2019; Cvetkovic et al., 2017). Since both cold and high light produce ROS, altered leaf number and bolting time are expected, yet only leaf number differences were observed in *iojap*. Although, many mutations that cause dysfunctions in leaves and chloroplast development also skew bolting time and flower development (Pogson et al., 2015), the *iojap* mutations do not.

So far, the phenotypes observed are primarily observed in the shoot, where photosynthesis is heavily required. This lack of photosynthesis would also have systemic effects that would disrupt root development, even in the presence of sucrose. On the other hand, in developmental processes where photosynthesis is not heavily relied upon (e.g. germination, etiolation), we do not see a low temperature phenotype (**Figure 9 & 10**). *Arabidopsis* requires stratification at a lower temperature (4˚C) to synchronize germination. During this time the seed imbibes water, and the existing proplastids to become active and begins to differentiate towards chloroplasts (Whatley, 1978). This is similar to what occurs in the leaf development, yet at all temperatures there is no difference of germination efficiency between WT and all *iojap* mutant alleles. What we do observe is that the time it takes to germinate

(emergence of the radicle), changes with temperature for all genotypes. This is to be expected, since most reactions, both enzymatic and chemical, reduce in rate as temperature decreases. In the case of *Arabidopsis,* the average time for germination was around 48 hours, 5 days and 16 days for 22˚C, 12˚C and 4˚C, respectively. Many plastid mutants are embryo lethal, but those that are not often show deleterious effects during seedling development. One such mutant is *plastid protein import2,* which lacks the ability to produce TOC159 protein. This mutant germinates with the same frequency of WT but dies shortly after germination (Tada et al., 2014). Furthermore, adding 3-(3,4-dichlorophenyl)- 1,1-dimethylurea (DCMU), a PSII inhibitor to developing or imbibing seeds did not result in reduced food stores or germination frequency (Allorent et al., 2013; Sela et al., 2020). This may be why we don't see germination dysfunction in *iojap* and why sucrose added to the media does not rescue the phenotype. Furthermore, *iojap* mutant in maize had a reduced germination frequency from 26% to 10% of WT, dependent on *Z. mays* variety (Coe et al., 1982), yet in *Arabidopsis* this phenotype is absent. Thus, is seems as IOJAP is required for processes that rely on photosynthesis heavily, such as leaf development. This hypothesis is supported by study of elongation of the hypocotyl during skotomorphogenesis. When a seed germinates in the absence of light, the hypocotyl begins to elongate toward the surface. The plastids of hypocotyl tissue are leucoplasts, a non-photosynthetic plastid, having the energy for this process derived from the endosperm (Dumas and Rogowsky, 2008). When I looked at the effects of *iojap* on etiolation by measuring hypocotyl length, there was no reduction of length at all temperatures (**Figure 10**). Interestingly, the *iojap* mutants trended longer than WT, especially at 4˚C, where *ijT3* was significantly longer than WT. Similar to *iojap* mutants, *cpna2-4*, is a mutant of nuclear encoded protein that is sensitive to low temperatures. Although its function is different being a part of the plastid chaperonin 60 complex involved in protein folding. At 22˚C, *cpna2-4* resembles WT in many metrics,

but when grown at low temperature (15˚C and 10˚C), both cotyledons and young leaves have a reduction in F_v/F_m and are pale yellow in color (Sela et al., 2020). Yet, at both optimal and low temperatures, *cpna2-4* has reduced hypocotyl length in *Arabidopsis*, unlike what is observed in *iojap*. Furthermore, some of *cpna2-4* phenotypes observed at 22˚C could be rescued by exogenous sucrose in the media, but were unable to be rescued at low temperature phenotypes (Sela et al., 2020). Thus, like *iojap* mutants, it is not an energy problem, but a problem related to developmental stage. In the case of IOJAP, this point in development is not involved in either hypocotyl elongation during etiolation or germination, but a factor in early stages of chloroplast development, such as young emerging leaves. Therefore, IOJAP function is important at a specific moment in chloroplast development different from CPNA2, and the function of IOJAP itself is sensitive to low temperature. If IOJAP functions in translation or transcription, then it would be likely to have phenotypes in any process that involves plastid transcription or translation, yet this in not what was observed. For instance, the *toc159*/+ mutant reduces import capacity which would be a systemic alteration, affecting any plastid processes, as observed in the reduction of hypocotyl length (Sela et al., 2020). These finding suggests that IOJAP functions in a specific plastid developmental process absent in germination and hypocotyl elongation but present in early leaf development. This speculation that IOJAP functioning is specific for early stages of chloroplast development is bolstered by transient expression analysis using confocal microscopy, where IOJAP-CFP is strongly observed in smaller chloroplasts, and less present in larger, seemingly more developed chloroplasts (**Figure 12**). Furthermore, IOJAP-CFP signals were often observed in large punctate arrangements, rather around the periphery of chloroplasts, unlike the small punctate arrangement as observed in BiFC experiment with nucleoid proteins (Wang et al., 2016a, 2017). However, IOJAP-CFP can be shown in other cases in a more pervasive diffuse arrangement in both

sizes of chloroplast. The structures that are observed from the CFP signal may be due to the dose given by transient expression that exceeds native expression load. Nevertheless, the construct itself, when in a stable line, is able to complement the low temperature phenotype at 12˚C in both *ijT1* and *ijT2* backgrounds.

Whether or not IOJAP is required for early chloroplast development or simply delays the whole development process, is still under investigation. Whatever the function is, it does not seem to be required for processes such as germination, hypocotyl growth during etiolation, or time of bolting (**Figure, 8-10**). Therefore, the function of IOJAP may lie in those processes where proplastids are differentiating into chloroplast while also bearing a high energy load, such as leaf development and de-etiolation, to which we investigate further in 'Chapter 3.'

CHAPTER THREE
PHYSIOLOGICAL AND MOLECULAR DEFECTS IN *IOJAP* MUTANTS

Introduction

Arabidopsis is a rosette annual plant that organizes its leaves in a spiral phyllotaxy, having each successive leaf spatially separated from the previous by around 137.5˚ angle (Bowman, 1994; Byrne et al., 2003). As the plant grows, the older leaves are located just below the younger leaves forming a rosette. Leaf development is a long and complex process, from leaf primordia to maturation. From the onset of the emergence of leaf primordia the cells begin to divide, while at the same time proplastids differentiate into chloroplasts and divide in synchrony with the leaf cells (Nelissen et al., 2016; Pogson et al., 2015). This process is spatially and temporally regulated. For instance, cells at the tip of the leaf cells will stop dividing and begin to expand while cells at the basal portion of the leaf will continue to divide. (Nelissen et al., 2016). Therefore, during leaf growth, we have different maturity sections of both leaf cells and chloroplasts. Furthermore, young leaves as a whole are more resilient to abiotic stresses, such as low temperatures, and thus acclimate more robustly compared to mature leaves (Takagi et al., 2003; Wanner and Junttila, 1999). Many mutations that cause chloroplast developmental result in leaf abnormalities such as paleness or variegation, such as we see in *iojap* maize (Coe et al., 1988; Jenkins, 1924). However, in maize this phenotype persists through leaf maturity, while in *Arabidopsis* not only is variegation absent but chlorosis in young leaves (Wang et al., 2016a) is transient, recovering as the leaf matures.

Although proplastid differentiation into chloroplasts in leaves is similar to de-etiolation, de-etiolation is simpler in that the etioplast is primed to change rapidly, and the required energy source is allocated from the seed. During etiolation the proplastids in the cotyledons differentiate into etioplasts.

This intermediate state contains pro-lamellar bodies (PLB), that set the stage for thylakoid biogenesis (Bahl et al., 1976; Galey et al., 1980). Internally, they contain proteins, ribosomes, chaperones, redox regulators, NADPH:protochlorophyllide oxidoreductase (POR), and protochlorophyllide (Blomqvist et al., 2006; Franck et al., 2000; Komatsu et al., 1999; Plöscher et al., 2009; Reisinger et al., 2008; von Zychlinski et al., 2005). Upon illumination protochlorophyllide is almost instantly converted into chlorophyll along with a quick transcriptional response by PEP of photosynthesis genes, and a large spike in translation of PSI and PSII reaches maximal accumulation within 15 minutes and 2 hours respectively (Baker and Butler, 1976; Domanskii et al., 2003; Kim and Mullet, 2003; Kim et al., 1994; Kleffmann et al., 2007; Klein and Mullet, 1986, 1987; Reinbothe et al., 1999; Wellburn and Hampp, 1979).

Variegation occurs when some cells contain plastids that are unable to develop into chloroplasts, while in other cells the chloroplast fully developed. In many cases, the variegation occurs at optimal temperature and remains permanent, as is the case of *immutans* (*im)* in Arabidopsis (Wu et al., 1999) and *iojap* in maize (Jenkins, 1924). Additionally, chloroplast development can be delayed, usually due to the delayed transition of proplastids to chloroplasts in young leaves. This is seen in many chloroplast mutants such as *sig2*, *pp71*, *svr11*, and *iojap* in Arabidopsis (Liu et al., 2018; Wang et al., 2016a; Xu et al., 2019). Many chloroplast mutations have no visible effect on plant growth, but when stressed by low temperature they lead to a young leaf virescent phenotype, such as *rpl33* in tobacco. In these cases however, the damage is reversible, as both color and photosynthesis is restored when transferred to warmer temperatures (Rogalski et al., 2008). We also see this in *Arabidopsis* plastid mutant *gun5*, which looks similar to WT at 22˚C, but when exposed to low temperatures (4˚C), new leaves begin to yellow. This yellowing is a result of highly underdeveloped thylakoid stacks, which revert close to WT when

transferred back to warmer temperatures (22˚C) (Kindgren et al., 2015). In nature, many plants can acclimate to low temperature, much of which is necessary to protect the chloroplast from ROS damage. Low temperature stress on a plastid mutant may overwhelm the chloroplast acclimation process. Furthermore, certain stages of chloroplast development may be more sensitive to chilling stress. For instance, in species that are ill adapted to low temperature, like maize, young leaves recovered far better than mature leave when they are transferred back to warm temperatures at 24˚C (Sowiński et al., 2005).

Chloroplasts are highly sensitive to abiotic stresses. This allows plants to react quickly to harmful changes in their environments. In the experiments in the previous chapter, cold stress elicited deleterious effects on shoot and root development. However, many other abiotic stresses have similar outcomes as chilling stress, which are the accumulation of ROS and, more specifically, singlet oxygen from PSII. Singlet oxygen primarily results from any perturbation of PSII, either directly by DCMU (Bechtold and Field, 2018b) and by high light (Aro et al., 1993; Tikkanen et al., 2012), or indirectly from salinity stress (Suo et al., 2017), osmotic stress (Reddy et al., 2004), or high heat (Katano et al., 2018). Furthermore, the inability to maintain photosystem repair via transcription (Pfannschmidt and Link, 1994) or translation (Chotewutmontri and Barkan, 2018; Tadini et al., 2020) also elicits a production of singlet oxygen, among other system failures. Additionally, many stresses lead to overlapping transcriptional changes (Kyong, 2007). These stresses often elicit numerous responses such as reduced root length, chlorosis, and necroses (Choudhury et al., 2013; Larkindale, 2005; Stepien and Johnson, 2009; Yu et al., 2012).

A frequently used, simple, fast, and non-invasive way to monitor chloroplast development or its reaction to various stresses is chlorophyll fluorescence (Govindje, 1995; Papageorgiou and Govindjee, 2011; Stirbet and Govindjee, 2011). Primarily, chlorophyll fluorescence focuses on PSII, and its

relationship of energy dissipation to photochemistry (Pérez-Bueno et al., 2019). For photochemistry to work, light is captured by the light harvesting antenna pigments which excites an electron of a pigment molecules. The energy is then passed to an open PSII reaction center where the specialized chlorophyll p680 electron is excited. A pigment molecule in an excited state has three options. The first option is to pass the energy to available electron acceptors towards photochemical work. The second option, if the PSII reaction center is closed (already has an electron), the energy is given off as heat. The third option is when the excited energy is released as light energy and fluorescence occurs (Baker, 2008; Murchie and Lawson, 2013). The competition between all three energy outcomes can be taken advantage of by using a very quick high intensity saturation light pulse that triggers light emission (maximum fluorescence, F_m) and compare that to minimum fluorescence (F_0), background noise. These two measurements allows the calculation of maximum quantum yield of PSII using the equation $(F_m-F_0)/F_m$ or F_v/F_m (Maxwell and Johnson, 2000). For most plants the average F_v/F_m is around 0.80 and any reduction from that is evidence of photoinhibition, or perturbance in chloroplast ability to maintain normal photosynthetic performance (Pérez-Bueno et al., 2019). Since photosynthetic capacity changes depending on different stages of chloroplast development, and all abiotic stresses directly or indirectly cause photoinhibition, F_v/F_m is an effective means of monitoring chloroplast health.

Already it has been observed that mutations in *iojap* result in variegation and abnormal and severely underdeveloped chloroplasts in *Z. mays* (Jenkins, 1924; Shumway and Weier, 1967). Likewise, in *Arabidopsis*, *iojap* mutations delayed chloroplast development and cause chlorosis in the basal region of young leaves, which resulted in a decrease in F_v/F_m (Wang et al., 2016a). Research described in Chapter 2 corroborated chlorosis in the basal region of young leaves, but also revealed variegation that was exacerbated by lower temperature (**Figure 6**). It was concluded that *iojap* mutation at optimal or

low temperature did not affect other physiological process such as bolting time, germination (**Figure 9**) or hypocotyl elongation (**Figure 10**) during etiolation. Further inquiries will focus on development processes that may rely on both plastid differentiation and require heavy photosynthetic activity, such as leaf development and de-etiolation of the cotyledons. Furthermore, variegation only manifests itself during low temperature, yet many abiotic stresses also produce a gene response and accumulation of ROS that cause photoinhibition. Therefore, in both cases, F_v/F_m will be used to monitor the health of the chloroplast in both physiological processes and the response to various abiotic stresses to address whether this phenotypic response is leaf developmentally specific and/or low temperature specific.

Methods

Leaf chronology: Seeds were germinated and grown vertically on standard media plates for 4 days at 22˚C. One seedling each was transferred to the center of a pot, packed lightly with germination soil. Each pot was placed in a tray, making 8 pots per genotype, and one tray for each temperature of 22˚C, 12˚C, and 4˚C. After transfer to soil, the tray was covered with a plastic dome and incubated at 22˚C under long day conditions (16 hours day, 8 hours night at 100 $\mu E \cdot m^{-2} \cdot s^{-1}$) for one day. Afterward, each tray was transferred to its respective temperature under long day conditions. Collection occurred when the tenth, eighth, and sixth leaf reached around 3 mm in length at 22˚C, 12˚C, and 4˚C respectively. Upon collection, the leaves were excised from youngest leaf to oldest leaf at the intersection of the blade and petiole. The leaves were placed in the FluoroCam 800MF closed system (Photon Systems Instruments, Czech Rep), dark acclimated for 30 seconds, and maximum quantum efficiency (F_v/F_m) was recorded. For every measurement for F_v/F_m a saturating pulse at 80% light intensity (3231.1 µE, 450 nm), actinic light 1 at 15% (123.8 µE, 620 nm), and actinic light 2 at 15% (223.0 µE, 450 nm), were used for pre-programed protocol. For each leaf, the average F_v/F_m was statistically analyzed in

GraphPad Prism (v.8) via Two-Way ANOVA with Dunnett's correction, comparing each mean within each row to WT mean in its respective column. Used Tukey's correction for comparing each mean within each row to each mean in its respective column. Three replicates were completed, each having a sample size of N=6 to 8 plants with $p<0.05$.

De-etiolation: About ~200 stratified seeds of WT, *ijT1*, *ijT2,* and *ijT3,* were plated on standard media plates, wrapped in parafilm, and placed horizontally at 22˚C and illuminated (100 $\mu E \cdot m^{-2} \cdot s^{-1}$) for 4 hours. Following illumination, plates were individually wrapped in aluminum foil, and incubated horizontally in darkness at 22˚C for 60 hours. The 60-hour incubation was set up to end so that light exposure started at 7 am (Zeitgeber time 0). After aluminum foil was removed, F_v/F_m was measured for each plate every two hours during daytime hours, with a FluoroCam 800MF closed system (Photon Systems Instruments, Czech Rep), until mutants reached WT levels (~0.80). For each time point F_v/F_m was statistically analyzed in GraphPad Prism (v.8) via Two-Way ANOVA with Dunnett's correction, comparing each mean within each row to WT mean in its respective column. Used Tukey's correction for comparing each mean within each row to each mean in its respective column. Three replicates were completed, each having a sample size of N=100 seedlings with $p<0.05$.

Cold sensitivity of mature leaves: Seeds of WT, *ijT1*, *ijT2*, and *ijT3* were germinated and grown on standard media plates vertically for 4 days at 22˚C. One seedling each was transferred to the center of a pot packed lightly with germination soil. Each pot was placed in a tray, making 8 pots per genotype. The seedlings were then incubated at 22˚C in long-day conditions until ten true leaves were formed, and then transferred to 12˚C. F_v/F_m was measured using a FluoroCam 800MF closed system (Photon Systems Instruments, Czech Rep) for the four oldest leaves, for six days after transfer to low temperature. For each time point F_v/F_m was statistically analyzed in GraphPad Prism (v.8) via Two-Way ANOVA with

Dunnett's correction, comparing each mean within each row to WT mean in its respective column. Used Tukey's correction for comparing each mean within each row to each mean in its respective column. Three replicates were completed, each having a sample size of N=6 plants to 8 with $p<0.05$.

Variegated leaves suffer reversible cold damage: Seeds of WT, *ijT1*, *ijT2*, and *ijT3* were germinated and grown on standard media plates vertically for 4 days at 22˚C. One seedling each was transferred to the center of a pot, packed lightly with germination soil. Each pot was placed in a tray, making 8 pots per genotype. The seedlings were then incubated at 12˚C in long-day conditions until eight true leaves were present then transferred to 22˚C. F_v/F_m was recorded once a day using for the four oldest leaves, for six days using a FluoroCam 800MF closed system (Photon Systems Instruments, Czech Rep). statistically analyzed in GraphPad Prism (v.8) via Two-Way ANOVA with Dunnett's correction, comparing each mean within each row to WT mean in its respective column. Used Tukey's correction for comparing each mean within each row to each mean in its respective column. Three replicates were completed, each having a sample size of N=6 to 8 plants with $p<0.05$.

Various abiotic stress treatments: Seeds of WT, *ijT1*, and *ijT2* were germinated on standard media at 22˚C for 3 days. After 3 days the seedlings were aseptically transferred in a sterile hood to a treatment plate and grown at 22˚C long day conditions, unless otherwise specified. The treatment plates consisted of standard media with chemical additives such as NaCl (100 mM, 150 mM), mannitol (100 mM, 200 mM and 300 mM), rifampicin (0.25 µg/mL, 2.5 µg/mL, and 25 µg/mL), lincomycin (0.1 µg/mL, 1 µg/mL, and 10 µg/mL), and DCMU (1 nM, 10 nM, and 100 nM). Solutions were dissolved in water or DMSO. Additionally, standard plates were used to subject plants to treatments of high light (600 $\mu E \cdot m^{-2} \cdot s^{-1}$ and 400 $\mu E \cdot m^{-2} \cdot s^{-1}$), and temperatures of 32˚C, 28˚C, 12˚C and 4˚C.

To compare primary root length, 6 to 7 seedlings per genotype were plated across the top-most line equally spaced between two 13 mm grids, then grown vertically during the incubation period. A Canon Rebel XS camera attached to a camera stand was used to take whole plate images for each treatment upon transfer to treatment plate. A second image was taken after the first primary root the reached 60 mm grid line or until the first signs of bleaching occurred. The difference of root length between the first and second image was calculated for each genotype per treatment and normalized to the average growth of WT for each treatment. Three replicates were completed, each having a sample size of N=12 to 14 with $p<0.05$.

In order to compare the differences between F_v/F_m values, seedlings were transferred to treatment plates, placing one seedling in the center of a 13 x 13 mm grid, having 12 grids for each genotype. Plates were placed horizontally during the incubation period and grown as described above. F_v/F_m was recorded for each genotype in their respective treatment, until the fourth true leaf of all seedlings was at least 3 mm in length, including petiole. The same data was used to calculate the percentage of difference between WT F_v/F_m control compared to WT of treatments. A FluoroCam 800MF (Photon Systems Instruments, Czech Rep) was used to record F_v/F_m values. Three replicates were completed, each having a sample size of N=12 to 14 seedlings with $p<0.05$. The same data was used to calculate the percent of difference between WT F_v/F_m control compared to WT of treatments, and analyzed using a One-Way ANOVA with Dunnett correction, comparing each mean to WT control.

Polysome gradient fractionation coupled with Q-PCR: *Plant Tissue Preparation:* Around 2000 (~0.04 g) seeds (WT or *jT1*), were prepared (refer to "Standard Growth Conditions"). In a sterile hood, each microfuge tube of seeds was mixed with 1 mL of sterile medium containing 0.05% phytagel (Sigma), with or without rifampicin (100 µg/mL) or lincomycin (1 µg/mL) and spread over standard

plant media plates containing corresponding chemical additives. Plates were wrapped in parafilm, and placed horizontally for stratification at 4˚C for 2 days. Plates were then exposed to light (100 µE) for 4 hours at 22˚C, and afterwards wrapped in aluminum foil to allow for 60 hours of etiolation. After light exposure, cotyledons along with hypocotyls were collected at 30 minutes and 3 hours after illumination as described below in 'Polysome Extraction'. *Polysome Extraction:* The protocol that follows was modified from Alice Barkan procedure (Barkan, 1993). For collection of plant tissue, plates of different time points were submerged in liquid nitrogen. Plant tissue was scraped off the plate using a RNase free steel spatula while submerged in liquid nitrogen, then quickly transferred into a mortar and pestle partially submerged in liquid nitrogen. Two milliliters of freshly made polysome extraction buffer (0.2M Tris, pH 9.0, 0.2M KCl, 35 mM $MgCl_2$, 25 mM EGTA, 5% sucrose, 1% TritonX-100, 2% polyoxyethylene-10-tridecyl ether, 0.5 mg/mL heparin, 50 mM Tris(2-carboxyethyl)phosphine, 100 µg/mL chloramphenicol, and 25 µg/mL cycloheximide) was added to the mortar then the tissue and buffer were ground into a fine powder. Ground tissue was thawed at room temperature and transferred to a 2 mL RNase-free microfuge tube (Invitrogen) to be incubated on ice for 10 minutes. The solution was then centrifuged at 14,000 relative centrifugal force (RCF) at 4˚C for 5 minutes to remove cellular debris. The supernatant was transferred to a new 2 mL microfuge tube. To the supernatant 10% sodium deoxycholate (1/20 volume of sample) was added, vortexed 5 seconds, incubated on ice for 5 minutes followed by centrifugation at 14,000 RCF at 4˚C for 15 minutes. The supernatant was transferred to a new microfuge tube. An aliquot of the sample (1 ml) was added to the sucrose gradient (see 'Preparation of Sucrose Gradients'), while another 1 mL aliquot was kept for total RNA, and was stored at -80˚C. *Preparation of Sucrose Gradients:* Stocks of 50% 45% 40% 35% 30% 25% 20% 15% 10% sucrose, were prepared in 1X gradient salt (40M Tris, pH 8.0, 20 mM KCl, 10 mM $MgCl_2$). A step gradient was

made using 14 mm x 89 mm polypropylene centrifuge tubes (Beckman Coulter), starting with 2 mL of 50% sucrose solution being added, which was placed in -80˚C for 10 minutes. This was followed by an addition of 1 mL of the other sucrose percentages in descending order, freezing after each addition. Gradients were stored at -80˚C, covered with foil. Before use, gradients were thawed overnight at 4˚C. *Sucrose Gradient Fractionation:* Sucrose gradients were run for 3 hours using an Optima L-90K Ultracentrifuge (Beckman Coulter) with SW40-Ti rotor at 33000 rotations per minute (193685 max RCF) at 4˚C. Sucrose gradients were collected using a Density Gradient Fractionator Model 185 with UA-5 absorbance (Instrument Specialty Co.). Fractions were collected in 800 µL aliquots into tubes containing 100 µL 5% SDS/0.2M EDTA solution, making a total of 11 fractions. RNA was then extracted from each fraction with an equal volume of 25:24:1 phenol:chloroform:isoamyl alcohol pH 5.2 (Fisher Bio Reagents) with 1/20 vol of 3M sodium acetate (pH 4.8). The solution was vortexed vigorously for 5 seconds, then set on ice for 5 minutes, the vortexed again for another 5 seconds. The mixed solution was centrifuged at 14,000 RCF at 4˚C for 10 minutes. The upper aqueous layer was transferred to a new 2 mL RNase-free microfuge tube (Invitrogen), with addition of 1 volume of 100% isopropanol and 15 µg/mL GlycoBlue (Invitrogen) and vortexed on medium speed for 1 second. The solution was stored at -20˚C for 1 hour, followed by centrifugation at 14,000 for 15 minutes at 4˚C. Supernatant was removed and 45 µL RNase-free water was added to resuspend the pellet. In addition, DNase Turbo (ThermoScientific) was added following the manufacturer's instructions for a 50 µL reaction. The reaction was incubated for 30 minutes at 37˚C, then placed on ice. The reaction volume was raised to 700 µL with RNase-free water, along with one volume of phenol:chloroform:isoamyl alcohol pH 5.2 (Fisher Bio Reagents). The mixture was then vortexed and centrifuged as described previously. A volume of 600 µL of the aqueous layer was transferred to a new 2 mL microfuge tube,

plus 2 volumes of 100% ethanol. The mixture was vortexed briefly and placed at -20˚C overnight, to be followed by centrifugation at 14000 RPM at 4˚C for 15 minutes. The supernatant was decanted off and the pellet was washed using 70% ethanol, vortexed then centrifuged at 14000 for 5 minutes at 4˚C. The wash was repeated one more time. Residual ethanol was removed by pipette followed by incubation at room temperature for 5 minutes, or until the ethanol was fully evaporated. The dried pellet was re-suspended in RNase free distilled water of 30 µL. NanoDrop™ One/OneC Microvolume UV-Vis Spectrophotometer was used to check for purity and concentration of the RNA. For a control, sucrose gradients were made with EDTA instead of $MgCl_2$, which dissociates ribosomes from mRNA. *Making of cDNA:* Reverse transcription was performed for each fraction and the total RNA counterpart, following the manufacturing instructions of Maxima Reverse Transcriptase. Each reaction contained 100 ng of RNA, and a master mix of gene specific primers. The completed reactions were diluted by a factor of 5 and stored at -20˚C. *Quantitative PCR of polysome fractions:* Quantitative PCR was performed using a CFX96 Touch Deep Well Real-Time PCR Detection System with Luna® Universal qPCR Master Mix (New England Bio Labs). The protocol for amplification followed the manufacturers instruction, adding an extension step of 68˚C, and the optimum annealing temperature of 60˚C. The amplification stage was followed by a melting curve, from 50˚C to 90˚C with a 0.5˚C step every 10 seconds. Primers were made targeting plastid specific genes and internal control references. Primers names and sequences are listed in the 'Appendix.'

Results

Here we investigate whether the detrimental effects of *iojap* in *Arabidopsis* present themselves differently depending on the maturity of the leaf. During the leaf morphology study, we observed that genotypes all suffered transient yellowing at the proximal area of young developing leaves (**Figure 13)**,

but it was more visible in *ijT3* (**Figure 13H**) at 12˚C. However, this yellowing dissipates as the leaf matures in optimal conditions (**Figure 13A-D**). Yet at lower temperatures, *iojap* mutants retain phenotypes such as variegation, yellowing, and virescence all through leaf development (**Figure 13F-H, J-L**). This suggested that the first sign of deleterious effects of *iojap* appears during the early development of leaves. We observed at 22˚C that all *iojap* mutant alleles had a reduced F_v/F_m signal, the only difference being the degree of severity (**Figure 14A**). The strongest phenotype was observed in *ijT3*, where F_v/F_m reading of leaves 1 through 7 were significantly lower than WT. The next affected allele was *ijT1,* where leaves 1 to 6 had a lower F_v/F_m signal than WT. Lastly *ijT2,* displayed the least reduction in F_v/F_m, with only leaves 1 to 5 having lower F_v/F_m signal than WT. It is worth noting that, although the young leaves had significantly lower quantum efficiency than WT, all alleles were able to reach WT F_v/F_m levels at some mature leaf state. Two-Way ANOVA with Tukey correction statistical analysis that compared all alleles to one another revealed that *ijT2* has a significantly higher F_v/F_m than *ijT1* and *ijT3* from leaf 1 to leaf 7, while *ijT1* was only statically higher than *ijT3* early in development (leaves 1 and 2). Lower temperature conditions of 12˚C and 4˚C increased the severity of reduced F_v/F_m in young leaves. For 12˚C growing conditions, all *iojap* mutants had statistically lower F_v/F_m ratio in all leaves (**Figure 14B**). Although neither of the alleles reached WT F_v/F_m levels, all alleles had an upward trajectory as leaves matured, suggesting chloroplast development was delayed, but could recover in due time. Allelic differences at 12˚C also occurred, where *ijT1* was near WT levels at 85% of WT, while

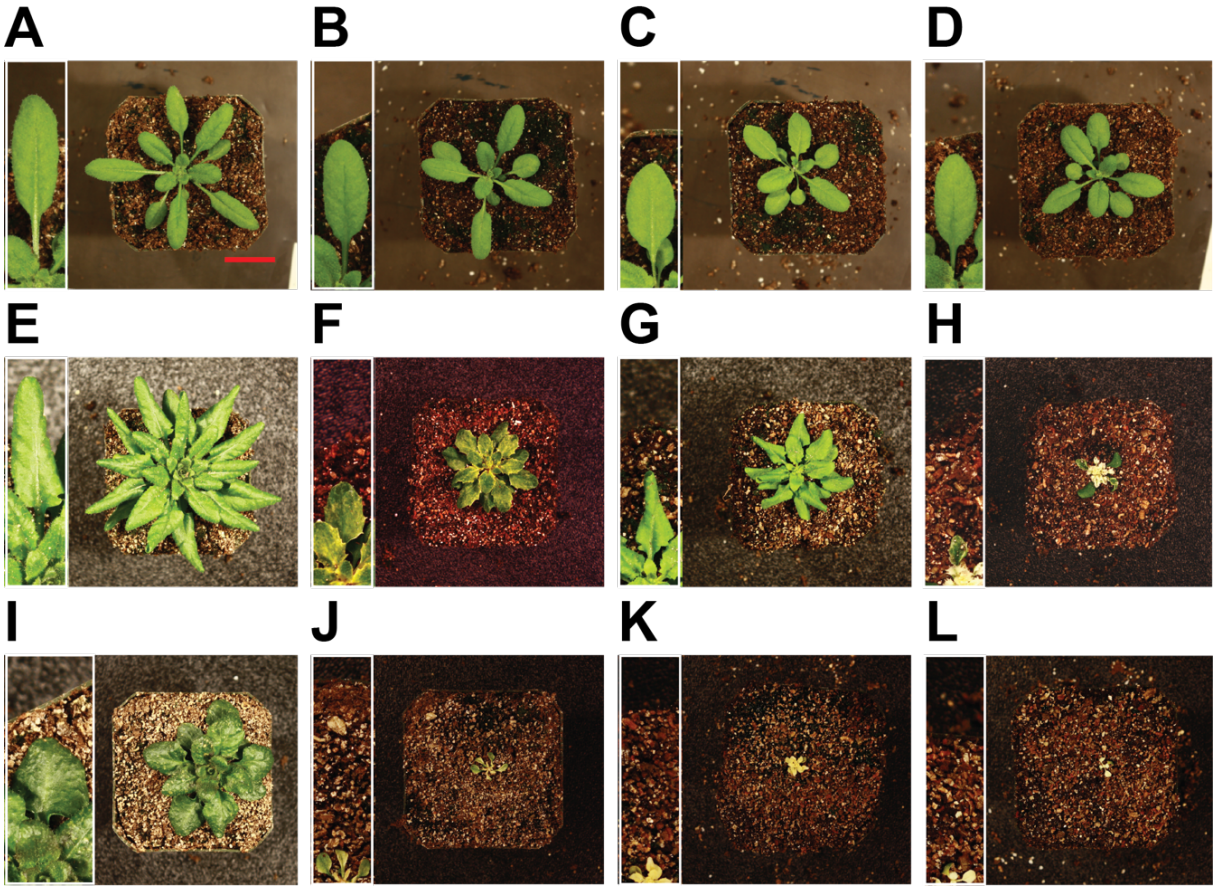

Figure 13: Images of Rosette and Mature Leaf Differences at Bolting.

Plants of WT (A, E, I), *ijT1* (B, F J), *ijT2* (C, G, K) and *ijT3* (D, H, L) were grown in soil at 22˚C (A-D), 12˚C (E-H) and 4˚C (I-L) and imaged at bolting of WT. Inserts with images of individual leaves were enlarged by a factor of four. Scale of 2 cm (red bar).

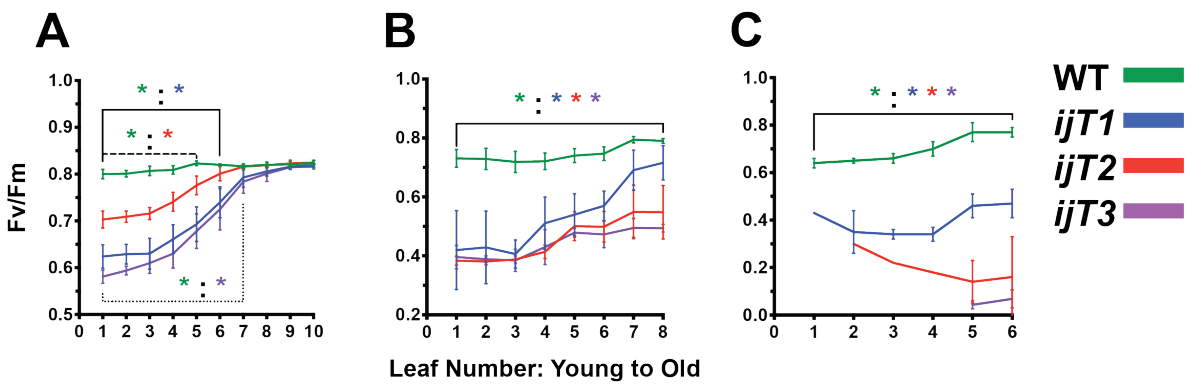

Figure 14: Delays in young leaf development, and increased sensitivity to chilling stress.

WT, *ijT1, ijT2,* and *ijT3* were transferred from plates to the soil at five days old and maintained for one day at 22˚C in long-day conditions (16 hr Light/ 8 hr Dark), then later transferred to their respective temperatures. Plants were collected at A) 10 (22˚C), B) 8 (12˚C), and C) 6 (4˚C) true leaves, where their leaves were excised and placed in chronological order to record F_v/F_m. A) WT maintained ~0.80 F_v/F_m levels, while younger leaves of *ijT1* (1 to 6), *ijT2 (1 to 5),* and *ijT3* (1 to 7) were significantly reduced. Remaining more matured leaves had similar F_v/F_m values as WT. B) All leaves from all iojap mutant alleles had a significant reduction of F_v/F_m compared to WT with a slow improvement of F_v/F_m as leaves got older. C) A slight reduction of WT F_v/F_m in younger leaves 1 through 4, compared to more mature leaves 5 and 6. All iojap mutant allele leaves were significantly reduced compared to WT. Only *ijT1* had recorded signals from all leaves, while *ijT2* and *ijT3* younger leaves were beyond the instrument's limits. Statical analysis of Two-Way ANOVA with Dunnett correction was performed ($p<0.05$, N=8).

ijT2 and *ijT3* were 65% and 60%, respectively. This was a different pattern of sensitivity that was observed at 22˚C, where *ijT2* was the least affected. Further statistical analysis comparing all genotypes revealed that *ijT1* had a significantly higher F_v/F_m than both *ijT2* and *ijT3* from leaves 7 to 8 and 6 to 8, respectively. Much like 12˚C, 4˚C conditions resulted in a further reduction of mutant F_v/F_m values compared to WT (**Figure 14C**). However, there seemed to be no upward trajectory for *ijT1*, and a definite downwards trajectory of F_v/F_m values for the remaining alleles. Furthermore, leaf 1 of *ijT2*, and leaves 1 to 5 of *ijT3* F_v/F_m signals were below the detection limit of the instrument. Early leaf development appeared to be more susceptible to low temperature, and the absence of IOJAP exacerbated this sensitivity. Furthermore, *iojap* mutants caused a reduction of F_v/F_m strongly in early leaf development at all temperatures, but some leaves could recover at optimal and mild low temperatures. This may be a specific leaf development event, where the proplastid differentiated to chloroplast or IOJAP may be required for any differentiation towards chloroplast, as in etioplast to chloroplast in de-etiolation.

To further test whether chloroplast development is altered in *iojap* mutants, we studied de-etiolation of WT, *ijT1*, *ijT2*, and *ijT3* mutants at 22˚C, 12˚C and 4˚C. We obtained similar results as in leaf development. At 22˚C, the F_v/F_m signal during cotyledon de-etiolation was severely reduced in all *iojap* mutants (**Figure 15A**). As time went on and the chloroplast matured, the F_v/F_m signal of all *iojap* alleles approached that of WT, ending around 87% to 80% that of WT. As expected, when de-etiolation occurred at 12˚C the severity of the decrease in F_v/F_m was greater than at 22˚C (**Figure 15B**), ending in the range of 55% to 45% that of WT. For all *iojap* mutants, F_v/F_m was significantly reduced for the time course of the experiment. Unlike at 22˚C, there was not a visibly large upward trend towards WT F_v/F_m over time, having greening rates of $1.15*10^{-4}$, $1.55*10^{-3}$, and $2.47*10^{-3}$ F_v/F_m per hour for *ijT1*, *ijT2* and

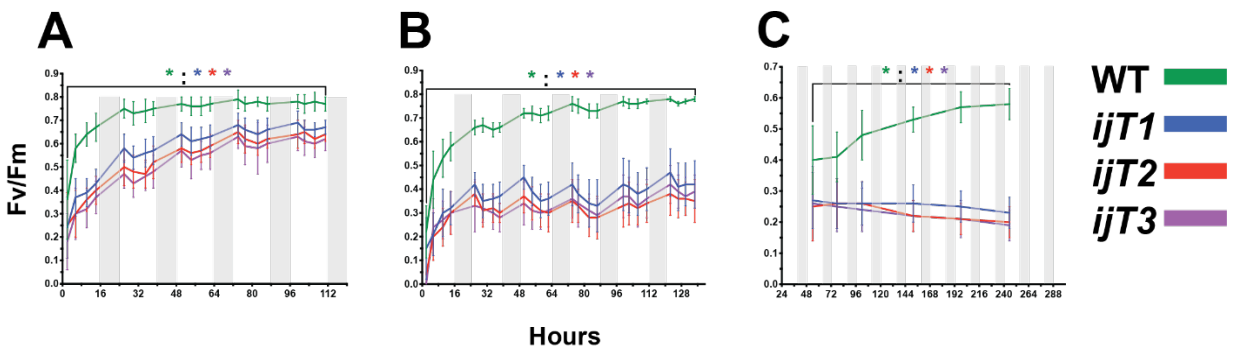

Figure 15: Delayed greening time exacerbated at low temperatures in *iojap* mutants.

Seeds of WT, *ijT1*, *ijT2*, and *ijT3* were etiolated for 50 hours at 22˚C then transferred to respective temperatures (22˚C, 12˚C, and 4˚C), to further incubate for another 10 hours. At Zeitgeber time zero, plates were exposed to light, and their F_v/F_m was measured every 3 hours or once a day. A) At 22˚C all *iojap* mutants F_v/F_m signal was significantly reduced at all time points but continued to increase toward WT values (~0.80) by day five. B) Greening at 12˚C, WT reached ~0.80 F_v/F_m value by days 5, while the *iojap* mutants F_v/F_m values were significantly reduced throughout the experiment. C) All mutants had a significantly lower F_v/F_m values than WT throughout the time course, as well as a continual reduction in F_v/F_m with time. Statistical analysis of Two-Way ANOVA with Dunnett correction was performed ($p<0.05$, N=8).

ijT3, respectively. These greening rates range from 3% to 53% that of WT (data not shown). The even lower temperature of 4˚C revealed that WT did not reach normal 0.8 F_v/F_m levels as in warm temperature, but instead plateaued at 0.55 (**Figure 15C**). However, during over the time course of the experiment from 48 to 240 hours WT had a positive slope. In all temperatures, *iojap* mutants had a significantly lower F_v/F_m signal compared to WT over the course of the experiment. Yet, opposite to that of 22˚C, the slopes for all *iojap* mutants were negative, thus the reduction of F_v/F_m signal grew larger with time, ending with a F_v/F_m signal relative to WT of 40%, 34% and 33%, for *ijT1*, *ijT2*, and *ijT3,* respectively. This suggests that the chloroplasts were getting worse or development had ceased. Overall, mutations in *iojap* disrupted early chloroplast development at 22˚C, as indicted by a decrease in F_v/F_m. This reduction in F_v/F_m and thus early chloroplast development was exacerbated at 12˚C and 4˚C.

The previous experiments showed that IOJAP is important for the development of functional chloroplasts. Now I want to see whether damage is dependent on the stage of leaf development, or also required for mature chloroplast to acclimate to low temperatures. To address the sensitivity of mature chloroplasts in *iojap* mutants WT, *ijT1*, *ijT2*, and *ijT3*, seedlings were grown in soil until they formed ten true leaves. At that time maximum quantum yield (F_v/F_m) was measured for the four oldest leaves. The plants were then immediately transferred to 12˚C followed by a single measurement for five sequential days. At the first measurement at 12˚C, all genotypes dropped in F_v/F_m value, but WT recovered back to initial value on day 3 (**Figure 16**). Unlike WT, the *iojap* mutants remained on a downward trend, never reaching their initial value throughout the course of the experiment (**Figure 16**). There was a slight difference in cold sensitivity among the *iojap* alleles, with *ijT1* similar to WT at 22˚C, and only after exposure to 12˚C was its F_v/F_m significantly reduced and remained this way. The other *iojap* alleles, *ijT2* and *ijT3* had significantly lower F_v/F_m than WT for the entire experiment. It would

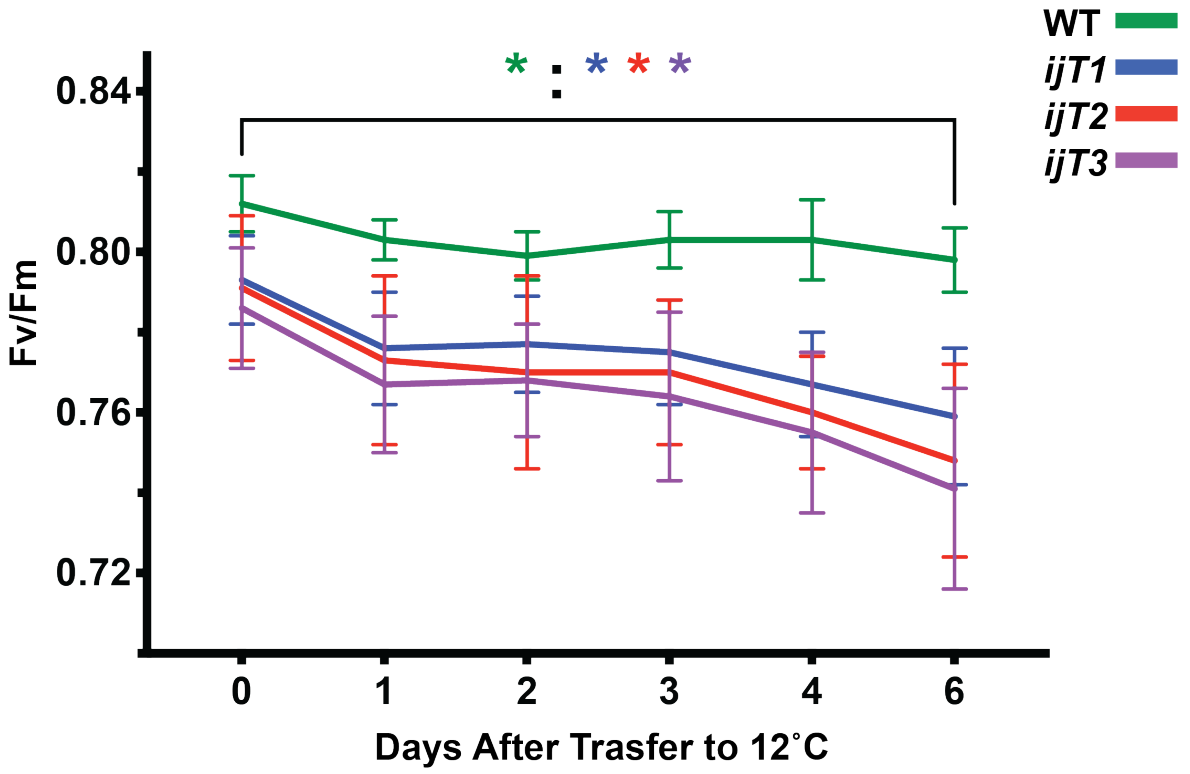

Figure 16: Mature chloroplasts in *iojap* mutants remain cold sensitive.

Four days old seedlings of WT, *ijT1*, *ijT2*, and *ijT3* were transferred to soil, incubated at 22˚C in long-day conditions until ten true leaves formed then transferred to 12˚C. F_v/F_m was recorded for the four oldest leaves, for six days. *ijT1* F_v/F_m was significantly reduced from one day after transfer to the end. WT F_v/F_m levels reminded relative constant while all three *iojap* alleles steadily declined. Statistical analysis of Two-Way ANOVA with Dunnett correction was performed ($p<0.05$, N=8).

seem that IOJAP is required for cold acclimation, even in matured leaves and the matured chloroplasts therein.

Unexpectedly, we found that mature chloroplast populations of *iojap* mutants, were more sensitive to low temperature. Next, we also wanted to know whether or not this cold damage was permanent. WT, *ijT1*, *ijT2*, and *ijT3* 4 days old seedlings were transferred to soil and grown at 12˚C until bolting. At this point, the four oldest leaves were chosen to measure their maximum quantum yield (F_v/F_m) from time of transfer to 22˚C, for five sequential days. As expected, all *iojap* mutants had a significantly reduced F_v/F_m than WT upon the initial measurement at 12˚C (**Figure 17**). Surprisingly, all *iojap* alleles recovered towards WT levels to some degree, although still maintained a significantly lower F_v/F_m than WT throughout the time course of the experiment (**Figure 17**). Curiously, *ijT1* and *ijT2,* had similar trajectories of recovery, while *ijT3* plateaued after the second day of transfer. Variegation caused by low temperature in *iojap* mutants is partially reversible, as seen by an increase F_v/F_m when transferred to 22˚C.

One of the most sensitive plant cellular processes to stress is photosynthesis (Sharkey and Schrader, 2006). Although the primary action of each form of abiotic stress is different, much of the transcriptional response and molecular changes overlap. The common denominator among all stresses is the accumulation of ROS and consequently photoinhibition (Sewelam et al., 2016). From this we hypothesized that any abiotic stress will induce the same phenotype as low temperature in *iojap* mutants. The abiotic stresses that were tested were high light, translation stress induced by the antibiotic spectinomycin, transcription stress caused by the antibiotic rifampicin, PSII stress caused by DCMU, high temperature stress, salinity stress, and osmotic stress. In order to compare these abiotic stresses treatments to chilling stress, we measured their effect on root length and F_v/F_m in mutants relative to

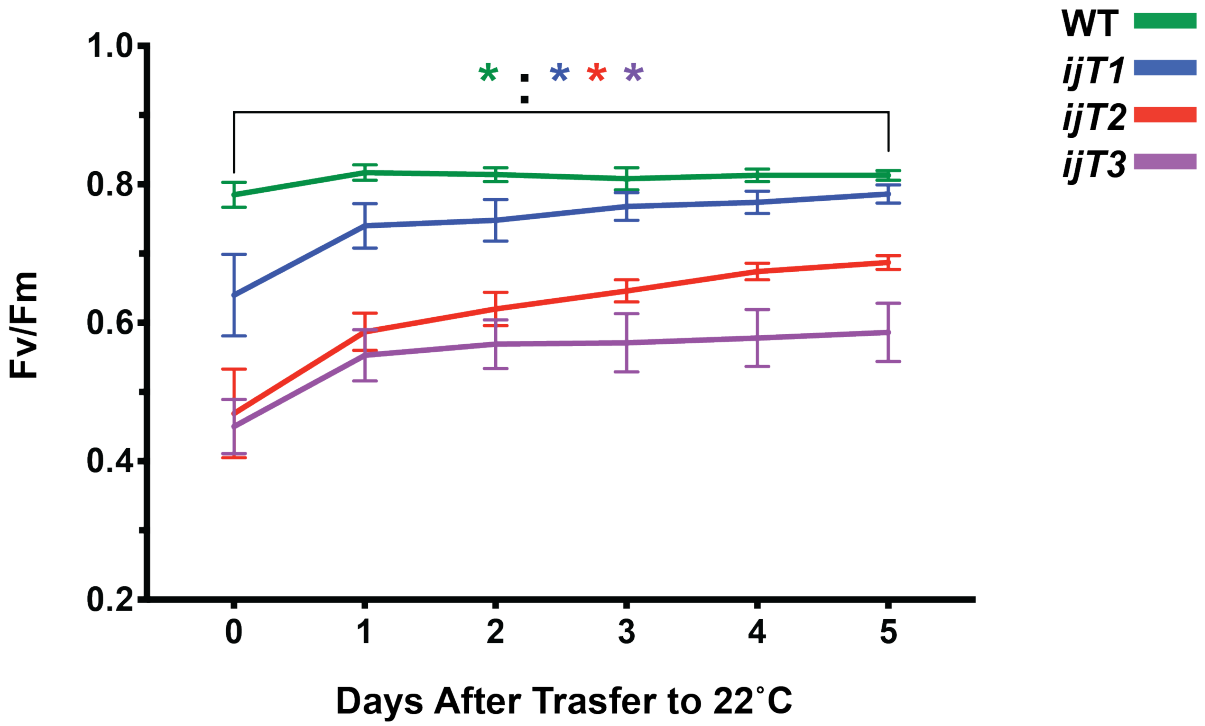

Figure 17: Chloroplast recovery from cold effect.

Plants were grown in soil at 12˚C until bolting then transferred to 22˚C. F_v/F_m was recorded for the four oldest leaves, for six days. All *iojap* mutants had a significantly lower F_v/F_m throughout the time course. Both *ijT1* and *ijT2* had a visibly positive slope toward WT F_v/F_m levels, while *ijT3* plateaued early.

WT (**Figure 18**). Neither of the abiotic stresses reduced root length or F_v/F_m signal to the degree that was observed at low temperature. For root length all abiotic stresses resulted in a root length that was 80% or greater relative to WT, with the exception of 1 µM spectinomycin treatment for *ijT1* having 68% of the root length of WT. Yet, the same treatment of *ijT2* resulted in a root length 96% relative to WT, making close to a 30% difference in root length between the *iojap* alleles. For comparison, *ijT1* and *ijT2* had a root length of 41% and 80% relative to WT, respectively, when grown at 12˚C. This drop in root length was further reduced to 25% for *ijT1,* and 40% for *ijT2* relative to WT, during the 4˚C treatment. This decrease was outside of the range of all other treatment having root length percentages ranging from 105% to 81%, relative to WT. Similarly, the results for F_v/F_m signal showed no severe observable reduction compared to WT at all other treatments other than low temperature. The range of the F_v/F_m signal relative to WT, was 102% to 91%, while low temperature treatment produced a range of 56% to 28% F_v/F_m signal relative to WT. Thus, *iojap* mutants were more strongly affected by low temperature stress than by any of the other stresses. Furthermore, 1 µM spectinomycin treatment for *ijT1* produced an Fv/Fm signal of around 92% relative to WT, that was counter to the effect observed reduction in root length. This led to an investigation whether abiotic treatments differentially affected F_v/F_m and root length.

To investigate the differential effects of abiotic treatments on F_v/F_m and root length we calculated the ratio of percent of F_v/F_m relative to WT over percentage of root length relative to WT for the given treatment (**Figure 19**). For all treatments, this ratio was close to 1, suggesting that the effect was similar for both F_v/F_m (shoot) and root. However, some treatments affected F_v/F_m and root length differently depending on genotype. For instance, in high light stress at 600 µE, root length of *ijT2* had a larger reduction, or was more sensitive, compared to its F_v/F_m value, while at 400 µE this was inverted.

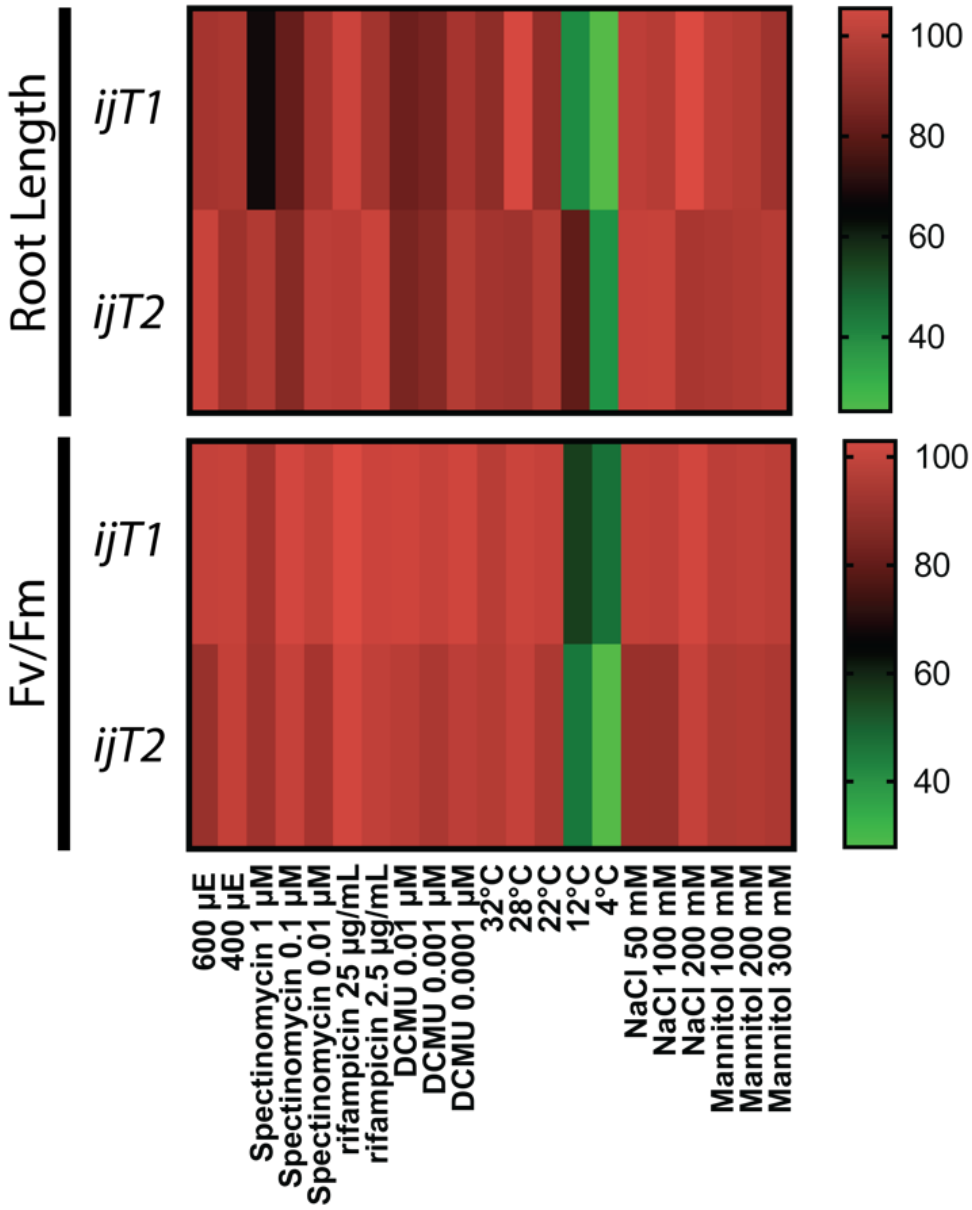

Figure 18: *Iojap* mutants do not show increased sensitivity to other stress treatments.

Seeds of WT, *ijT1*, and *ijT2* were germinated on standard plates, then transferred to treatment plates of spectinomycin, rifampicin (25 µg/ul, 2.5 µg/ul, and 0.25 µg/ul), DCMU (0.01 µM, 0.001 µM, and 0.0001 µM), NaCl (150 µM, 100 µM, and 50 µM), mannitol (300 µM, 200 µM, and 100 µM), and standard plates for high light (600 µE, 400 µE), 32˚C, 28˚C, 22˚C, 12˚C, and 4˚C. For root length, images were taken at transfer and after WT reached 30 mm root length or upon photobleaching. For F_v/F_m measurement, signals were recorded at four true leaves. Top Panel: There was a slight reduction in root length in 1 µM spectinomycin for *ijT1*, with all other treatments beside 12˚C and 4˚C being similar to WT. Bottom Panel: Severe reduction of F_v/F_m at 12˚C and 4˚C while other treatments were similar to WT. Each treatment was normalized to the corresponding WT of that treatment.

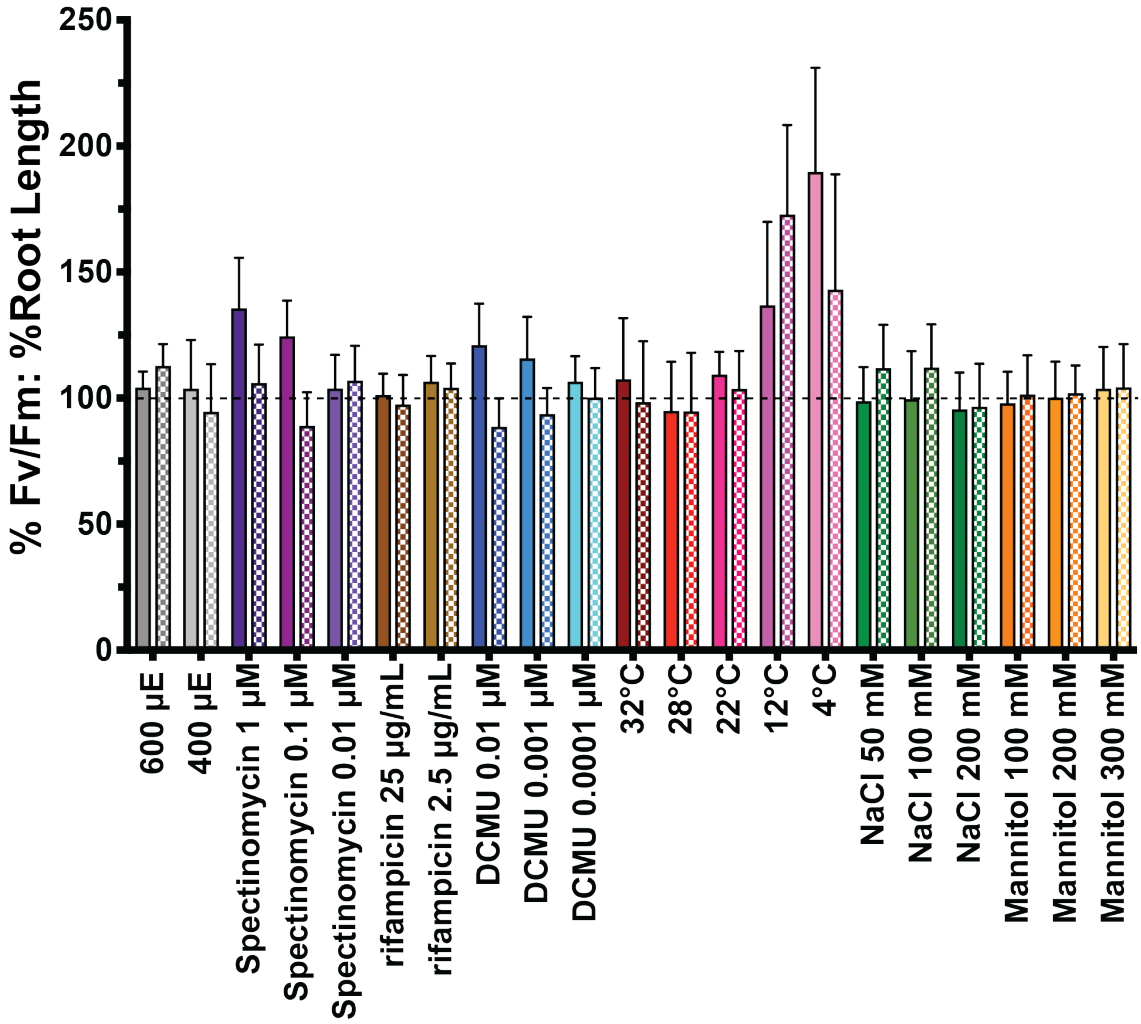

Figure 19: Abiotic stress treatment effect on shoot and root is dependent on *iojap* mutant alleles.

Data from the abiotic stress treatment was used to calculate the sensitivity of treatment in *iojap* mutants in shoots (F_v/F_m) compared to root length. The percent of F_v/F_m of *iojap* relative to WT over the percent *iojap* mutant root length relative to WT control. A percentage above 100 indicates the shoot was less sensitive to treatment than root length. Solid bars denote *ijT1*, and patterned bars denote *ijT2*. Error bars were calculated using error propagation.

A similar pattern was observed in spectinomycin, DCMU, low temperature, and NaCl treatments. For spectinomycin, *ijT1* root length was more sensitive to treatment, while *ijT2* was fairly consistent across concentrations, except for 0.1 μM spectinomycin where F_v/F_m was more sensitive. In DCMU treatments, *ijT1* root length was more affected by treatment while *ijT2* F_v/F_m had greater reduction. Another interesting pattern, was that at low temperature both *ijT1* and *ijT2* root length was more sensitive than F_v/F_m, however, severity of the sensitivity between genotypes at 12˚C was the inverted at 4˚C. When exposed to salinity (NaCl) stress *ijT2* root length was more sensitive than the shoot, while any effect that was observed in root or shoot was similar in *ijT1*. Although one does not expect reduced root length to exactly correlate with reduced F_v/F_m, this does suggest that some treatments alter these two metrics differently. Surprisingly though, some treatments did not conform to expectations. DCMU treatment which binds to PSII and blocks electron transfer, causing ROS accumulation (Hsu et al., 1986; Metz et al., 1986), should lead to a lower F_v/F_m value. However, all DCMU treatments did not reduced F_v/F_m signal of *iojap* having range of 93% to 100% F_v/F_m relative to WT. This begged the question to whether the treatment had miniscule effect on *iojap* because it had a severe effect on WT. If treatment on WT was too severe, then the gap of the difference between WT and *iojap* F_v/F_m may also decrease. This led us to test whether WT was also differentially affected in either of the abiotic treatments.

Most of the treatments used were selected based on published research that tested mutants under conditions that WT could normally acclimate to. To check whether WT was differentially affected in any abiotic treatments the percent of the WT F_v/F_m signal relative to WT F_v/F_m control (standard plate) was calculated (**Figure 20**). Some of the conditions affected F_v/F_m values in WT while others did not lead to a measurable decrease. WT F_v/F_m value was similar to control in most treatments, that is, WT was not sensitive to treatments, in most cases. However, WT was significantly reduced at all rifampicin

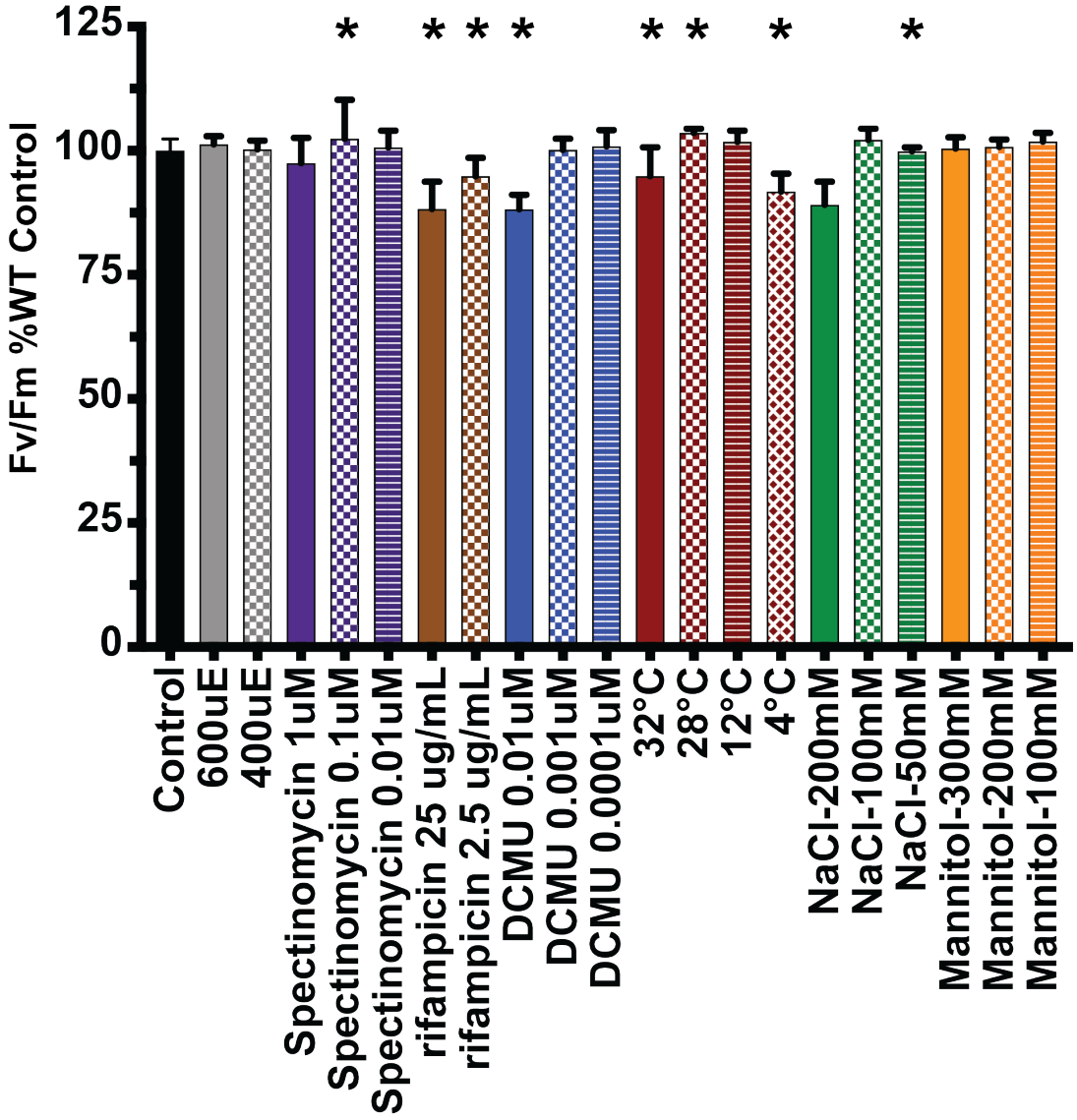

Figure 20: Effect of different stress treatments on F_v/F_m signal in WT.

The percent of WT F_v/F_m was calculated by the F_v/F_m value of abiotic treatment compared to WT control (standard plate, 22˚C). Each treatment is grouped by color, and a different pattern denoted same treatment with a different dose. Asterisk (*) denotes statistical difference compared to control.

concentrations, high temperature, 4˚C, and 200 mM NaCl (**Figure 20**). Furthermore, WT F_v/F_m was significantly reduced in 0.01 μM DCMU treatment, 82% relative to WT. This may explain why we didn't observe a larger reduction of F_v/F_m in *iojap* mutants because WT F_v/F_m reduction decreased the difference in reduction of *iojap* mutants. While this could be one factor for the small difference between WT and *iojap* mutants in some abiotic stresses, it does not account for all of them. In summary, like low temperature, WT was able to acclimate to most abiotic stresses applied in this study, which further underscores that the effect we observed in *iojap* seemingly is due to low temperature alone.

The exact cause of the low temperature phenotype is currently unknown but may rely on the function of IOJAP. Previous investigation in maize, bacteria, and mitochondria suggest IOJAP is involved in translation, since it was observed bound to the 50S ribosome (Han et al., 1993; Häuser et al., 2012; Li et al., 2015; Wanschers et al., 2012). However, a study in *Arabidopsis* suggests it may be involved in transcription and interreacts with PEP associated nucleoid proteins (Wang et al., 2016a, 2017). If IOJAP affects translation I predict that either translation or ribosome assembly is compromised. On the other hand, if IOJAP affects transcription, I predict the mutants will have reduced transcript processing and a reduction of PEP specific transcripts (Han et al., 1993; Wang et al., 2016a).

To investigate whether the deleterious effects of *iojap* were caused by a failure in transcription or transcription, polysome profile coupled with qPCR was employed. Unfortunately, not enough replicates were characterized, so this represents preliminary findings. The general premise is that if translation is aberrant then transcripts would be maintained to a similar level as WT but shift toward the lower end of the gradient, with fewer ribosome per mRNA. If transcription was reduced, we would see lower transcript levels but in the higher density fractions, with more ribosome per mRNA. Polysome profiles we generated using de-etiolated seedling exposed to light for 30 minutes and three hours, labeled T1

(**Figure 21A**) and T3 (**Figure 21B**) respectively. At each time point, four samples were collected: WT (black), *ijT1* (blue), WT with 1 µg/mL lincomycin (red), and 100 µg/mL rifampicin (green). Although each *iojap* allele reacted differentially to low temperature, they all are consistent in phenotype relative to WT. Therefore, *ijT1* was chosen as a representative to study whether *iojap* causes a defect in chloroplast translational or transcriptional. Lincomycin inhibits translation by binding to the 50S ribosome and prevents peptide bond formation (Spížek and Řezanka, 2017), while rifampicin binds to the PEP core protein RPOB subunit to inhibit transcription (Campbell et al., 2001). These treatments were used to mimic a translational and transcriptional mutant defect.

The polysome profiles (**Figure 21**) show both cytoplasmic and chloroplast mRNA and polysomes. In fractions 1 to 3, there is free mRNA not bound to a ribosome. Fractions 4 to 5 show peaks that correspond to both cytoplasmic and chloroplastic ribosome subunits and a single ribosome bound to mRNA. Fractions 6 to 8 and 9 to 11 are low density polysomes and high density polysome, respectively. All polysome profiles were normalized and aligned by their starting points and ending points, where the starting point is defined by a drastic increase in absorbance from baseline (pigments and mRNA in solution), and ending point is defined by a drastic increase of absorbance by blue pushing solution containing bromophenol blue. Overall, all polysome profiles show the distinct features of free mRNA, ribosome and its subunits, and trailing polysomes. However, rifampicin profile ribosome subunit and monosome peaks were shifted right relative to the rest of rest of the profiles, from fraction 4 to 5 to fraction 5 to 6. This is most likely due to slight elution speed differences. Otherwise the rest of the profiles line up well, with the slight shift to the right in *ijT1* T1 peak (blue) of the ribosome monosome (**Figure 21A**). Also, there was a slight perturbance in lincomycin T1 (red) profile, a sudden dip in absorbance before the ribosome subunit peaks (**Figure 21A**).

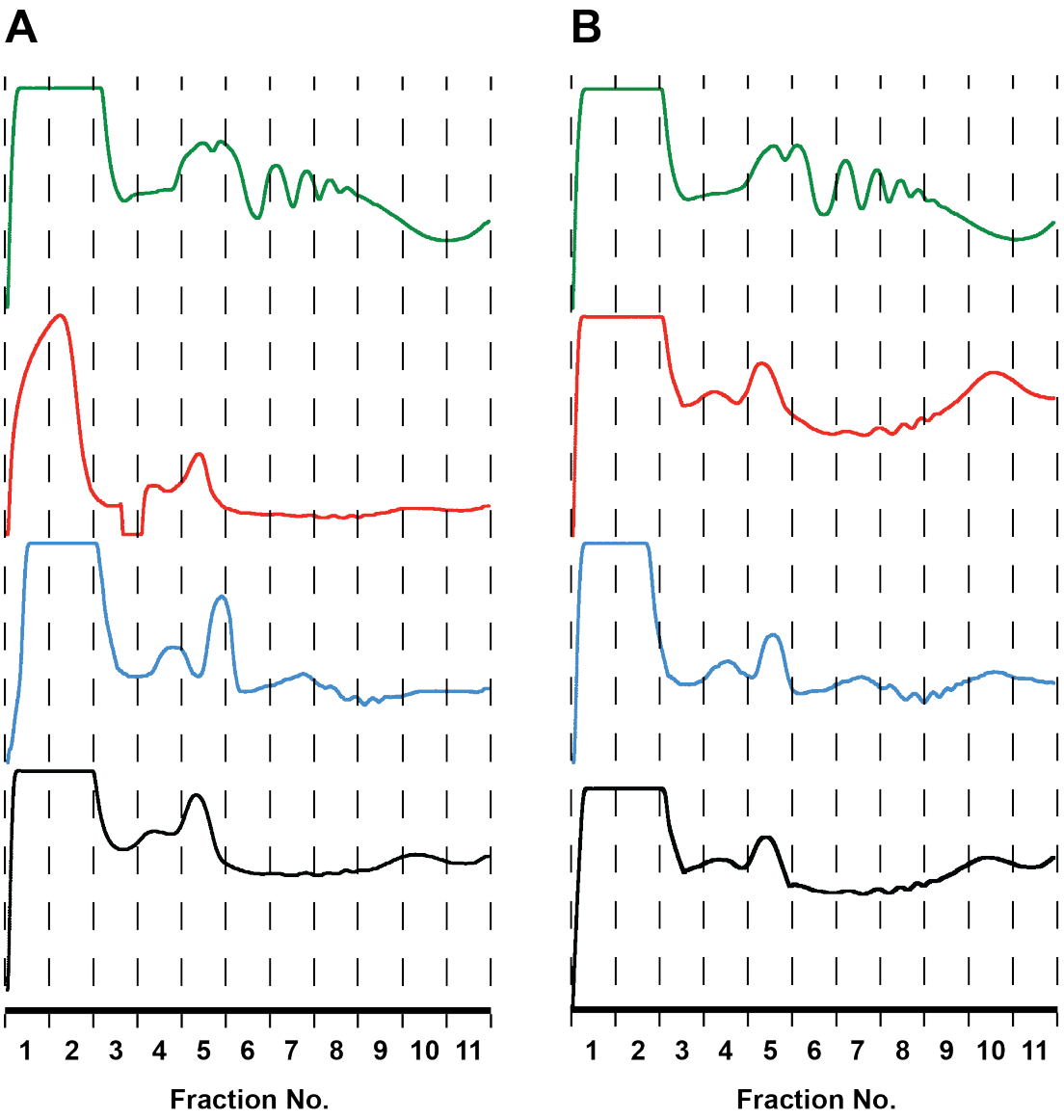

Figure 21: Reduced polysome profiles peaks in *iojap* and treated samples.

Polysome profiles of de-etiolated seedlings of WT (black), *ijT1* (blue), WT treated with lincomycin 1 ug/mL (red), or rifampicin 100 µg/mL (green), were collected after A) 30 minutes and B) 3 hours of light exposure. Profiles were normalized from the first sharp increase of signal and last sharp increase of signal. Eleven fractions were collected and reflect least dense (fraction 1) to most dense (fraction 11).

Fractions of the polysome profiles for both T1 and T3 for WT and *ijT1* were used to isolate and purify mRNA for the amplification of *PSBA*, *CLPP*, *ACCD*, and *GX17* by qPCR. These genes represent three classes of transcriptionally controlled genes, class I (PEP only), II (NEP and PEP) and III (NEP only) where *PSBA*, *CLPP*, and *ACCD* belong to these three categories, respectively. For an internal control, a cytoplasmic gene, *gx17* was used. Each fraction was normalized to the total RNA of internal reference gene, and then by the amount of cDNA produced in each fraction. Then the gene of interest for a specific time point was compared to that gene in WT, making a differential level of expression relative to WT for a given treatment (**Figure 22**). The gene *PSBA* analysis of T3 cannot be compared due to a failure to amplify the polysome fractions 6 to 10. Fractions for *CLPP* revealed that *ijT1* has a higher level of expression in the free mRNA fraction 1 to 3, while in T3 mRNA levels were relatively similar but still suggest higher level of transcript in the fraction 1 to 5 which are free mRNA, ribosome subunits and monosome. ACCD fractions for T1 and similar to that of *CLPP*, having *ijT1* expression of this transcript in fractions 1 to 5. However, in T3, most fraction are slightly higher than WT, but skewed toward fractions 1 to 5. This indicates *CLPP* transcripts were higher in fractions containing free mRNA and mRNA bound to few ribosomes.

The results for polysome profile coupled-qPCR are preliminary and need more data. Yet, these data suggest that in *ijT1* transcript concentration shift towards fractions 1 to 5 (lower density) that contain free mRNA and monosome and its subunits for all plastid genes tested. This may indicate a translational defect, either not having enough ribosomes or a low translation activity such that the available transcripts have low ribosome loading.

Discussion

As noted previously in Chapter 2, mutations in *iojap* seem specific to processes that combine

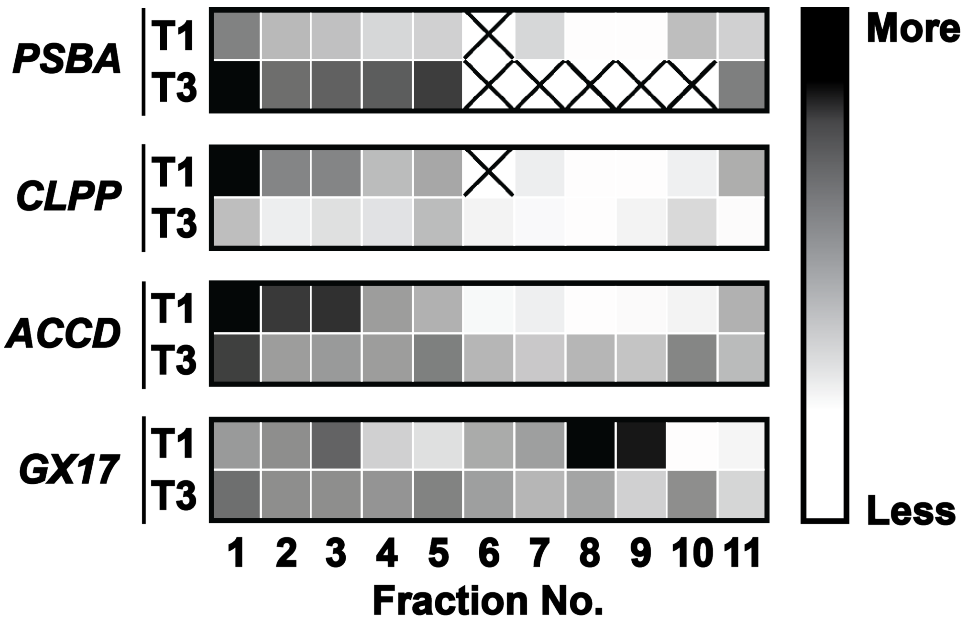

Figure 22: Heatmap of changes in plastid transcript abundance in different polysome fractions of *ijT1*.

Transcripts abundance was normalized to internal reference gene *GX17*, comparing *ijT1* transcripts to WT in each time point, T1 (30 minutes), and T3 (3 hours) after light exposure. The differences between *ijT1* transcripts compared to WT are presented as a ratio, where the total RNA equals 1. Expression difference represented by a color gradient, where *ijT1* transcript expression is more than WT (black) and less than WT (white). Genes analyzed were *PSBA*, *CLPP*, and *ACCD* that are primarily transcribed by PEP, NEP + PEP and NEP, respectively.

differentiation from proplastid to chloroplast and a requirement for a heavy load of photosynthesis. This was based on the observation that no phenotype was observed during germination (**Figure 9**), where chloroplast differentiation occurs, as well as in skotomorphogenesis were growth relies on endosperm energy source (**Figure 10)**. *Iojap* mildly affects leaf development at 22˚C, near the basal region of the leaf, and lower temperatures (12˚C and 4˚C) exacerbate the phenotype (**Figure 6**). Since, the basal region of the leaf in *Arabidopsis* contains differentiating chloroplasts (Nelissen et al., 2016), we suspected younger leaves would be more susceptible to any deleterious effects from *iojap,* especially at low temperatures. In fact, this is what we observed. In all *iojap* alleles, the younger leaves were severely reduced in F_v/F_m compared to WT at low temperatures (**Figure 14**). Additionally, we also observed a similar pattern at 22˚C, having young *iojap* leaves expressing the strongest phenotype, an observation not clearly visualized by leaf morphology (**Figure 6**). Another feature of *iojap* mutation, is that at both 22˚C and 12˚C, the F_v/F_m levels become more similar to WT at a later developmental stage. This illustrates two things. One, the hurdle or damage from the lack of *iojap* was overcome or compensated quickly at 22˚C and more slowly at 12˚C. Furthermore, to reach WT levels of maximum quantum efficiency, the leaf did not require a full population of health chloroplast, as seen by the variegation at 12˚C. However, at the lowest temperature (4˚C), *ijT2* and *ijT3*, were unable to recover, and progressively got worse with leaf age (**Figure 14**). Therefore, the damaged accrued by the loss of IOAJP was not able to be compensated. This pattern was observed during leaf development and was also paralleled during de-etiolation (**Figure 15**). This suggests that IOJAP function is required in processes that the differentiation of proplastids to chloroplasts and etioplast to chloroplast have in common (Nelissen et al., 2016; Pogson et al., 2015). It is interesting to note that young leaves as a whole have been reported to be more resilient and acclimated faster to low temperatures, (Takagi et al., 2003;

Wanner and Junttila, 1999), especially when they start developing when the plant is already in cold conditions (Sowiński et al., 2005; Stitt and Hurry, 2002; Wang et al., 2016b). Yet, this ability is lost in *iojap* mutants, and maybe linked to the delayed development of thylakoid membranes (Wang et al., 2016a). The predicted role of IOJAP in chloroplast development suggests that low temp stress should not affect mature chloroplasts. Yet, when plants grown at 22˚C were subjected to 12˚C, mature leaves of *iojap* mutants progressively decreased their F_v/F_m values, while WT recovered to 22˚C F_v/F_m levels (**Figure 16**). This observation is very different from what is observed in maize where severe variegation not only occurs at optimal temperature, but is permanent, the *iojap* white tissue chloroplast do not recover (Jenkins, 1924; Shumway and Weier, 1967). Moreover, *iojap* mature leaves on plants grown at 12˚C that were transferred to 22˚C, recovered toward WT levels (**Figure 17**). Taken together, this may suggest that IOJAP plays an important role in an early stage of chloroplast development, that is sensitive to cold, but any damage accrued or developmental stasis that is induced can be reversed. Furthermore, mature chloroplasts are still susceptible to low temperature, and the function of IOJAP is required to maintain chloroplast heath under chilling stress. However, the decreased F_v/F_m observed in both warm to cold and cold to warm, could be from a significant portion of the chloroplast population stuck or delayed enough to be in that sensitive developmental state. Another possibility is that without IOJAP, the chloroplast has an inherent level of stress that can be overcome or dealt with at optimal conditions, but cold stress specifically magnifies this problem. This results in deleterious effects we observed in *iojap.*

When we subjected *iojap* plants to other forms of stress, such as salinity, drought, photosynthesis inhibitor, translation inhibitor, transcription inhibitor, high light, and high temperature, the results were surprising (**Figure 18**). None of the treatments elicited phenotypes as severe as what was observed in low temperature. Although all other treatments had some reduction in root length and

F_v/F_m relative to WT, most did not reach root lengths lower than 80% of WT. The exception to this trend was spectinomycin (translation inhibitor), where the root length was 70% of WT. Oddly enough, this concentration of spectinomycin (1 μM), often caused photobleaching, but unexpectedly led to significantly higher F_v/F_m signals than the WT control (**Figure 19**). Another interesting observation is that *ijT1* root length was more sensitive to spectinomycin (1 μM) than *ijT2*. In comparison to the other treatment, both 12˚C and 4˚C all were below 50% of that of WT. The treatment levels for high light, temperature, salinity, and osmotic stress were selected to be near the edge of the acclimation ability of *Arabidopsis*. However, when WT F_v/F_m levels of treatments are compared to the F_v/F_m levels of the control, there was a significant reduction of F_v/F_m in many treatments (**Figure 20**). Yet these treatments still did not produce a severe reduction in F_v/F_m or root length in the *iojap* mutants. This could mean that the phenotypes we observe are directly linked to cold, or that the treatments were detrimental to both WT and *iojap* to such an extent that any difference were negligible. For example, in 200 mM and 300 mM mannitol treatments, WT root length is around 50% of control plate (data not shown), and also showed visible deleterious effects such as translucent leaves, and an increase lateral root formation. Thus, the effect of mannitol on WT at the said concentrations, were so severe it damaged both WT and *iojap* mutants to the extend, it was beyond the capacity of either genotype to handle. At the same time 12˚C does not elicit a phenotype in WT and yet we see a severe effect in *iojap* mutants. Thus, the lack of effect of other abiotic treatments in WT, does not warrant the presumption the treatment was ineffective nor surprising to be absent in *iojap* especially the phenotype is low temperature dependent. Nevertheless, the other stresses were unable to causes a differential effect between WT and the *iojap* mutants comparable to what was observed at low temperature.

Abiotic stresses cause a certain level of accumulation of ROS, therefore if the cause of cold stress was due to high ROS production, we would expect similar phenotypes from other stresses. Yet, none of the other stress treatments were comparable to chilling stress, which would suggest another mechanism of malfunction. On the other hand, the majority of literature suggests that IOJAP is involved in translation regulation or ribosome assemble in maize, mammalian mitochondria and bacteria (Häuser et al., 2012; Li et al., 2015; Rorbach et al., 2012; Siemenroth et al., 1980). But for some reason at 22˚C there a subtle to no difference in *iojap* root length (**Figure 4**), or in F_v/F_m in mature leaves (**Figure11 & 14**). With the assumption that *iojap* translation is less efficient at 22˚C, and low temperature results in stress load beyond the capability of *iojap* mutants, then, we would expect spectinomycin, a translation inhibitor, to mimic the *iojap* low temperature phenotype. But this is not what was observed. Spectinomycin treatment resulted in an F_v/F_m and root length similar to WT (**Figure 19**). Likewise, one study in *Arabidopsis* suggested that IOJAP functions in transcription (Wang et al., 2016a), yet rifampicin treatment was also ineffective in phenocopying the *iojap* cold phenotype. Maybe, IOJAP functions in the cold gene response, however, *iojap* is continuously expressed throughout for most of the plant life cycle and developmental stages and does not change when exposed to the cold. This may indicate IOJAP function may not be a response to the cold, but the particular function in itself is sensitive to the cold. If IOJAP function is to increase stability, either ensuring strong binding interaction or processivity in translation, then cold causes these processes to be more unstable, while at 22˚C this process maintains a certain level of stability, and thus few defects occur. This is similar to what is observed in *crass* and *cp20a* mutants. CRASS protein binds to the 30S subunit, while CP29a binds to mRNA transcripts in chloroplasts (Kupsch et al., 2012; Pulido et al., 2018). Both mutants have a WT phenotype at 22˚C, and look visually normal, but elicit decrease translation and reduced F_v/F_m when

exposed to lower temperatures. Both are speculated to be required for stability of either ribosome assembly, ribosome interaction with the transcript, or stability of the mRNA itself. In the absence of CRASS or CP29A, the stability they offer is no longer there, and that is further disrupted by low temperature. Another possibility is that IOJAP increases the stability of ribosome interactions with the transcript or of the monosome itself during translation. It was found that cold temperature increases the frequency of ribosomal pausing in tomatoes. Focusing on the PSII D1 transcript, *PSBA*, it was demonstrated that exposure to low temperature increased ribosome pausing to such a degree, that D1 production was reduced, causing a reduction of F_v/F_m (Grennan and Ort, 2007). This may suggest that certain translation processes are sensitive to the cold, and IOJAP may be functioning to ameliorate cold effects.

The largest hole in the IOJAP story is the role it plays in the chloroplast. Much of the work in maize, bacteria, and mitochondria suggest it is involved either in translation or in ribosome assembly. However, one study in maize suggests that lack of IOJAP causes aberrant mRNA processing, but this could be due to low levels of protein to process mRNA transcripts. Yet, another study showed that *iojap* had reduced PEP transcripts and translation was barely affected (Wang et al., 2016a). This study set out to bridge that gap by performing polysome profiling coupled to qPCR. However, due to time limitations, only a few samples could be completely analyzed. The analysis that was completed gave promising results. When looking at *CLPP* and *ACCD* gene expression and position in polysome gradient relative to WT, there was a higher level of transcript in fractions 1 to 5 that contain the free RNA, ribosome subunit, and monosome. This suggests that translation was reduced compared to WT. Since *CLPP* and *ACCD* are class II and class III respectively, then *iojap* does not seem to have only PEP-specific effects. The class I gene studied, *PSBA* could not be fully analyzed, but for the early time point (T1), where

there was a higher representation of *PSBA* in fractions 1 to 5, which matches the pattern we see for the other genes in this study. Altogether the polysome profile coupled to qPCR experiment suggests that translation is reduced overall, while transcription was not affected. However, further analysis is required. Other treatments in waiting for analysis are lincomycin and rifampicin. Lincomycin is a chloroplast translation inhibitor, while rifampicin reduces PEP transcription. If one of these treatments patterns resemble that of *ijT1* then it will either support or reject the current pre-liminary results.

CHAPTER FOUR
CONCLUSION AND FUTURE DIRECTIONS

IOJAP research has been ongoing for close to 100 years and was first reported in maize by Merel T Jenkins in 1924. Since then, the *iojap* maize mutant was extensively characterized showing leaf abnormalities, variegation, and reproductive defects (Coe et al., 1988; Jenkins, 1924). Here, we added to this characterization of *iojap* mutants using *Arabidopsis thaliana*. Unlike maize, a monocot, *Arabidopsis* is a dicot, and thus offers insights into the different effects of loss of IOJAP function between these two clades. This work established that the *iojap* phenotype is subtle at optimal conditions, causing only a small decrease in root length and reduction in maximum quantum efficiency (F_v/F_m), particularly in young leaves. Our finding was also corroborated by a recent study that demonstrated that *iojap* mutant affected young leaves, causing chlorosis near the basal region (Wang et al., 2016a). This observation was expanded upon here, demonstrating not only that young leaves were more affected in *iojap* mutants but this reduction in F_v/F_m also occurred in early stage of chloroplast development from proplastid or etioplast to chloroplast. Hence, during de-etiolation (greening), *iojap* mutants lagged behind WT, having reduced F_v/F_m signal. More interestingly, though, was the discovery that any defect that was observed at optimal temperature was strongly exacerbated by growing *iojap* mutant plants at low temperature (12˚C and 4˚C). Surprisingly, growth at low temperature also revealed similar phenotypes as those observed in maize, such as variegation, and aberrant leaf morphology. What may be as intriguing is that of the abiotic stresses tested, low temperature stress alone precipitated these severe *iojap* mutant phenotypes. Additionally, while maize incurred germination defects (Coe et al., 1982), this was not observed in *Arabidopsis.* Another, novel characterization in regard to *iojap* was the lack of deleterious effects on etiolation, relative to its hypocotyl length. Both processes of germination and etiolation remained stable in low temperature, bolstering the idea, that *iojap* mutants disrupt early development of chloroplasts.

Another aspect of this study was to understand the molecular role IOJAP plays in plant development. In most of the literature, IOJAP was found to regulate translation, and is verified to bind to the ribosome, specifically RPL14 (Han and Martienssen, 1995; Siemenroth et al., 1980). Yet, a most recent paper suggested that, in *Arabidopsis*, IOJAP is involved in transcription. This claim was bolstered by IOJAP interaction with PEP associated nucleoid proteins and a reduction in PEP targeted transcripts (Wang et al., 2016a). To address this discrepancy of possible IOJAP functions, polysome profiling of a few ribosomal transcripts by qPCR was attempted on de-etiolating seedlings, early in the transformation from etioplast to chloroplast. Preliminary findings suggest that *iojap* mutant transcripts were skewed toward low ribosome loading. This may indicate a translational defect. If it were a transcription defect, then it was assumed to lead to an increase in high polysome loading per transcript. Also, the genes tested represent the three categories of plastid transcripts, class I (PEP only), class II (NEP and PEP), and class III (NEP only). In other studies, there were only a decrease in PEP targeted transcripts, yet in this study, each class was similarly affected. However, the results presented here are not conclusive and more work needs to be done.

A possible way to assess the gaps in knowledge of IOJAP function would be to further investigate possible dysfunctions in chloroplast transcription and translation. One approach would be to expand the polysome profiling coupled with qPCR by analyzing the behavior of additional genes in the transcript categories, such as rbcL (class I), rRNA16S (class II) and rpoA (class III). Furthermore, this procedure can be repeated using the transcription inhibitor tagetitoxin, or the translation inhibitor lincomycin. These two chemicals are presumed to mimic a transcriptional or translational mutation defect, respectively. However, while polysome profiling coupled with qPCR is relatively economic, it is also laborious and can have multiple sources for potential error. A more robust and comprehensive

approach would be ribosome foot printing. This would allow us to observe the translational output as well as transcriptome abundance in one step. Also, this is a quantitative genome-wide approach, allowing analysis of the entire transcriptome of the chloroplast.

A question that still needs to be addressed about IOJAP in *Arabidopsis* is whether it interacts with the 50S ribosome, as observed in maize and other non-plant species. Although, it was observed that IOJAP interreacts with PEP nucleoid associated proteins, no attempts have been made to investigate whether or not *Arabidopsis* IOJAP also interacts with the ribosome. A two-pronged approach could be used. First, pull down assays using IOJAP, IOJAP minus the DUF143 domain, or IOJAP DUF143 only as bait, and PRPL14, PEP-associated nucleoid protein FLN1, and PEP protein RPOC1 as prey. In recent work, GFP fusion constructs of IOJAP DUF143 only and IOJAP minus DUF143 were investigated. IOJAP DUF143 only was able to localize to the chloroplast nucleoid but was unable to interact with FLN1. However, IOJAP minus DUF143 localized diffusely to the nucleoid and was able to interact with FLN1. This suggest the DUF143 domain and the N- and C-terminal extensions both offer binding interaction that may be independent from one another. Thus, the pull-down described above will allow for the testing of binding of the ribosome and what feature of IOJAP in necessary to do so. Secondly, transient expression using BIFC constructs could be performed. Constructs containing a plastid transit peptide fused to PRPL14 and PRPL19 would be made having the C-terminus YFP, while IOJAP having the N-terminal part of YFP. These constructs could then be expressed using the transient expression system described in chapter 2. Since this method was used to determine the positive interaction of FLN1, FLN1 fused to C-terminal YFP will be used as a control. Together both would confirm whether or not IOJAP also interacts with the chloroplast ribosome.

LIST OF REFERENCES

Aach, H., Bode, H., Robinson, D.G., and Graebe, J.E. (1997). ent-Kaurene synthase is located in proplastids of meristematic shoot tissues. Planta *202*, 211–219.

Ahmed, T., Yin, Z., and Bhushan, S. (2016). Cryo-EM structure of the large subunit of the spinach chloroplast ribosome. Sci Rep *6*.

Albrecht, V., Ingenfeld, A., and Apel, K. (2006). Characterization of the snowy cotyledon 1 mutant of Arabidopsis thaliana: the impact of chloroplast elongation factor G on chloroplast development and plant vitality. Plant Mol. Biol. *60*, 507–518.

Allen, R.D. (1995). Dissection of Oxidative Stress Tolerance Using Transgenic Plants. Plant Physiol *107*, 1049–1054.

Allorent, G., Courtois, F., Chevalier, F., and Lerbs-Mache, S. (2013). Plastid gene expression during chloroplast differentiation and dedifferentiation into non-photosynthetic plastids during seed formation. Plant Mol Biol *82*, 59–70.

Aluru, M.R., Yu, F., Fu, A., and Rodermel, S. (2006). Arabidopsis variegation mutants: new insights into chloroplast biogenesis. J Exp Bot *57*, 1871–1881.

Angelovici, R., Galili, G., Fernie, A.R., and Fait, A. (2010). Seed desiccation: a bridge between maturation and germination. Trends in Plant Science *15*, 211–218.

Armenteros, J.J.A., Salvatore, M., Emanuelsson, O., Winther, O., Heijne, G. von, Elofsson, A., and Nielsen, H. (2019a). Detecting sequence signals in targeting peptides using deep learning. Life Science Alliance *2*.

Armenteros, J.J.A., Salvatore, M., Emanuelsson, O., Winther, O., Heijne, G. von, Elofsson, A., and Nielsen, H. (2019b). Detecting sequence signals in targeting peptides using deep learning. Life Science Alliance *2*.

Aro, E.-M., Virgin, I., and Andersson, B. (1993). Photoinhibition of Photosystem II. Inactivation, protein damage and turnover. Biochimica et Biophysica Acta (BBA) - Bioenergetics *1143*, 113–134.

Bahl, J., Francke, B., and Monéger, R. (1976). Lipid composition of envelopes, prolamellar bodies and other plastid membranes in etiolated, green and greening wheat leaves. Planta *129*, 193–201.

Bain, J.M. (1968). A CRYSTALLINE INCLUSION IN THE CHLOROPLASTS OF THE OUTER HYPODERMAL CELLS OF THE BANANA FRUIT. 8.

Baker, N.R. (2008). Chlorophyll Fluorescence: A Probe of Photosynthesis In Vivo. Annual Review of Plant Biology *59*, 89–113.

Baker, N.R., and Butler, W.L. (1976). Development of the Primary Photochemical Apparatus of Photosynthesis during Greening of Etiolated Bean Leaves. Plant Physiol. *58*, 526–529.

Barkan, A. (1988). Proteins encoded by a complex chloroplast transcription unit are each translated from both monocistronic and polycistronic mRNAs. EMBO J. *7*, 2637–2644.

Barkan, A. (1993). Nuclear Mutants of Maize with Defects in Chloroplast Polysome Assembly Have Altered Chloroplast RNA Metabolism. The Plant Cell *5*, 389–402.

Barkan, A. (2011). Expression of Plastid Genes: Organelle-Specific Elaborations on a Prokaryotic Scaffold. Plant Physiology *155*, 1520–1532.

Baumgartner, B.J., Rapp, J.C., and Mullet, J.E. (1993). Plastid Genes Encoding the Transcription/Translation Apparatus Are Differentially Transcribed Early in Barley (Hordeum vulgare) Chloroplast Development (Evidence for Selective Stabilization of psbA mRNA). Plant Physiol. *101*, 781–791.

Bechtold, U., and Field, B. (2018a). Molecular mechanisms controlling plant growth during abiotic stress. J Exp Bot *69*, 2753–2758.

Bechtold, U., and Field, B. (2018b). Molecular mechanisms controlling plant growth during abiotic stress. J Exp Bot *69*, 2753–2758.

Bieri, P., Leibundgut, M., Saurer, M., Boehringer, D., and Ban, N. (2017). The complete structure of the chloroplast 70S ribosome in complex with translation factor pY. EMBO J *36*, 475–486.

Blomqvist, L.A., Ryberg, M., and Sundqvist, C. (2006). Proteomic analysis of the etioplast inner membranes of wheat (Triticum aestivum) by two-dimensional electrophoresis and mass spectrometry. Physiologia Plantarum *128*, 368–381.

Bobik, K., and Burch-Smith, T.M. (2015). Chloroplast signaling within, between and beyond cells. Front. Plant Sci. *6*.

Bogorad, L. (2008). Evolution of early eukaryotic cells: genomes, proteomes, and compartments. Photosyn. Res. *95*, 11–21.

Börner, T., Zhelyazkova, P., Legen, J., and Schmitz-Linneweber, C. (2014). Chloroplast Gene Expression—RNA Synthesis and Processing. In Plastid Biology, (Springer, New York, NY), pp. 3–47.

Börner, T., Aleynikova, A.Yu., Zubo, Y.O., and Kusnetsov, V.V. (2015). Chloroplast RNA polymerases: Role in chloroplast biogenesis. Biochimica et Biophysica Acta (BBA) - Bioenergetics *1847*, 761–769.

Bouvier, F., Backhaus, R.A., and Camara, B. (1998). Induction and Control of Chromoplast-specific Carotenoid Genes by Oxidative Stress. J. Biol. Chem. *273*, 30651–30659.

Bowman, J.L. (1994). Arabidopsis: an atlas of morphology and development (New York, NY: Springer).

Boyes, D.C., Zayed, A.M., Ascenzi, R., McCaskill, A.J., Hoffman, N.E., Davis, K.R., and Görlach, J. Growth Stage–Based Phenotypic Analysis of Arabidopsis: A Model for High Throughput Functional Genomics in Plants. 12.

Bruce, B.D. (2000). Chloroplast transit peptides: structure, function and evolution. Trends in Cell Biology *10*, 440–447.

van Buer, J., Prescher, A., and Baier, M. (2019). Cold-priming of chloroplast ROS signalling is developmentally regulated and is locally controlled at the thylakoid membrane. Scientific Reports *9*, 3022.

Butland, G., Peregrín-Alvarez, J.M., Li, J., Yang, W., Yang, X., Canadien, V., Starostine, A., Richards, D., Beattie, B., Krogan, N., et al. (2005). Interaction network containing conserved and essential protein complexes in Escherichia coli. Nature *433*, 531–537.

Byrne, M.E., Groover, A.T., Fontana, J.R., and Martienssen, R.A. (2003). Phyllotactic pattern and stem cell fate are determined by the Arabidopsis homeobox gene BELLRINGER. Development *130*, 3941–3950.

Campbell, E.A., Korzheva, N., Mustaev, A., Murakami, K., Nair, S., Goldfarb, A., and Darst, S.A. (2001). Structural mechanism for rifampicin inhibition of bacterial RNA polymerase. Cell *104*, 901–912.

Casadoro, G., and Rascio, N. (1977). Morphogenesis of membrane-bound bodies in belladonna (Atropa belladonna L.) plastids. Journal of Ultrastructure Research *61*, 186–192.

Charuvi, D., Kiss, V., Nevo, R., Shimoni, E., Adam, Z., and Reich, Z. (2012). Gain and Loss of Photosynthetic Membranes during Plastid Differentiation in the Shoot Apex of *Arabidopsis*. Plant Cell *24*, 1143–1157.

Chi-Ham, C.L., Keaton, M.A., Cannon, G.C., and Heinhorst, S. (2002). The DNA-compacting protein DCP68 from soybean chloroplasts is ferredoxin:sulfite reductase and co-localizes with the organellar nucleoid. Plant Mol. Biol. *49*, 621–631.

Chinnusamy, V., Zhu, J.-K., and Sunkar, R. (2010). Gene regulation during cold stress acclimation in plants. Methods Mol. Biol. *639*, 39–55.

Chotewutmontri, P., and Barkan, A. (2016). Dynamics of Chloroplast Translation during Chloroplast Differentiation in Maize. PLOS Genetics *12*, e1006106.

Chotewutmontri, P., and Barkan, A. (2018). Multilevel effects of light on ribosome dynamics in chloroplasts program genome-wide and psbA-specific changes in translation. PLOS Genetics *14*, e1007555.

Choudhury, S., Panda, P., Sahoo, L., and Panda, S.K. (2013). Reactive oxygen species signaling in plants under abiotic stress. Plant Signaling & Behavior *8*, e23681.

Ciarmiello, L.F., Woodrow, P., Fuggi, A., Pontecorvo, G., and Carillo, P. (2011). Plant Genes for Abiotic Stress. Abiotic Stress in Plants - Mechanisms and Adaptations.

Coe, E.H., Thompson, D.L., and Walbot, V. (1982). NUCLEAR GENES AND CHLOROPLAST MODIFICATIONS IN MAIZE. 18.

Coe, E.H., Thompson, D., and Walbot, V. (1988). Phenotypes Mediated by the Iojap Genotype in Maize. American Journal of Botany *75*, 634.

Consonni, G., Geuna, F., Gavazzi, G., and Tonelli, C. (1993). Molecular homology among members of the R gene family in maize. Plant J. *3*, 335–346.

Courtois, F., Merendino, L., Demarsy, E., Mache, R., and Lerbs-Mache, S. (2007). Phage-type RNA polymerase RPOTmp transcribes the rrn operon from the PC promoter at early developmental stages in Arabidopsis. Plant Physiol. *145*, 712–721.

Crosatti, C., Rizza, F., Badeck, F.W., Mazzucotelli, E., and Cattivelli, L. (2013). Harden the chloroplast to protect the plant. Physiologia Plantarum *147*, 55–63.

Cvetkovic, J., Müller, K., and Baier, M. (2017). The effect of cold priming on the fitness of Arabidopsis thaliana accessions under natural and controlled conditions. Scientific Reports *7*, 44055.

Demarsy, E., Buhr, F., Lambert, E., and Lerbs-Mache, S. (2012). Characterization of the plastid-specific germination and seedling establishment transcriptional programme. J Exp Bot *63*, 925–939.

Deruère, J., Römer, S., d'Harlingue, A., Backhaus, R.A., Kuntz, M., and Camara, B. (1994). Fibril assembly and carotenoid overaccumulation in chromoplasts: a model for supramolecular lipoprotein structures. Plant Cell *6*, 119–133.

Domanskii, V., Rassadina, V., Gus-Mayer, S., Wanner, G., Schoch, S., and Rüdiger, W. (2003). Characterization of two phases of chlorophyll formation during greening of etiolated barley leaves. Planta *216*, 475–483.

Dumas, C., and Rogowsky, P. (2008). Fertilization and early seed formation. Comptes Rendus Biologies *331*, 715–725.

Dyall, S.D., Brown, M.T., and Johnson, P.J. (2004). Ancient invasions: from endosymbionts to organelles. Science *304*, 253–257.

El-Gebali, S., Mistry, J., Bateman, A., Eddy, S.R., Luciani, A., Potter, S.C., Qureshi, M., Richardson, L.J., Salazar, G.A., Smart, A., et al. (2019). The Pfam protein families database in 2019. Nucleic Acids Res *47*, D427–D432.

Ellis, R.J. (1979). The plastids: Their chemistry, structure, growth and inheritance, 2nd edn: by J. T. O. Kirk and R. A. E. Tilney-Bassett, Elsevier/North-Holland Biomedical Press, Amsterdam, New York and Oxford, 1978. $150.00/Dfl. 337.00 (xx + 960 pages) ISBN 0 444 80022 0. Trends in Biochemical Sciences *4*, N305.

Emanuel, C., Weihe, A., Graner, A., Hess, W.R., and Börner, T. (2004). Chloroplast development affects expression of phage-type RNA polymerases in barley leaves. Plant J. *38*, 460–472.

Ensminger, I., Busch, F., and Huner, N.P.A. (2006). Photostasis and cold acclimation: sensing low temperature through photosynthesis. Physiologia Plantarum *126*, 28–44.

Esau, K. (1975). Crystalline inclusion in thylakoids of spinach chloroplasts. Journal of Ultrastructure Research *53*, 235–243.

Fernández, A.P., and Strand, A. (2008). Retrograde signaling and plant stress: plastid signals initiate cellular stress responses. Curr. Opin. Plant Biol. *11*, 509–513.

Francia, E., Rizza, F., Cattivelli, L., Stanca, A.M., Galiba, G., Tóth, B., Hayes, P.M., Skinner, J.S., and Pecchioni, N. (2004). Two loci on chromosome 5H determine low-temperature tolerance in a "Nure" (winter) x "Tremois" (spring) barley map. Theor. Appl. Genet. *108*, 670–680.

Franck, F., Sperling, U., Frick, G., Pochert, B., van Cleve, B., Apel, K., and Armstrong, G.A. (2000). Regulation of etioplast pigment-protein complexes, inner membrane architecture, and protochlorophyllide a chemical heterogeneity by light-dependent NADPH:protochlorophyllide oxidoreductases A and B. Plant Physiol. *124*, 1678–1696.

Fung, S., Nishimura, T., Sasarman, F., and Shoubridge, E.A. (2013). The conserved interaction of C7orf30 with MRPL14 promotes biogenesis of the mitochondrial large ribosomal subunit and mitochondrial translation. Molecular Biology of the Cell *24*, 184–193.

Galagan, J.E., Sisk, P., Stolte, C., Weiner, B., Koehrsen, M., Wymore, F., Reddy, T.B.K., Zucker, J.D., Engels, R., Gellesch, M., et al. (2010). TB database 2010: Overview and update. Tuberculosis *90*, 225–235.

Galey, J., Francke, B., and Bahl, J. (1980). Ultrastructure and lipid composition of etioplasts in developing dark-grown wheat leaves. Planta *149*, 433–439.

Galperin, M.Y. (2004). "Conserved hypothetical" proteins: prioritization of targets for experimental study. Nucleic Acids Research *32*, 5452–5463.

Gatenby, A.A., Castleton, J.A., and Saul, M.W. (1981). Expression in E. coli of maize and wheat chloroplast genes for large subunit of ribulose bisphosphate carboxylase. Nature *291*, 117–121.

Gilkerson, J., Perez-Ruiz, J., Chory, J., and Callis, J. (2012). The plastid-localized pfkB-type carbohydrate kinases FRUCTOKINASE-LIKE 1 and 2 are essential for growth and development of Arabidopsis thaliana. BMC Plant Biol *12*, 102.

Gilmour, S.J., Hajela, R.K., and Thomashow, M.F. (1988). Cold Acclimation in Arabidopsis thaliana. Plant Physiology *87*, 745–750.

Goldberg, R.B., de Paiva, G., and Yadegari, R. (1994). Plant Embryogenesis: Zygote to Seed. Science *266*, 605–614.

Gombos, Z., Wada, H., and Murata, N. (1994). The recovery of photosynthesis from low-temperature photoinhibition is accelerated by the unsaturation of membrane lipids: a mechanism of chilling tolerance. Proc Natl Acad Sci U S A *91*, 8787–8791.

Goulas, E., Schubert, M., Kieselbach, T., Kleczkowski, L.A., Gardeström, P., Schröder, W., and Hurry, V. (2006). The chloroplast lumen and stromal proteomes of Arabidopsis thaliana show differential sensitivity to short- and long-term exposure to low temperature. Plant J. *47*, 720–734.

Govindje, e (1995). Sixty-Three Years Since Kautsky: Chlorophyll a Fluorescence. Functional Plant Biol. *22*, 131.

Graf, M., Arenz, S., Huter, P., Dönhöfer, A., Novácek, J., and Wilson, D.N. (2017). Cryo-EM structure of the spinach chloroplast ribosome reveals the location of plastid-specific ribosomal proteins and extensions. Nucleic Acids Res. *45*, 2887–2896.

Greaves, J.A. (1996). Improving suboptimal temperature tolerance in maize- the search for variation. J Exp Bot *47*, 307–323.

Grennan, A.K., and Ort, D.R. (2007). Cool temperatures interfere with D1 synthesis in tomato by causing ribosomal pausing. Photosynth Res *94*, 375–385.

Gruissem, W., and Zurawski, G. (1985). Analysis of promoter regions for the spinach chloroplast rbcL, atpB and psbA genes. EMBO J *4*, 3375–3383.

Gunning, B.E.S. (2001). Membrane geometry of "open" prolamellar bodies. Protoplasma *215*, 4–15.

Gutteridge, S., Brunkard, J.O., and Burch-Smith, T.M. (2018). Ties that bind: the integration of plastid signalling pathways in plant cell metabolism. Essays Biochem *62*, 95–107.

Hajdukiewicz, P.T., Allison, L.A., and Maliga, P. (1997). The two RNA polymerases encoded by the nuclear and the plastid compartments transcribe distinct groups of genes in tobacco plastids. EMBO J *16*, 4041–4048.

Han, C., and Martienssen, R. (1995). The Iojap (Ij) protein is associated with 50S chloroplast ribosomal subunits.

Han, C., and Martienssen, R.A. (2001). The Iojap (Ij) protein is associated with 50S chloroplast ribosomal subunits.

Han, C., Patrie, W., Polacco, M., and Coe, EdwardH. (1993). Aberrations in plastid transcripts and deficiency of plastid DNA in striped and albino mutants in maize. Planta *191*.

Han, C.D., Coe Jr, E.H., and Martienssen, R.A. (1992). Molecular cloning and characterization of iojap (ij), a pattern striping gene of maize. The EMBO Journal *11*, 4037.

Harris, J.B., and Arnott, H.J. (1973). Effects of senescence on chloroplasts of the tobacco leaf. Tissue Cell *5*, 527–544.

Harsányi, A., Böddi, B., Bóka, K., and Gáborjányi, R. (2005). Pathogen Affected Greening Process of Barley Seedlings Infected with BSMV by Seed Transmission. CEREAL RESEARCH COMMUNICATIONS *33*, 209–211.

Hashimoto, H. (1985). Changes in distribution of nucleoids in developing and dividing chloroplasts and etioplasts ofArena sativa. Protoplasma *127*, 119–127.

Häuser, R., Pech, M., Kijek, J., Yamamoto, H., Titz, B., Naeve, F., Tovchigrechko, A., Yamamoto, K., Szaflarski, W., Takeuchi, N., et al. (2012). RsfA (YbeB) Proteins Are Conserved Ribosomal Silencing Factors. PLoS Genetics *8*, e1002815.

He, M., He, C.-Q., and Ding, N.-Z. (2018). Abiotic Stresses: General Defenses of Land Plants and Chances for Engineering Multistress Tolerance. Front Plant Sci *9*.

Heidarvand, L., and Maali Amiri, R. (2010). What happens in plant molecular responses to cold stress? Acta Physiol Plant *32*, 419–431.

Hernández-Pinzón, I., Ross, J.H., Barnes, K.A., Damant, A.P., and Murphy, D.J. (1999). Composition and role of tapetal lipid bodies in the biogenesis of the pollen coat of Brassica napus. Planta *208*, 588–598.

Hernández-Verdeja, T., and Strand, Å. (2018). Retrograde Signals Navigate the Path to Chloroplast Development. Plant Physiology *176*, 967–976.

Hess, W.R., and Börner, T. (1999). Organellar RNA polymerases of higher plants. Int. Rev. Cytol. *190*, 1–59.

Hess, W.R., Prombona, A., Fieder, B., Subramanian, A.R., and Börner, T. (1993). Chloroplast rps15 and the rpoB/C1/C2 gene cluster are strongly transcribed in ribosome-deficient plastids: evidence for a functioning non-chloroplast-encoded RNA polymerase. The EMBO Journal *12*, 563–571.

Houde, M., Dhindsa, R.S., and Sarhan, F. (1992). A molecular marker to select for freezing tolerance in Gramineae. Mol. Gen. Genet. *234*, 43–48.

Hsieh, K., and Huang, A.H.C. (2004). Endoplasmic reticulum, oleosins, and oils in seeds and tapetum cells. Plant Physiol. *136*, 3427–3434.

Hsu, B.D., Lee, J.Y., and Pan, R.L. (1986). The two binding sites for DCMU in Photosystem II. Biochem Biophys Res Commun *141*, 682–688.

Hsu, S.-C., Belmonte, M.F., Harada, J.J., and Inoue, K. (2010). Indispensable Roles of Plastids in Arabidopsis thaliana Embryogenesis. Curr Genomics *11*, 338–349.

Hu, J., and Bogorad, L. (1990). Maize chloroplast RNA polymerase: the 180-, 120-, and 38-kilodalton polypeptides are encoded in chloroplast genes. Proc Natl Acad Sci U S A *87*, 1531–1535.

Hübschmann, T., and Börner, T. (1998). Characterisation of transcript initiation sites in ribosome-deficient barley plastids. Plant Mol. Biol. *36*, 493–496.

Huner, N.P.A., Öquist, G., and Sarhan, F. (1998). Energy balance and acclimation to light and cold. Trends in Plant Science *3*, 224–230.

Hurkman, W.J., and Kennedy, G.S. (1976). Fine structure and development of proteoplasts in primary leaves of mung bean. Protoplasma *89*, 171–184.

Jackson, R.J., Kaminski, A., and Pöyry, T.A.A. (2007). 8 Coupled Termination-Reinitiation Events in mRNA Translation. Cold Spring Harbor Monograph Archive *48*, 197–223.

Jarvis, P., and López-Juez, E. (2013). Biogenesis and homeostasis of chloroplasts and other plastids. Nature Reviews Molecular Cell Biology *14*, 787–802.

Jenkins, M.T. (1924). HERITABLE CHARACTERS OF MAIZE XX—Iojap-Striping, a Chlorophyll Defect. J Hered *15*, 467–472.

Josse, E.-M., and Halliday, K.J. (2008). Skotomorphogenesis: The Dark Side of Light Signalling. Current Biology *18*, R1144–R1146.

Juneau, P., Lay, P.L., Böddi, B., Samson, G., and Popovic, R. (2002). Relationship Between the Structural and Functional Changes of the Photosynthetic Apparatus During Chloroplast–Chromoplast Transition in Flower Bud of Lilium longiflorum¶. Photochemistry and Photobiology *75*, 377–381.

Kapoor, S., Suzuki, J.Y., and Sugiura, M. (1997). Identification and functional significance of a new class of non-consensus-type plastid promoters. The Plant Journal *11*, 327–337.

Katano, K., Honda, K., and Suzuki, N. (2018). Integration between ROS Regulatory Systems and Other Signals in the Regulation of Various Types of Heat Responses in Plants. Int J Mol Sci *19*.

Kiel, M.C., Kaji, H., and Kaji, A. (2007). Ribosome recycling: An essential process of protein synthesis. Biochemistry and Molecular Biology Education *35*, 40–44.

Kijek, J.J. (2013). RsfS (YbeB) is an universally conserved ribosome silencing factor. Freie Universität Berlin.

Kim, J., and Mullet, J.E. (2003). A mechanism for light-induced translation of the rbcL mRNA encoding the large subunit of ribulose-1,5-bisphosphate carboxylase in barley chloroplasts. Plant Cell Physiol. *44*, 491–499.

Kim, J., Eichacker, L.A., Rudiger, W., and Mullet, J.E. (1994). Chlorophyll Regulates Accumulation of the Plastid-Encoded Chlorophyll Proteins P700 and D1 by Increasing Apoprotein Stability. Plant Physiology *104*, 907–916.

Kindgren, P., Dubreuil, C., and Strand, Å. (2015). The Recovery of Plastid Function Is Required for Optimal Response to Low Temperatures in Arabidopsis. PLOS ONE *10*, e0138010.

Kleffmann, T., von Zychlinski, A., Russenberger, D., Hirsch-Hoffmann, M., Gehrig, P., Gruissem, W., and Baginsky, S. (2007). Proteome Dynamics during Plastid Differentiation in Rice. Plant Physiol *143*, 912–923.

Klein, R.R., and Mullet, J.E. (1986). Regulation of chloroplast-encoded chlorophyll-binding protein translation during higher plant chloroplast biogenesis. J. Biol. Chem. *261*, 11138–11145.

Klein, R.R., and Mullet, J.E. (1987). Control of gene expression during higher plant chloroplast biogenesis. Protein synthesis and transcript levels of psbA, psaA-psaB, and rbcL in dark-grown and illuminated barley seedlings. J. Biol. Chem. *262*, 4341–4348.

Kobayashi, K., Baba, S., Obayashi, T., Sato, M., Toyooka, K., Keränen, M., Aro, E.-M., Fukaki, H., Ohta, H., Sugimoto, K., et al. (2012). Regulation of Root Greening by Light and Auxin/Cytokinin Signaling in *Arabidopsis*. Plant Cell *24*, 1081–1095.

Komatsu, S., Muhammad, A., and Rakwal, R. (1999). Separation and characterization of proteins from green and etiolated shoots of rice (Oryza sativa L.): towards a rice proteome. Electrophoresis *20*, 630–636.

Koornneef, M., Alonso-Blanco, C., Peeters, A., and Soppe, W. (1998). GENETIC CONTROL OF FLOWERING TIME IN ARABIDOPSIS. Annual Review of Plant Physiology and Plant Molecular Biology *49*.

Krupinska, K., Melonek, J., and Krause, K. (2013). New insights into plastid nucleoid structure and functionality. Planta *237*, 653–664.

Kühn, K., Bohne, A.-V., Liere, K., Weihe, A., and Börner, T. (2007). Arabidopsis Phage-Type RNA Polymerases: Accurate in Vitro Transcription of Organellar Genes. The Plant Cell *19*, 959–971.

Kupsch, C., Ruwe, H., Gusewski, S., Tillich, M., Small, I., and Schmitz-Linneweber, C. (2012). Arabidopsis chloroplast RNA binding proteins CP31A and CP29A associate with large transcript pools and confer cold stress tolerance by influencing multiple chloroplast RNA processing steps. Plant Cell *24*, 4266–4280.

Kuroiwa, T. (1991). The Replication, Differentiation, and Inheritance of Plastids with Emphasis on the Concept of Organelle Nuclei. In International Review of Cytology, K.W. Jeon, and M. Friedlander, eds. (Academic Press), pp. 1–62.

Kyong, C.W. (2007). Cluster Analysis and Comparison of Various Chloroplast and Nuclear Transcriptomes in Arabidopsis thaliana. Ludwig Maximilians University in Munich.

Laloi, C., and Havaux, M. (2015). Key players of singlet oxygen-induced cell death in plants. Front Plant Sci *6*, 39.

Lancer, H.A., Cohen, C.E., and Schiff, J.A. (1976). Changing Ratios of Phototransformable Protochlorophyll and Protochlorophyllide of Bean Seedlings Developing in the Dark. Plant Physiol. *57*, 369–374.

Larkindale, J. (2005). Heat Stress Phenotypes of Arabidopsis Mutants Implicate Multiple Signaling Pathways in the Acquisition of Thermotolerance. PLANT PHYSIOLOGY *138*, 882–897.

Lee, B.-H. (2009). Ecotype-dependent genetic regulation of bolting time in the Arabidopsis mutants with increased number of leaves. J Microbiol Biotechnol *19*, 542–546.

Lee, D.W., Lee, J., and Hwang, I. (2017). Sorting of nuclear-encoded chloroplast membrane proteins. Curr. Opin. Plant Biol. *40*, 1–7.

Leister, D. (2016). Towards understanding the evolution and functional diversification of DNA-containing plant organelles. F1000Res *5*, 330.

Letunic, I., and Bork, P. (2019). Interactive Tree Of Life (iTOL) v4: recent updates and new developments. Nucleic Acids Res *47*, W256–W259.

Li, X., Sun, Q., Jiang, C., Yang, K., Hung, L.-W., Zhang, J., and Sacchettini, J. (2015). Structure of Ribosomal Silencing Factor Bound to Mycobacterium tuberculosis Ribosome. Structure *23*, 1858–1865.

Liang, Z., Zhu, N., Mai, K.K., Liu, Z., Tzeng, D., Osteryoung, K.W., Zhong, S., Staehelin, L.A., and Kang, B.-H. (2018). Thylakoid-Bound Polysomes and a Dynamin-Related Protein, FZL, Mediate Critical Stages of the Linear Chloroplast Biogenesis Program in Greening Arabidopsis Cotyledons. The Plant Cell *30*, 1476–1495.

Liere, K., and Börner, T. (2013). Development-Dependent Changes in the Amount and Structural Organization of Plastid DNA. In Plastid Development in Leaves during Growth and Senescence, B. Biswal, K. Krupinska, and U.C. Biswal, eds. (Dordrecht: Springer Netherlands), pp. 215–237.

Liere, K., Weihe, A., and Börner, T. (2011). The transcription machineries of plant mitochondria and chloroplasts: Composition, function, and regulation. J. Plant Physiol. *168*, 1345–1360.

Link, G. (1996). Green life: Control of chloroplast gene transcription. BioEssays *18*, 465–471.

Liu, X., Zhou, Y., Xiao, J., and Bao, F. (2018). Effects of Chilling on the Structure, Function and Development of Chloroplasts. Front Plant Sci *9*.

Liu, Y.-G., Mitsukawa, N., Oosumi, T., and Whittier, R.F. (1995). Efficient isolation and mapping of Arabidopsis thaliana T-DNA insert junctions by thermal asymmetric interlaced PCR. The Plant Journal *8*, 457–463.

Ljubesic, N. (1972). Ultrastructural changes of plastids during the yellowing of the fruit of Cucurbita pepo var. pyriformis. Acta Bot Croatica.

Lopez-Juez, E., and Pyke, K.A. (2004). Plastids unleashed: their development and their integration in plant development. Int. J. Dev. Biol. *49*, 557–577.

Lukatkin, A.S., Brazaitytė, A., Bobinas, Č., and Duchovskis, P. (2012). Chilling injury in chilling-sensitive plants: a review. *99*, 14.

Lyska, D., Meierhoff, K., and Westhoff, P. (2013). How to build functional thylakoid membranes: from plastid transcription to protein complex assembly. Planta *237*, 413–428.

Madeira, F., Park, Y. mi, Lee, J., Buso, N., Gur, T., Madhusoodanan, N., Basutkar, P., Tivey, A.R.N., Potter, S.C., Finn, R.D., et al. (2019). The EMBL-EBI search and sequence analysis tools APIs in 2019. Nucleic Acids Research *47*, W636–W641.

Maier, U.-G., Zauner, S., Woehle, C., Bolte, K., Hempel, F., Allen, J.F., and Martin, W.F. (2013). Massively Convergent Evolution for Ribosomal Protein Gene Content in Plastid and Mitochondrial Genomes. Genome Biol Evol *5*, 2318–2329.

Majeran, W., Friso, G., Ponnala, L., Connolly, B., Huang, M., Reidel, E., Zhang, C., Asakura, Y., Bhuiyan, N.H., Sun, Q., et al. (2010). Structural and Metabolic Transitions of C4 Leaf Development and Differentiation Defined by Microscopy and Quantitative Proteomics in Maize. The Plant Cell *22*, 3509–3542.

Majeran, W., Friso, G., Asakura, Y., Qu, X., Huang, M., Ponnala, L., Watkins, K.P., Barkan, A., and Wijk, K.J. van (2012). Nucleoid-Enriched Proteomes in Developing Plastids and Chloroplasts from Maize Leaves: A New Conceptual Framework for Nucleoid Functions. Plant Physiology *158*, 156–189.

Mansfield, S.G., and Briarty, L.G. (1991). Early embryogenesis in *Arabidopsis thaliana* . II. The developing embryo. Can. J. Bot. *69*, 461–476.

Marinos, N.G. (1967). Multifunctional plastids in the meristematic region of potato tuber buds. J. Ultrastruct. Res. *17*, 91–113.

Martin, W., Rujan, T., Richly, E., Hansen, A., Cornelsen, S., Lins, T., Leister, D., Stoebe, B., Hasegawa, M., and Penny, D. (2002). Evolutionary analysis of Arabidopsis, cyanobacterial, and chloroplast genomes reveals plastid phylogeny and thousands of cyanobacterial genes in the nucleus. Proc. Natl. Acad. Sci. U.S.A. *99*, 12246–12251.

Martinoia, E., Heck, U., J. Dalling, M., and Matile, PH. (1983). Changes in Chloroplast Number and Chloroplast Constituents in Senescing Barley Leaves. Biochemie Und Physiologie Der Pflanzen *178*, 147–155.

Maxwell, K., and Johnson, G.N. (2000). Chlorophyll fluorescence—a practical guide. J Exp Bot *51*, 659–668.

Meinke, D.W. (2020). Genome-wide identification of EMBRYO-DEFECTIVE (EMB) genes required for growth and development in Arabidopsis. New Phytologist *226*, 306–325.

Meinke, D., Muralla, R., Sweeney, C., and Dickerman, A. (2008). Identifying essential genes in Arabidopsis thaliana. Trends Plant Sci. *13*, 483–491.

Melonek, J., Oetke, S., and Krupinska, K. (2016). Multifunctionality of plastid nucleoids as revealed by proteome analyses. Biochim. Biophys. Acta *1864*, 1016–1038.

Menke, W. (1962). Structure and Chemistry of Plastids. Annu. Rev. Plant. Physiol. *13*, 27–44.

Metz, J.G., Pakrasi, H.B., Seibert, M., and Arntzen, C.J. (1986). Evidence for a dual function of the herbicide-binding Dl protein in photosystem II. FEBS LETTERS *205*, 6.

Millen, R.S., Olmstead, R.G., Adams, K.L., Palmer, J.D., Lao, N.T., Heggie, L., Kavanagh, T.A., Hibberd, J.M., Gray, J.C., Morden, C.W., et al. (2001). Many Parallel Losses of infA from Chloroplast DNA during Angiosperm Evolution with Multiple Independent Transfers to the Nucleus. Plant Cell *13*, 645–658.

Miller, G., Suzuki, N., Ciftci-Yilmaz, S., and Mittler, R. (2010). Reactive oxygen species homeostasis and signalling during drought and salinity stresses. Plant Cell Environ. *33*, 453–467.

Minorsky, P.V. (2002). Plant Physiology. Plant Physiology *129*, 5–6.

Miryeganeh, M., Yamaguchi, M., and Kudoh, H. (2018). Synchronisation of Arabidopsis flowering time and whole-plant senescence in seasonal environments. Scientific Reports *8*, 10282.

Mittler, R. (2002). Oxidative stress, antioxidants and stress tolerance. Trends Plant Sci. *7*, 405–410.

Mullet, J.E. (1993). Dynamic regulation of chloroplast transcription. Plant Physiol *103*, 309–313.

Murchie, E.H., and Lawson, T. (2013). Chlorophyll fluorescence analysis: a guide to good practice and understanding some new applications. Journal of Experimental Botany *64*, 3983–3998.

Myouga, F., Akiyama, K., Motohashi, R., Kuromori, T., Ito, T., Iizumi, H., Ryusui, R., Sakurai, T., and Shinozaki, K. (2010). The Chloroplast Function Database: a large-scale collection of Arabidopsis Ds/Spm- or T-DNA-tagged homozygous lines for nuclear-encoded chloroplast proteins, and their systematic phenotype analysis. The Plant Journal *61*, 529–542.

Nakagawa, S., Niimura, Y., and Gojobori, T. (2017). Comparative genomic analysis of translation initiation mechanisms for genes lacking the Shine-Dalgarno sequence in prokaryotes. Nucleic Acids Res. *45*, 3922–3931.

Nakata, M.T., Sato, M., Wakazaki, M., Sato, N., Kojima, K., Sekine, A., Nakamura, S., Shikanai, T., Toyooka, K., Tsukaya, H., et al. (2018). Plastid translation is essential for lateral root stem cell patterning in Arabidopsis thaliana. Biology Open *7*.

Nelissen, H., Gonzalez, N., and Inzé, D. (2016). Leaf growth in dicots and monocots: so different yet so alike. Current Opinion in Plant Biology *33*, 72–76.

Nesbit, A.D., Whippo, C., Hangarter, R.P., and Kehoe, D.M. (2015). Translation initiation factor 3 families: what are their roles in regulating cyanobacterial and chloroplast gene expression? Photosyn. Res. *126*, 147–159.

Neuhaus, H.E., and Emes, M.J. (2000). NONPHOTOSYNTHETIC METABOLISM IN PLASTIDS. Annu. Rev. Plant Physiol. Plant Mol. Biol. *51*, 111–140.

Newcomb, E.H. (1967). Fine structure of protein-storing plastids in bean root tips. J. Cell Biol. *33*, 143–163.

Ohyama, K., Fukuzawa, H., Kohchi, T., Shirai, H., Sano, T., Sano, S., Umesono, K., Shiki, Y., Takeuchi, M., Chang, Z., et al. (1986). Chloroplast gene organization deduced from complete sequence of liverwort Marchantia polymorpha chloroplast DNA. Nature *322*, 572–574.

Olen, B., Auld, S., and University, O.S. (2019). Farming: Weather is Leading Cause of U.S. Crop Loss – How Do You Assess the Risk?

Olinares, P.D.B., Ponnala, L., and van Wijk, K.J. (2010). Megadalton complexes in the chloroplast stroma of Arabidopsis thaliana characterized by size exclusion chromatography, mass spectrometry, and hierarchical clustering. Mol. Cell Proteomics *9*, 1594–1615.

Pacini, E., Taylor, P.E., Singh, M.B., and Knox, R.B. (1992). Development of Plastids in Pollen and Tapetum of Rye-grass, Lolium perenne L. Ann Bot *70*, 179–188.

Papageorgiou, G.C., and Govindjee, null (2011). Photosystem II fluorescence: slow changes--scaling from the past. J. Photochem. Photobiol. B, Biol. *104*, 258–270.

Park, H., Kreunen, S.S., Cuttriss, A.J., DellaPenna, D., and Pogson, B.J. (2002). Identification of the Carotenoid Isomerase Provides Insight into Carotenoid Biosynthesis, Prolamellar Body Formation, and Photomorphogenesis. The Plant Cell *14*, 321–332.

Parthier, B. (1988). GERONTOPLASTS - THE YELLOW END IN THE ONTOGENESIS OF CHLORO- PLASTS. 28.

Pennington, R.T. (2002). Willis, K.J., McElwain, J.C. The evolution of plants. Ann Bot *90*, 678–679.

Peoples, M.B., and Dalling, M.J. (1988). The interplay between proteolysis and amino acid metabolism during senescence and nitrogen reallocation.

Pérez-Bueno, M.L., Pineda, M., and Barón, M. (2019). Phenotyping Plant Responses to Biotic Stress by Chlorophyll Fluorescence Imaging. Front. Plant Sci. *10*.

Pfalz, J., and Pfannschmidt, T. (2013). Essential nucleoid proteins in early chloroplast development. Trends in Plant Science *18*, 186–194.

Pfannschmidt, T., and Link, G. (1994). Separation of two classes of plastid DNA-dependent RNA polymerases that are differentially expressed in mustard (Sinapis alba L.) seedlings. Plant Mol Biol *25*, 69–81.

Pfannschmidt, T., Blanvillain, R., Merendino, L., Courtois, F., Chevalier, F., Liebers, M., Grübler, B., Hommel, E., and Lerbs-Mache, S. (2015). Plastid RNA polymerases: orchestration of enzymes with different evolutionary origins controls chloroplast biogenesis during the plant life cycle. J Exp Bot *66*, 6957–6973.

Plöscher, M., Granvogl, B., Zoryan, M., Reisinger, V., and Eichacker, L.A. (2009). Mass spectrometric characterization of membrane integral low molecular weight proteins from photosystem II in barley etioplasts. Proteomics *9*, 625–635.

Pogorelko, G.V., Kambakam, S., Nolan, T., Foudree, A., Zabotina, O.A., and Rodermel, S.R. (2016). Impaired Chloroplast Biogenesis in Immutans, an Arabidopsis Variegation Mutant, Modifies Developmental Programming, Cell Wall Composition and Resistance to Pseudomonas syringae. PLOS ONE *11*, e0150983.

Pogson, B.J., Ganguly, D., and Albrecht-Borth, V. (2015). Insights into chloroplast biogenesis and development. Biochimica et Biophysica Acta (BBA) - Bioenergetics *1847*, 1017–1024.

Pouteau, S., and Albertini, C. (2009). The significance of bolting and floral transitions as indicators of reproductive phase change in Arabidopsis. J Exp Bot *60*, 3367–3377.

Powikrowska, M., Oetke, S., Jensen, P.E., and Krupinska, K. (2014). Dynamic composition, shaping and organization of plastid nucleoids. Front Plant Sci *5*.

Price, J.L., and Thomson, W.W. (1967). Occurrence of a Crystalline Inclusion in the Chloroplasts of Macadamia Leaves. Nature *214*, 1148–1149.

Provart, N.J., Gil, P., Chen, W., Han, B., Chang, H.-S., Wang, X., and Zhu, T. (2003). Gene Expression Phenotypes of Arabidopsis Associated with Sensitivity to Low Temperatures. Plant Physiology *132*, 893–906.

Pulido, P., Zagari, N., Manavski, N., Gawronski, P., Matthes, A., Scharff, L.B., Meurer, J., and Leister, D. (2018). CHLOROPLAST RIBOSOME ASSOCIATED Supports Translation under Stress and Interacts with the Ribosomal 30S Subunit. Plant Physiology *177*, 1539–1554.

Pyke, K.A. (1999). Plastid Division and Development. The Plant Cell *11*, 549–556.

Pyke, K.A., and Leech, R.M. (1994). A Genetic Analysis of Chloroplast Division and Expansion in Arabidopsis thaliana. Plant Physiol. *104*, 201–207.

Reddy, A.R., Chaitanya, K.V., and Vivekanandan, M. (2004). Drought-induced responses of photosynthesis and antioxidant metabolism in higher plants. Journal of Plant Physiology *161*, 1189–1202.

Reinbothe, C., Lebedev, N., and Reinbothe, S. (1999). A protochlorophyllide light-harvesting complex involved in de-etiolation of higher plants. Nature *397*, 80–84.

Reisinger, V., Hertle, A.P., Plöscher, M., and Eichacker, L.A. (2008). Cytochrome b6f is a dimeric protochlorophyll a binding complex in etioplasts. FEBS J. *275*, 1018–1024.

Reyes-Prieto, A., Weber, A.P.M., and Bhattacharya, D. (2007). The origin and establishment of the plastid in algae and plants. Annu. Rev. Genet. *41*, 147–168.

Rhoades, M.M. (1943). Genic Induction of an Inherited Cytoplasmic Difference. Proc Natl Acad Sci U S A *29*, 327–329.

Rhoades, M.M. (1946). Plastid Mutations. Cold Spring Harb Symp Quant Biol *11*, 202–207.

Rhoades, M.M. (1950). Gene Induced Mutation of a Heritable Cytoplasmic Factor Producing Male Sterility in Maize. Proc Natl Acad Sci U S A *36*, 634–635.

Richter, U., Kühn, K., Okada, S., Brennicke, A., Weihe, A., and Börner, T. (2010). A mitochondrial rRNA dimethyladenosine methyltransferase in Arabidopsis. Plant J *61*, 558–569.

Rogalski, M., Schöttler, M.A., Thiele, W., Schulze, W.X., and Bock, R. (2008). Rpl33, a nonessential plastid-encoded ribosomal protein in tobacco, is required under cold stress conditions. Plant Cell *20*, 2221–2237.

Rolland, N., Curien, G., Finazzi, G., Kuntz, M., Maréchal, E., Matringe, M., Ravanel, S., and Seigneurin-Berny, D. (2012). The biosynthetic capacities of the plastids and integration between cytoplasmic and chloroplast processes. Annu. Rev. Genet. *46*, 233–264.

Rolland, N., Bouchnak, I., Moyet, L., Salvi, D., and Kuntz, M. (2018). The Main Functions of Plastids. In Plastids, E. Maréchal, ed. (New York, NY: Springer US), pp. 73–85.

Rorbach, J., Gammage, P.A., and Minczuk, M. (2012). C7orf30 is necessary for biogenesis of the large subunit of the mitochondrial ribosome. Nucleic Acids Research *40*, 4097–4109.

Ross, J.H.E., Milanesi, C., Murphy, D.J., and Cresti, M. (2000). Rapid-freeze fixation and substitution improves tissue preservation of microspores and tapetum in Brassica napus. Sex Plant Reprod *12*, 237–240.

Ruelland, E., and Zachowski, A. (2010). How plants sense temperature. Environmental and Experimental Botany *69*, 225–232.

Sakai, A., Takano, H., and Kuroiwa, T. (2004). Organelle nuclei in higher plants: structure, composition, function, and evolution. Int. Rev. Cytol. *238*, 59–118.

Sato, E.M., Hijazi, H., Bennett, M.J., Vissenberg, K., and Swarup, R. (2015). New insights into root gravitropic signalling. J. Exp. Bot. *66*, 2155–2165.

Savage, L.J., Imre, K.M., Hall, D.A., and Last, R.L. (2013). Analysis of Essential Arabidopsis Nuclear Genes Encoding Plastid-Targeted Proteins. PLOS ONE *8*, e73291.

Scharff, L.B., Childs, L., Walther, D., and Bock, R. (2011). Local absence of secondary structure permits translation of mRNAs that lack ribosome-binding sites. PLoS Genet. *7*, e1002155.

Scharff, L.B., Ehrnthaler, M., Janowski, M., Childs, L.H., Hasse, C., Gremmels, J., Ruf, S., Zoschke, R., and Bock, R. (2017). Shine-Dalgarno Sequences Play an Essential Role in the Translation of Plastid mRNAs in Tobacco. The Plant Cell *29*, 3085–3101.

Sela, A., Piskurewicz, U., Megies, C., Mène-Saffrané, L., Finazzi, G., and Lopez-Molina, L. (2020). Embryonic Photosynthesis Affects Post-Germination Plant Growth. Plant Physiology *182*, 2166–2181.

Sewelam, N., Kazan, K., and Schenk, P.M. (2016). Global Plant Stress Signaling: Reactive Oxygen Species at the Cross-Road. Front. Plant Sci. *7*.

Shajani, Z., Sykes, M.T., and Williamson, J.R. (2011). Assembly of bacterial ribosomes. Annu. Rev. Biochem. *80*, 501–526.

Sharma, M.R., Wilson, D.N., Datta, P.P., Barat, C., Schluenzen, F., Fucini, P., and Agrawal, R.K. (2007). Cryo-EM study of the spinach chloroplast ribosome reveals the structural and functional roles of plastid-specific ribosomal proteins. PNAS *104*, 19315–19320.

Sharma, M.R., Dönhöfer, A., Barat, C., Marquez, V., Datta, P.P., Fucini, P., Wilson, D.N., and Agrawal, R.K. (2010). PSRP1 Is Not a Ribosomal Protein, but a Ribosome-binding Factor That Is Recycled by the Ribosome-recycling Factor (RRF) and Elongation Factor G (EF-G). J. Biol. Chem. *285*, 4006–4014.

Shcherbakova, K., Nakayama, H., and Shimamoto, N. (2015). Role of 100S ribosomes in bacterial decay period. Genes to Cells *20*, 789–801.

Shiina, T., Tsunoyama, Y., Nakahira, Y., and Khan, M.S. (2005). Plastid RNA polymerases, promoters, and transcription regulators in higher plants. Int. Rev. Cytol. *244*, 1–68.

Shinozaki, K., Ohme, M., Tanaka, M., Wakasugi, T., Hayashida, N., Matsubayashi, T., Zaita, N., Chunwongse, J., Obokata, J., Yamaguchi-Shinozaki, K., et al. (1986). The complete nucleotide sequence of the tobacco chloroplast genome: its gene organization and expression. EMBO J *5*, 2043–2049.

Shumway, L.K., and Weier, T.E. (1967). The Chloroplast Structure of Iojap Maize. American Journal of Botany *54*, 773.

Siemenroth, A., Börner, T., and Metzger, U. (1980). Biochemical studies on the iojap mutant of maize. Plant Physiology *65*, 1108–1110.

Sijben-Müller, G., Hallick, R.B., Alt, J., Westhoff, P., and Herrmann, R.G. (1986). Spinach plastid genes coding for initiation factor IF-1, ribosomal protein S11 and RNA polymerase alpha-subunit. Nucleic Acids Res. *14*, 1029–1044.

Sinclair, S.A., Larue, C., Bonk, L., Khan, A., Castillo-Michel, H., Stein, R.J., Grolimund, D., Begerow, D., Neumann, U., Haydon, M.J., et al. (2017). Etiolated Seedling Development Requires Repression of Photomorphogenesis by a Small Cell-Wall-Derived Dark Signal. Current Biology *27*, 3403-3418.e7.

Soitamo, A.J., Piippo, M., Allahverdiyeva, Y., Battchikova, N., and Aro, E.-M. (2008). Light has a specific role in modulating Arabidopsis gene expression at low temperature. BMC Plant Biol. *8*, 13.

Soll, J., and Schleiff, E. (2004). Plant cell biology: Protein import into chloroplasts. Nature Reviews Molecular Cell Biology *5*, 198–208.

Sorek, R., Zhu, Y., Creevey, C.J., Francino, M.P., Bork, P., and Rubin, E.M. (2007). Genome-wide experimental determination of barriers to horizontal gene transfer. Science *318*, 1449–1452.

de Souza, A., Wang, J.-Z., and Dehesh, K. (2017). Retrograde Signals: Integrators of Interorganellar Communication and Orchestrators of Plant Development. Annual Review of Plant Biology *68*, 85–108.

Sowiński, P., Rudzińska-Langwald, A., Adamczyk, J., Kubica, I., and Fronk, J. (2005). Recovery of maize seedling growth, development and photosynthetic efficiency after initial growth at low temperature. Journal of Plant Physiology *162*, 67–80.

Spížek, J., and Řezanka, T. (2017). Lincosamides: Chemical structure, biosynthesis, mechanism of action, resistance, and applications. Biochem Pharmacol *133*, 20–28.

Stepien, P., and Johnson, G.N. (2009). Contrasting Responses of Photosynthesis to Salt Stress in the Glycophyte Arabidopsis and the Halophyte Thellungiella: Role of the Plastid Terminal Oxidase as an Alternative Electron Sink. Plant Physiol. *149*, 1154–1165.

Stirbet, A., and Govindjee (2011). On the relation between the Kautsky effect (chlorophyll a fluorescence induction) and Photosystem II: Basics and applications of the OJIP fluorescence transient. Journal of Photochemistry and Photobiology B: Biology *104*, 236–257.

Stitt, M., and Hurry, V. (2002). A plant for all seasons: alterations in photosynthetic carbon metabolism during cold acclimation in Arabidopsis. Curr. Opin. Plant Biol. *5*, 199–206.

Stitt, M., and Zeeman, S.C. (2012). Starch turnover: pathways, regulation and role in growth. Curr. Opin. Plant Biol. *15*, 282–292.

Strittmatter, G., Gozdzicka-Jozefiak, A., and Kössel, H. (1985). Identification of an rRNA operon promoter from Zea mays chloroplasts which excludes the proximal tRNAValGAC from the primary transcript. EMBO J *4*, 599–604.

Sugiura, M. (1992). The chloroplast genome. Plant Mol. Biol. *19*, 149–168.

Sun, Y., and Zerges, W. (2015a). Translational regulation in chloroplasts for development and homeostasis. Biochimica et Biophysica Acta (BBA) - Bioenergetics *1847*, 809–820.

Sun, Y., and Zerges, W. (2015b). Translational regulation in chloroplasts for development and homeostasis. Biochimica et Biophysica Acta (BBA) - Bioenergetics *1847*, 809–820.

Suo, J., Zhao, Q., David, L., Chen, S., and Dai, S. (2017). Salinity Response in Chloroplasts: Insights from Gene Characterization. Int J Mol Sci *18*.

Suzuki, N., Koussevitzky, S., Mittler, R., and Miller, G. (2012). ROS and redox signalling in the response of plants to abiotic stress. Plant Cell Environ. *35*, 259–270.

Svensson, J.T., Crosatti, C., Campoli, C., Bassi, R., Stanca, A.M., Close, T.J., and Cattivelli, L. (2006). Transcriptome Analysis of Cold Acclimation in Barley Albina and Xantha Mutants. Plant Physiology *141*, 257–270.

Swiatecka-Hagenbruch, M., Emanuel, C., Hedtke, B., Liere, K., and Börner, T. (2008). Impaired function of the phage-type RNA polymerase RpoTp in transcription of chloroplast genes is compensated by a second phage-type RNA polymerase. Nucleic Acids Res *36*, 785–792.

Tada, A., Adachi, F., Kakizaki, T., and Inaba, T. (2014). Production of viable seeds from the seedling lethal mutant ppi2-2 lacking the atToc159 chloroplast protein import receptor using plastic containers, and characterization of the homozygous mutant progeny. Front. Plant Sci. *5*.

Tadini, L., Pesaresi, P., Kleine, T., Rossi, F., Guljamow, A., Sommer, F., Mühlhaus, T., Schroda, M., Masiero, S., Pribil, M., et al. (2016). GUN1 Controls Accumulation of the Plastid Ribosomal Protein S1 at the Protein Level and Interacts with Proteins Involved in Plastid Protein Homeostasis. Plant Physiol. *170*, 1817–1830.

Tadini, L., Jeran, N., Peracchio, C., Masiero, S., Colombo, M., and Pesaresi, P. (2020). The plastid transcription machinery and its coordination with the expression of nuclear genome: Plastid-Encoded Polymerase, Nuclear-Encoded Polymerase and the Genomes Uncoupled 1-mediated retrograde communication. Philosophical Transactions of the Royal Society B: Biological Sciences *375*, 20190399.

Takagi, T., Nakamura, M., Hayashi, H., Inatsugi, R., Yano, R., and Nishida, I. (2003). The leaf-order-dependent enhancement of freezing tolerance in cold-acclimated Arabidopsis rosettes is not correlated with the transcript levels of the cold-inducible transcription factors of CBF/DREB1. Plant Cell Physiol. *44*, 922–931.

Takahashi, M., and Asada, K. (1988). Superoxide production in aprotic interior of chloroplast thylakoids. Arch. Biochem. Biophys. *267*, 714–722.

Takahashi, S., and Murata, N. (2008). How do environmental stresses accelerate photoinhibition? Trends Plant Sci. *13*, 178–182.

Tarasenko, V.I., Katyshev, A.I., Yakovleva, T.V., Garnik, E.Y., Chernikova, V.V., Konstantinov, Y.M., and Koulintchenko, M.V. (2016). RPOTmp, an Arabidopsis RNA polymerase with dual targeting, plays an important role in mitochondria, but not in chloroplasts. J Exp Bot *67*, 5657–5669.

Taylor, N.L., Tan, Y.-F., Jacoby, R.P., and Millar, A.H. (2009). Abiotic environmental stress induced changes in the Arabidopsis thaliana chloroplast, mitochondria and peroxisome proteomes. J Proteomics *72*, 367–378.

Theocharis, A., Clément, C., and Barka, E.A. (2012). Physiological and molecular changes in plants grown at low temperatures. Planta *235*, 1091–1105.

Thomashow, M.F. (1999). PLANT COLD ACCLIMATION: Freezing Tolerance Genes and Regulatory Mechanisms. Annu. Rev. Plant Physiol. Plant Mol. Biol. *50*, 571–599.

Thomson, W.W., and Whatley, J.M. (1980). Development of Nongreen Plastids. Annual Review of Plant Physiology *31*, 375–394.

Tikkanen, M., Grieco, M., Nurmi, M., Rantala, M., Suorsa, M., and Aro, E.-M. (2012). Regulation of the photosynthetic apparatus under fluctuating growth light. Philos. Trans. R. Soc. Lond., B, Biol. Sci. *367*, 3486–3493.

Tiller, N., and Bock, R. (2014). The Translational Apparatus of Plastids and Its Role in Plant Development. Molecular Plant *7*, 1105–1120.

Timmis, J.N., Ayliffe, M.A., Huang, C.Y., and Martin, W. (2004). Endosymbiotic gene transfer: organelle genomes forge eukaryotic chromosomes. Nat. Rev. Genet. *5*, 123–135.

Ting, J.T., Wu, S.S., Ratnayake, C., and Huang, A.H. (1998). Constituents of the tapetosomes and elaioplasts in Brassica campestris tapetum and their degradation and retention during microsporogenesis. Plant J. *16*, 541–551.

Tripathy, B.C., and Oelmüller, R. (2012). Reactive oxygen species generation and signaling in plants. Plant Signal Behav *7*, 1621–1633.

Trösch, R., Barahimipour, R., Gao, Y., Badillo-Corona, J.A., Gotsmann, V.L., Zimmer, D., Mühlhaus, T., Zoschke, R., and Willmund, F. (2018). Commonalities and differences of chloroplast translation in a green alga and land plants. Nature Plants *4*, 564–575.

Uemura, M., and Steponkus, P.L. (1997). Effect of Cold Acclimation on the Lipid Composition of the Inner and Outer Membrane of the Chloroplast Envelope Isolated from Rye Leaves. Plant Physiol *114*, 1493–1500.

Uemura, M., Tominaga, Y., Nakagawara, C., Shigematsu, S., Minami, A., and Kawamura, Y. (2006). Responses of the plasma membrane to low temperatures. Physiologia Plantarum *126*, 81–89.

Vágújfalvi, A., Galiba, G., Cattivelli, L., and Dubcovsky, J. (2003). The cold regulated transcriptional activator Cbf3 is linked to the frost-tolerance gene Fr-A2 on wheat chromosome 5A. Mol Genet Genomics *269*, 60–67.

Van Dingenen, J., Blomme, J., Gonzalez, N., and Inzé, D. (2016). Plants grow with a little help from their organelle friends. EXBOTJ *67*, 6267–6281.

Vera, A., and Sugiura, M. (1995). Chloroplast rRNA transcription from structurally different tandem promoters: an additional novel-type promoter. Curr Genet *27*, 280–284.

Vera, A., Hirose, T., and Sugiura, M. (1996). A ribosomal protein gene (rpl32) from tobacco chloroplast DNA is transcribed from alternative promoters: similarities in promoter region organization in plastid housekeeping genes. Mol. Gen. Genet. *251*, 518–525.

Walbot, V., and Coe, E.H. (1979). Nuclear gene iojap conditions a programmed change to ribosome-less plastids in Zea mays. Proceedings of the National Academy of Sciences *76*, 2760–2764.

Wang, M., Jiang, L., Da, Q., Liu, J., Feng, D., Wang, J., Wang, H.-B., and Jin, H.-L. (2016a). DELAYED GREENING 238, a Nuclear-Encoded Chloroplast Nucleoid Protein, Is Involved in the Regulation of Early Chloroplast Development and Plastid Gene Expression in *Arabidopsis thaliana*. Plant and Cell Physiology *57*, 2586–2599.

Wang, M., Jiang, L., Da, Q., Liu, J., Feng, D., Wang, J., Wang, H.-B., and Jin, H.-L. (2017). Domain of Unknown Function 143 is required for the functioning of PEP-associated protein DG238 in the chloroplast. J. Plant Biol. *60*, 604–611.

Wang, S., Bai, G., Wang, S., Yang, L., Yang, F., Wang, Y., Zhu, J.-K., and Hua, J. (2016b). Chloroplast RNA-Binding Protein RBD1 Promotes Chilling Tolerance through 23S rRNA Processing in Arabidopsis. PLoS Genet. *12*, e1006027.

Wang, X., Fan, C., Zhang, X., Zhu, J., and Fu, Y.-F. (2013). BioVector, a flexible system for gene specific-expression in plants. BMC Plant Biol *13*, 198.

Wang, Y., Zhang, J., Shi, X., Peng, Y., Li, P., Lin, D., Dong, Y., and Teng, S. (2016c). Temperature-sensitive albino gene *TCD5* , encoding a monooxygenase, affects chloroplast development at low temperatures. EXBOTJ *67*, 5187–5202.

Wanner, L.A., and Junttila, O. (1999). Cold-Induced Freezing Tolerance in Arabidopsis. Plant Physiology *120*, 391–400.

Wanschers, B.F.J., Szklarczyk, R., Pajak, A., van den Brand, M.A.M., Gloerich, J., Rodenburg, R.J.T., Lightowlers, R.N., Nijtmans, L.G., and Huynen, M.A. (2012). C7orf30 specifically associates with the large subunit of the mitochondrial ribosome and is involved in translation. Nucleic Acids Research *40*, 4040–4051.

Waters, M.T., and Langdale, J.A. (2009). The making of a chloroplast. The EMBO Journal *28*, 2861–2873.

Waters, M.T., Fray, R.G., and Pyke, K.A. (2004). Stromule formation is dependent upon plastid size, plastid differentiation status and the density of plastids within the cell. Plant J. *39*, 655–667.

Wellburn, A.R., and Hampp, R. (1979). Appearance of photochemical function in prothylakoids during plastid development. Biochimica et Biophysica Acta (BBA) - Bioenergetics *547*, 380–397.

Whatley, J.M. (1977). Variations in the Basic Pathway of Chloroplast Development. The New Phytologist *78*, 407–420.

Whatley, J.M. (1978). A Suggested Cycle of Plastid Developmental Interrelationships. The New Phytologist *80*, 489–502.

Whitfeld, P.R., Leaver, C.J., Bottomley, W., and Atchison, B. (1978). Low-molecular-weight (4.5S) ribonucleic acid in higher-plant chloroplast ribosomes. Biochem J *175*, 1103–1112.

Wise, R.R. (2006). The structure and function of plastids (Dordrecht: Springer).

Wu, D., Wright, D.A., Wetzel, C., Voytas, D.F., and Rodermel, S. (1999). The IMMUTANS variegation locus of Arabidopsis defines a mitochondrial alternative oxidase homolog that functions during early chloroplast biogenesis. Plant Cell *11*, 43–55.

Xu, D., Marino, G., Klingl, A., Enderle, B., Monte, E., Kurth, J., Hiltbrunner, A., Leister, D., and Kleine, T. (2019). Extrachloroplastic PP7L Functions in Chloroplast Development and Abiotic Stress Tolerance. Plant Physiology *180*, 323–341.

Yadav, S.K. (2010). Cold stress tolerance mechanisms in plants. A review. Agronomy for Sustainable Development *30*.

Yamaguchi, K., and Subramanian, A.R. (2000). The plastid ribosomal proteins. Identification of all the proteins in the 50 S subunit of an organelle ribosome (chloroplast). J. Biol. Chem. *275*, 28466–28482.

Yamaguchi, K., von Knoblauch, K., and Subramanian, A.R. (2000). The plastid ribosomal proteins. Identification of all the proteins in the 30 S subunit of an organelle ribosome (chloroplast). J. Biol. Chem. *275*, 28455–28465.

Yamasaki, T., Kudoh, T., Kamimura, Y., and Katoh, S. (1996). A Vertical Gradient of the Chloroplast Abundance among Leaves of Chenopodium album. Plant Cell Physiol *37*, 43–48.

Yoon, H.S., Hackett, J.D., Ciniglia, C., Pinto, G., and Bhattacharya, D. (2004). A molecular timeline for the origin of photosynthetic eukaryotes. Mol. Biol. Evol. *21*, 809–818.

Yu, F., Fu, A., Aluru, M., Park, S., Xu, Y., Liu, H., Liu, X., Foudree, A., Nambogga, M., and Rodermel, S. (2007). Variegation mutants and mechanisms of chloroplast biogenesis. Plant, Cell & Environment *30*, 350–365.

Yu, H.-D., Yang, X.-F., Chen, S.-T., Wang, Y.-T., Li, J.-K., Shen, Q., Liu, X.-L., and Guo, F.-Q. (2012). Downregulation of Chloroplast RPS1 Negatively Modulates Nuclear Heat-Responsive Expression of HsfA2 and Its Target Genes in Arabidopsis. PLOS Genetics *8*, e1002669.

Yu, Y., Mu, H.H., Mu-Forster, C., and Wasserman, B.P. (1998). Polypeptides of the maize amyloplast stroma. Stromal localization of starch-biosynthetic enzymes and identification of an 81-kilodalton amyloplast stromal heat-shock cognate. Plant Physiol. *116*, 1451–1460.

Yukawa, M., Kuroda, H., and Sugiura, M. (2007). A new in vitro translation system for non-radioactive assay from tobacco chloroplasts: effect of pre-mRNA processing on translation in vitro. Plant J. *49*, 367–376.

Zeeman, S.C., Smith, S.M., and Smith, A.M. (2004). The breakdown of starch in leaves. New Phytologist *163*, 247–261.

Zhang, L., Paakkarinen, V., van Wijk, K.J., and Aro, E.M. (1999). Co-translational assembly of the D1 protein into photosystem II. J. Biol. Chem. *274*, 16062–16067.

Zhelyazkova, P., Sharma, C.M., Förstner, K.U., Liere, K., Vogel, J., and Börner, T. (2012). The Primary Transcriptome of Barley Chloroplasts: Numerous Noncoding RNAs and the Dominating Role of the Plastid-Encoded RNA Polymerase. The Plant Cell *24*, 123–136.

Zimorski, V., Ku, C., Martin, W.F., and Gould, S.B. (2014). Endosymbiotic theory for organelle origins. Curr. Opin. Microbiol. *22*, 38–48.

Zoschke, R., and Bock, R. (2018). Chloroplast Translation: Structural and Functional Organization, Operational Control, and Regulation. The Plant Cell *30*, 745–770.

Zoschke, R., Liere, K., and Börner, T. (2007). From seedling to mature plant: arabidopsis plastidial genome copy number, RNA accumulation and transcription are differentially regulated during leaf development. Plant J. *50*, 710–722.

Zybailov, B., Rutschow, H., Friso, G., Rudella, A., Emanuelsson, O., Sun, Q., and van Wijk, K.J. (2008). Sorting signals, N-terminal modifications and abundance of the chloroplast proteome. PLoS ONE *3*, e1994.

von Zychlinski, A., Kleffmann, T., Krishnamurthy, N., Sjölander, K., Baginsky, S., and Gruissem, W. (2005). Proteome analysis of the rice etioplast: metabolic and regulatory networks and novel protein functions. Mol. Cell Proteomics *4*, 1072–1084.

APPENDIX

PRIMERS SEQUENCES AND SUPPLIES

Table 4: Arabidopsis genetic lines.

Genotypes	Back ground	SALK No.
WT	Columbia-0	N.A.
ijT1	Columbia-0	N.A.
ijT2	Columbia-0	SALK_121803.40.80.x
ijT3	Columbia-0	SALKseq_053017.1

Table 5: Laboratory materials in alphabetical order.

Materials	Company
Aluminum foil	Fisher
Fafard Superfine Germination Mix	SunGro Horticulture
Falcon® tube (50 mL)	Fisher
Fisherbrand™ Petri Dishes Square Grid (100 x 15 mm)	Fisher
Microfuge Tube (1.5 mL)	Fisher
Murashige and Skoog Basal Salt Mixture	Sigma
Parafilm	Bemis™ Parafilm™
Phytagel ™	Sigma
Polypropylene centrifuge tubes (14 mm x 89 mm)	Beckman Coulter
RNase-free microfuge tube (2 mL)	Invitrogen
U.S.A Standard Test Sieve (300 µm)	Fisher
Square Grid Plates	Fisher
Sucrose	Fisher
Traditional Square Pot (2.5 in)	Kord
Trays (10 x 20 x 2.5 in)	Living Whole Foods

Table 6: Laboratory chemicals in alphabetical order.

Chemicals	Company
25:24:1 phenol:chloroform:isoamyl alcohol pH 5.2	Fisher Bioagents
3-(3,4-dichlorophenyl)-1,1-dimethylurea (DCMU)	Sigma
6-Benzylaminopurine hydrochloride	Sigma
Acetosyringone	BioworldSupplier
Agarose (Low-EEO/Multi-Purpose/Molecular Biology Grade)	Fisher Bioreagents™
BD Bacto™ Dehydrated Agar	BD Diagnostic Systems
Bleach	Clorox
Chloramphenicol	Fisher Bioreagents™
Cycloheximide, 95%	ACROS Organics™
D-Mannitol	Fisher Chemical™
Dimethyl sulfoxide, DMSO - anhydrous, 99.9%	Sigma
Ethanol (100%)	Decons Laboartory Inc.
Ethylene glycol-bis(β-aminoethyl ether)-N,N,N′,N′-tetraacetic acid (EGTA)	ACROS Organics™
Ethylenediaminetetraacetic acid (EDTA)	Sigma
Glacial acetic acid	Fisher Chemical™
GlycoBlue™	Invitrogen
Heparin	Fisher Bioagents
Hydrochloric acid (HCl)	Fisher Chemical™
Kanamycin	Fisher Bioreagents™
LB Broth	Fisher Bioreagents™
Lincomycin hydrochloride	Alfa Aesar™
Magnesium chloride (MgCl2) anhydrous, ≥98%	Sigma
Murashige and Skoog Basal Salt Mixture	Sigma
Peptone	Fisher Bioreagents™
Polyoxyethylene-10-tridecyl ether	Sigma
Potassium chloride (KCl)	Fisher Chemical™
Rifampicin, ≥98%	TCI America™
Silwet L-77	Sigma
Sodium acetate	Fisher Chemical™
Sodium chloride (NaCl)	Fisher Chemical™
Sodium dodecyl sulfate	Sigma
Tris(2-carboxyethyl)phosphine (TCP)	Sigma
Tris(hydroxymethyl)aminomethane hydrochloride (Tris-HCl)	Fisher Bioreagents™
Triton-x100	Sigma
Yeast Extract	Fisher Bioreagents™

Table 7: Vectors and live cultures in alphabetical order.

Vectors	Company
Early Gate pEG100	The Arabidopsis Information Resource (TAIR)
GEC-C-3xCFP (Fu44)	The Arabidopsis Information Resource (TAIR)
GEC-C-3xMyc (Fu48)	The Arabidopsis Information Resource (TAIR)
pAN159 (cox-YFP)	Nebenführ Lab, University of Tennessee
pAN363 (prSSU-YFP)	Nebenführ Lab, University of Tennessee

Live Cultures
Agrobacterium tumefaciens (GV3101)
DB3.1 *E. coli*
TOP10 *E. coli*

Table 8: Molecular kits and enzymes in alphabetical order.

Kits	Company
Wizard® SV Gel and PCR Clean-Up System	Promega
Zyppy™ Plasmid Miniprep Kit instructions.	Zymo Research

Enzymes	Company
Clonase	New England Biolabs
DNase Turbo	ThermoScientific™
EcoRI-HF	New England Biolabs
EcoRI-HF	New England Biolabs
Luna® Universal qPCR Master Mix (New England Bio Labs	New England Biolabs
Maxima Reverse Transcriptase	ThermoScientific™
Phusion PCR	New England Biolabs
RT maxima	New England Biolabs
SpeI-HF	New England Biolabs
SpeI-HF	New England Biolabs
T4 DNA Ligase	New England Biolabs
XhoI	New England Biolabs
XohI	New England Biolabs

Table 9: Instruments and software in alphabetical order.

Instruments	Company
BioRad Gene Pulser-Xcell	Bio-Rad Laboratories, Inc.
Polaroid MP4 Land Camera	Polaroid Corp.
Canon Reble XS camera with a 55 mm lens	Canon USA Inc.
CFX96 Touch Deep Well Real-Time PCR Detection System with	Bio-Rad Laboratories, Inc.
Density Gradient Fractionator Model 185 with UA-5 absorbance	Instrument Specialty Co.
Electrophoresis Aparatus Thermal EC Classic™	Thermo Scientific™
FluoroCam 800MF closed system	Photon Systems Instruments
Leica SP8 White Laser Confocal System.	Leica Microsystems
NanoDrop™ One/OneC Microvolume UV-Vis	Thermo Scientific™
Optima L-90K Ultracentrifuge	Beckman Coulter
SW40-Ti rotor	Beckman Coulter
Zeis Divcovery V8 with CL 1500 ECO stereo lights	Carl Zeiss Microscopy, LLC

Software	Company
DNASTAR Lasergene	DNASTAR, Inc.
GraphPad Prism (v.8)	GraphPad Software
Image J	National Institutes of Health

Table 10: Primers and their sequences in alphabetical order.

Primers	Sequence
accD_Q-lit-F	TGTGGATTCAATGCGACAAT
accD_Q-lit-R	TTTTGCGCAGAGTCAATACG
accD-RT-1	AATGATATCCCCCAACAT
AD1	NTCGASTWTSGWGTT
AD2	NGTCGASWGANAWGAA
clpP_Q-F1	TATCCCGTCTCATTCTGCGA
clpP_Q-R1	CTCCCGTTTGTGCCTCATAA
clpP-RT-1	ACATAAAAACATCCCGTTC
cpijT2-LP	AACAAGAGGCTTGACAAAGAGG
GEC-alpha-CFP-R	AACAGCTCCTCGCCCTTG
grx17-Q-F2	TATCTACCGCCGATGCTCTC
grx17-Q-R2	CCCTCTCGCACTTCGTTATC
GW-cpIJ-CL-R	GCAAAAGAATTCGTTCCGTGGTTGTGACTGA
GW-cpIJ-CL-F1	CGAACTAGTAGAACAAAGGCGAAGGGTTTTAGAT
GW-cpIJ-CL-F	CGAATACTCGAGAATACTTTTATCAGAACAAAGGCG
gx17-RT-2	CCAATTAACTCACCTTTGTA
IJ_e3-SEQ-F	CCGCCCTCAAATTGATGCAAT
IT5-LP	TCCACAAAGTGCTGGATTCCC
IT5-RP	TGTGTACCGTATTTGTCGTCCCA
KT5-LP	CCATATATCTTCTCGAGGAATGCAG
KT5-RP	CGGGAACCAGAGTCTGAGGAGA
LBa1	TGGTTCACGTAGTGGGCCATCG
psbA_Q-F1	CAGGCTGAGCACAACATTCT
psbA_Q-R1	ACCAAGGAACCATGCATAGC
psbA-RT-3	CATACCATCAGAAAAACTTC
RBa1	GTTTCTGACGTATGTGCTTAGC
Rv-ij-LB	CCTTATAATTGCTGTTGGCGACT
Rv-iojap	TCTCTGCATCATCGTCAACC
SEQ-35S-F	CGCACAATCCCACTATCCTTCGCA
SP1	CGGGAGAGCCGTTGTAAG
SP2	CCCTCGCAGAGATCCGAATTAT
SP2.1	CATCTCCCTCGCAGAGATCC
SP2.2	GCGGAGGGTAGCATGTTGAT
SP3.1	GGAACGAGCAGAAGTCCTCC
SP4.1	CAGGACCGCCATCAATCGTA
SP4.2	CGCAGTTCCGCAAATAGCC
SP5	GCAGAGATGAACACGACCATCA
SP6	CTCGCGCCACTTCTTCACG

VITA

Thomas Jay Payne grew up in Michigan, where he fostered a curiosity of nature. After high school, he attended Central Michigan University, where he received his Bachelor of Science degree in Biochemistry. For a short time, he tried his hand in polymer chemistry but decided he would rather pursue a career in biology. To achieve his goal, Thomas attended the Graduate School at University of Tennessee, in. the department of Biochemistry & Cellular and Molecular Biology. There he concentrated on plant molecular biology, where he investigated the effects of low temperature on a chloroplast mutant *iojap* in *Arabidopsis thaliana*. He learned many new skills to help him succeed in a industrial career, creating genetically modified crops and plants for food and market application. Thomas is extremely grateful for his chance to achieve a Ph.D. and owes his success to his mentor, family, and friends.